Numerical Groundwater Modelling as a Tool to Quantify Shallow Aquifer Water Ingress through Mining-Related Open Voids

George Pieter van Dyk
2008102218

Submitted in fulfilment of the requirements for the degree

Magister Scientiae in Geohydrology

in the

Faculty of Natural and Agricultural Sciences

(Institute for Groundwater Studies)

at the

University of the Free State

Supervisor: Dr Amy Allwright

Date 27/11/2023

Declaration

I, George Pieter van Dyk, hereby declare that this dissertation submitted for the Master of Science Degree to the Institute for Groundwater Studies, Faculty of Science, University of the Free State, Bloemfontein, South Africa, is my own independent work. This thesis has not been submitted to any other institution of higher education. I further declare that all sources cited have been acknowledged by means of a list of references.

George Pieter van Dyk

2008102218

27 November 2023

Acknowledgements

I would like to thank everyone that supported me in completing this dissertation, my moderator Amy Allwright for guidance and my wife Cilleste van Dyk for the constant support and motivation and family and friends.

Abstract

The quantification of water ingress volumes and rates from different aquifer systems through open voids can aid in related studies concerning water quality, decanting potential, and stability evaluations especially in areas where historic mining has played a significant role in altering the groundwater environment. The objective of the research and approach is to evaluate if numerical groundwater modelling can be used as a tool to quantify ingress rates from shallow aquifer systems during rapid recharge events when these aquifer systems become saturated and water seeps through individual mine related open voids on a regional scale, eventually reaching historic mining infrastructure and deeper hard rock aquifers.

A case study that focused on the East Rand Basin was used to evaluate if numerical modelling can be used to produce quantified ingress rates from shallow aquifer systems through mine-related open voids. The East Rand Basin has a rich history of mine related activities which still has a large influence on the regional aquifer systems.

The research included gathering spatial and site-specific data required to construct and represent a numerical groundwater model in FEFLOW groundwater modelling software. The representative model was used to simulate a scenario that included monthly rainfall records that indicated elevated rainfall events and applied as time dependant recharge to the shallow aquifer systems identified along the Blesbokspruit and associated tributaries. The mapped mine-related open voids that fell within the shallow aquifers systems were assigned as discrete features to represent open voids leading to the mapped historic underground mine workings. The simulation included hydraulic head raises with each consecutive rainfall event to saturate the shallow aquifer systems and the ingress rates were recorded at each individual open void.

The outcome of the numerical modelling assessment proved that ingress rates can be quantified with results indicating that a maximum of 12 000 m^3/d can flow from the shallow aquifer systems during heavy rainfall events through 33 (out of 69) mapped open voids. The results were compared to a similar study (Waal, 2013), that indicated a good comparison in inflow rates. The model illustrated that roughly 16% of surface-related water (including ingress through shallow aquifer systems) could come from 46% of mine related open voids.

Numerical groundwater modelling proved to be a valuable tool to quantify ingress rates from aquifer systems through open voids, however data availability and data quality add major limitations to the result accuracy and model confidence.

Contents

Chapter 1 Introduction 1

1.1 Research question/hypothesis. 4

1.2 Research aims and objectives. 4

1.3 Research methodology. 4

Chapter 2 Literature review 7

2.1 Modelling the interaction between surface and groundwater systems 7

2.2 Surface water/groundwater modelling software packages 10

2.3 Groundwater and surface water interaction in the Witwatersrand Gold Fields 11

Chapter 3 Site characterisation and conceptualisation 16

3.1 Data review and acquisition 20

3.1.1 Spatial data 21

3.1.2 Site specific data 32

3.2 Conceptual model 53

Chapter 4 Numerical Groundwater Flow Model 57

4.1 Model construction. 57

4.2 Model evaluation. 59

4.3 Simulation results 68

4.4 Model application: Shallow aquifer ingress into mine related open voids. 71

4.4.1 Numerical model application and model input 71

4.4.2 Model application criteria. 72

4.4.3 Model application results. 74

Chapter 5 Discussion of Numerical Groundwater Modelling as a Tool to Quantify Shallow Aquifer Water Ingress through Mining-Related Open Voids 81

Chapter 6 Conclusions and Recommendations 86

6.1 Recommendations 87

Chapter 7 References 89

Appendix A Rainfall Records 93

Appendix B Groundwater Chloride Concentrations 104

Appendix C Recharge Estimations and Assumptions 108

Appendix D Recharge Potential and related Geology 112

Appendix E Groundwater Levels 114

Appendix F Time Dependant Recharge Model Input 117

List of Figures

Figure 1-1 Conceptual illustration of the numerical model objective during static conditions 2

Figure 1-2 Conceptual illustration of the numerical model objective during a flooding event 3

Figure 2-1 Conceptual illustration of the groundwater – surface water interaction processes. 9

Figure 2-2 Major River systems over the Witwatersrand Goldfields area taken from (Winde, 2015) 12

Figure 2-3 Sinkhole event densities identified in Gauteng and associated causes as dewatering or ingress (Taken from Dippenaar, 2018) 15

Figure 3-1 The Witwatersrand Gold Fields and the East Rand Basin Boundaries (Taken from Tucker, 2016) 18

Figure 3-2 The East Rand Basin and mapped Mining Footprint (Taken from CGS, 2018) 19

Figure 3-3 Topography and surface drainage of the sub-catchment area 23

Figure 3-4 Mapped Geology of the East Rand Basin 27

Figure 3-5 Geological key for Figure 3-4. 28

Figure 3-6 Schematic drawing of the sub surface geology of the East Rand Basin (Taken from Frimmel, 2019). 29

Figure 3-7 Wetland areas in relation to Alluvial deposits along the surface drainages. 31

Figure 3-8 Rainfall Station within the sub catchment area 34

Figure 3-9 Rainfall records for station 476644. 35

Figure 3-10 Rainfall records for station 476736. 35

Figure 3-11 Rainfall records for station 476766. 36

Figure 3-12 Rainfall records for station 476835 36

Figure 3-13 Chloride concentrations in and around the sub catchment 38

Figure 3-14 Figure indicating the rainwater chloride concentrations over South Africa Taken from (van Wyk et al., 2011) 40

Figure 3-15 Recharge percentages and Geology for the Sub Catchment 42

Figure 3-16 Geological key for Figure 3-15 43

Figure 3-17 Correlation between measured hydraulic head and topography. 46

Figure 3-18 Groundwater levels in and around the sub catchment area 47

Figure 3-19 Measured Hydraulic Head as interpolated from the reported groundwater levels 48

Figure 3-20 Historic Mining footprint as well as mapped shafts and ingress positions. 52

Figure 3-21 Limited ingress into mine related open from shallow aquifers during static conditions (not to scale) 55
Figure 3-22 Ingress into Mine related open voids during rapid recharge events (not to scale). 56
Figure 4-1 Horizontal and vertical finite element discretisation of the model domain, showing the surface features included (rivers, structures and mining outlines) 59
Figure 4-2 Model calibration input parameters: Hydraulic Conductivity and Recharge 62
Figure 4-3 Model representation input: Historic Mine hydraulic conductivity and Hydraulic Head Boundary Conditions 63
Figure 4-4 Correlation between measured and simulated hydraulic head. 66
Figure 4-5 Measured vs Simulated Hydraulic Head 66
Figure 4-6 Correlation between simulated and measured hydraulic head excluding outliers. 67
Figure 4-7 Measured vs Simulated Hydraulic Head excluding outliers 67
Figure 4-8 Simulated Hydraulic Head to represent the static groundwater conditions 69
Figure 4-9 Simulated Surface to Groundwater Level to evaluate that hydraulic head is below topography 70
Figure 4-10 Selected mine related voids to the shallow aquifer systems. 73
Figure 4-11 Hydraulic Head increases during the rapid recharge event. 77
Figure 4-12 Estimated inflows rates during the rapid recharge events. 78
Figure 4-13 Cumulative inflow rates during the rapid recharge events from the mine related open voids... 79
Figure 4-14 Hydraulic head increase during rainfall events: Rainfall event >300 mm. 80

List of Tables

Table 2-1 Ground water - Surface water interaction processes 8
Table 3-1 Model input data and sources 20
Table 3-2 Geological description and stratigraphy 26
Table 3-3 Rainfall station and recorded years 33
Table 3-4 Rainwater chloride concentrations for South Africa Taken from (van Wyk et al., 2011) 39
Table 3-5 Aquifer parameters determined from (Scholtz, 2013) 49
Table 3-6 Aquifer parameters summarised for the different aquifer systems (Scholtz, 2013) 50
Table 3-7 Aquifer parameters analysed for boreholes at the West Wits Mine (Koekemoer, 2020) 50
Table 4-1 Numerical Model Input Parameters 61
Table 4-2 Time steps at which hydraulic head needs to be raised during elevated rainfall. 74
Table 4-3 Water ingress during different climatic conditions for the east rand basin (Waal, 2013) 76

Abbreviations

Cl	Chloride
km	Kilometre
L/s	Litres per second
m	Meters
m/a	Meters per annum
m/d	Meters per day
m^3	Cubic meters
m^3/ d	Cubic meters per day
m^3/hr	Cubic meters per hour
mamsl	Meters Above Mean Sea Level
MAP	Mean Annual Precipitation
mbgl	Meters below ground level
mbwl	Meters below water level
mg/L	Milligrams per litre
ml	Millilitres
mm	Millimetres
mm/a	Millimetres per annum
TSF	Tailings Storage facility
WRD	Waste Rock Dump

Chapter 1 Introduction

The Witwatersrand Gold Fields presents huge challenges regarding groundwater management due to the extensive historical mining and associated open voids that exist as remnants from the historical mining activities (DWAF, 2013). The mining related open voids can be old mine shafts or surface cavities that remained open due to sub-surface caving at shallow mine tunnels. These mining-related open voids can serve as preferential pathways for water to flow freely into the underground groundwater systems and could have extensive influence on how the groundwater aquifer systems behave during flooding periods if these voids are situated in close proximity to perennial streams and rivers, as well as smaller tributaries, typically associated with shallow alluvial aquifer systems. Increased water ingress from rapidly recharged shallow aquifer systems into open voids during flooding or excessive wet periods will have an impact on the groundwater quantity and quality of the deeper hard rock aquifer systems.

If ingress volumes could accurately be modelled numerically, the possibility exists to better quantify water management programs in terms of water quantity and quality. The conceptual idea is illustrated in Figure 1-1 and Figure 1-2 which indicates the groundwater conditions under normal static conditions and the shallow aquifer ingress into the mine-related open voids in the associated floodplain area of the river systems (Figure 1-1). During a flood event, the river would flood it's banks and fill the floodplain area with subsequent rapid recharge to the shallow alluvial aquifer systems (Figure 1-2). Any mine-related open void that exists in the shallow aquifer system or in close proximity to the shallow aquifer systems could experience increased inflows during the flooding event.

This dissertation and research will detail how numerical groundwater modelling may be used as a tool to determine and quantify shallow aquifer water ingress volumes and rates through open voids and make use of a case study to focus on ingress through mining-related open voids to underlying aquifer systems.

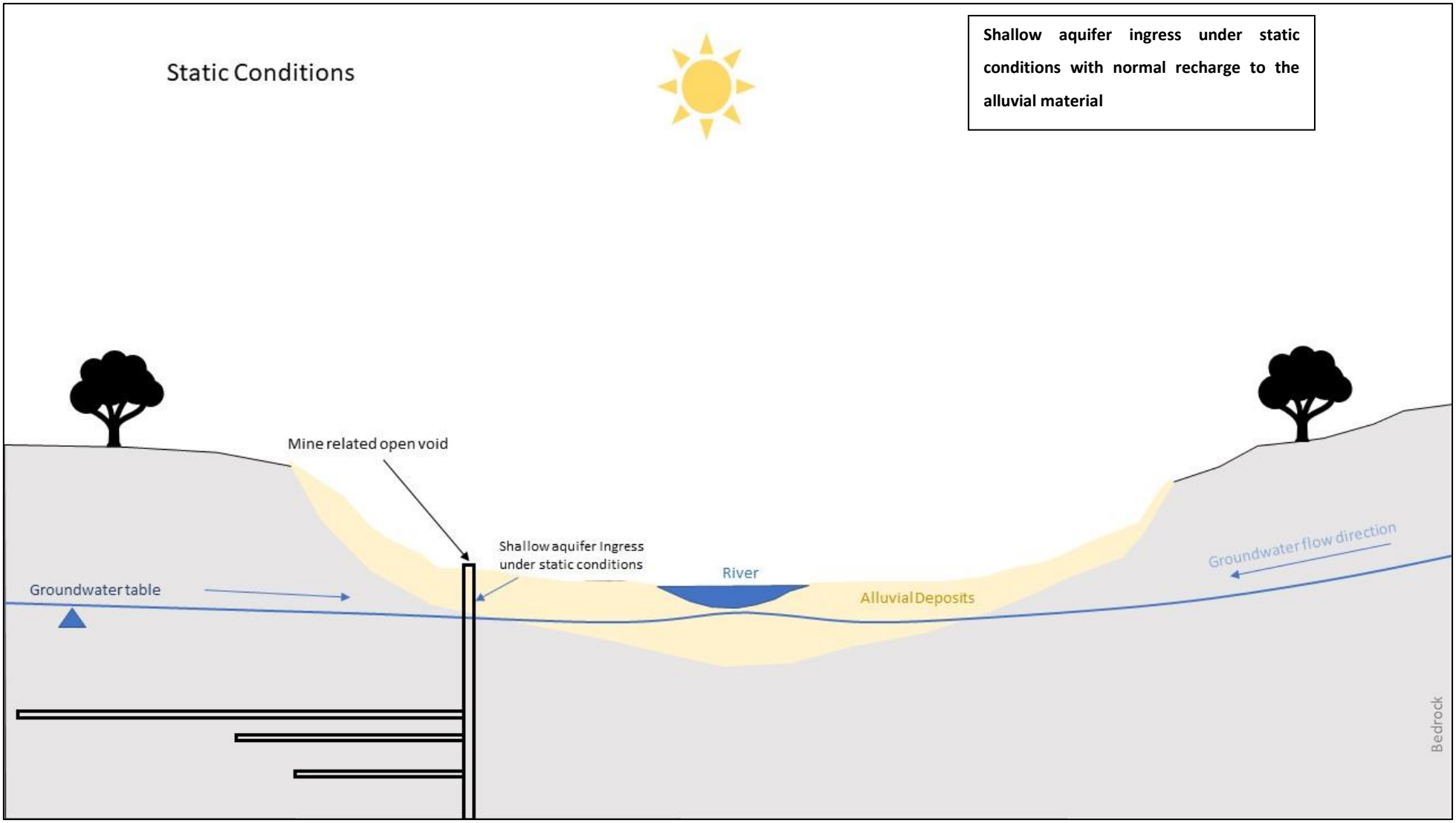

Figure 1-1 Conceptual illustration of the numerical model objective during static conditions

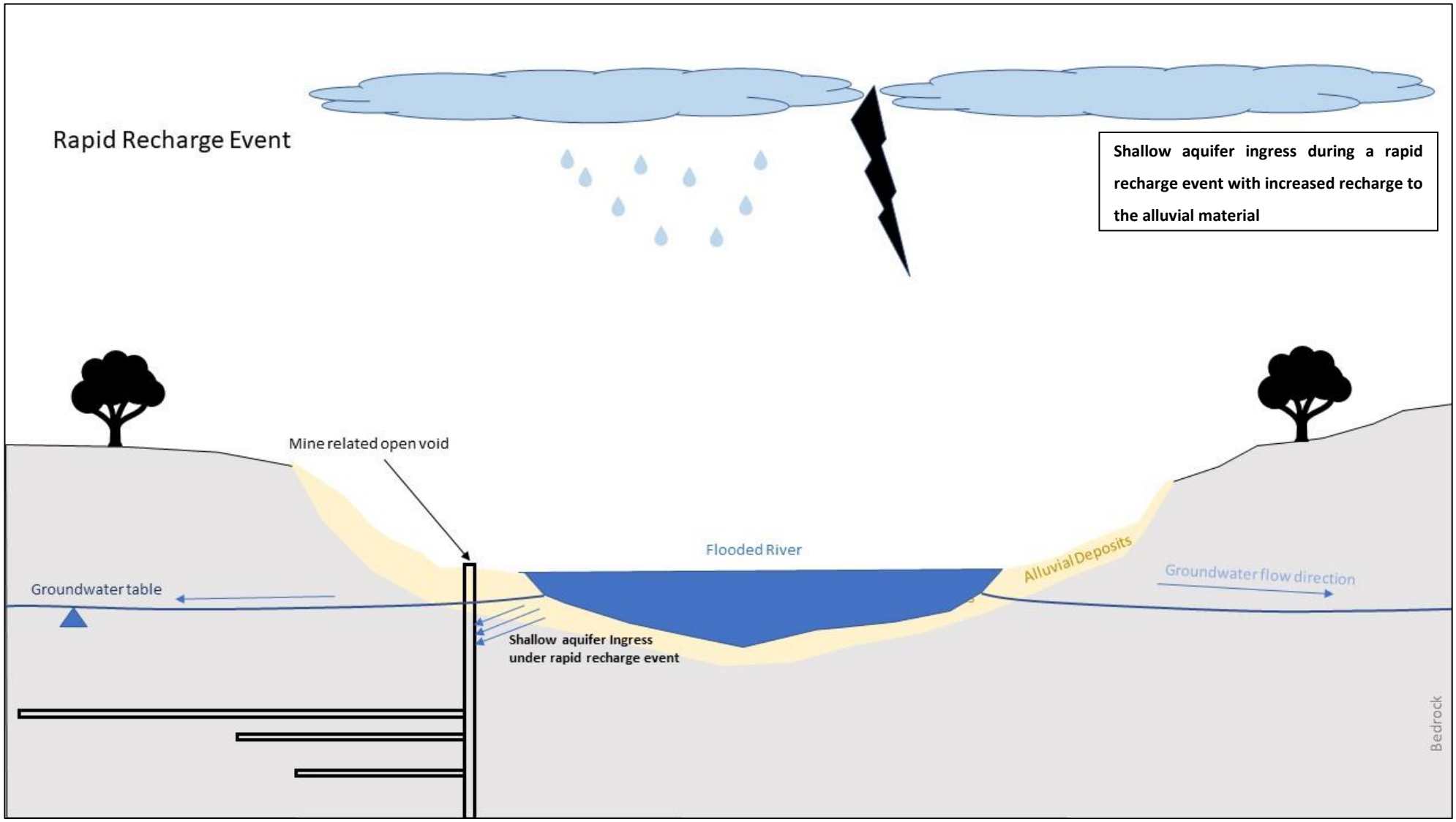

Figure 1-2 Conceptual illustration of the numerical model objective during a flooding event

1.1 Research question/hypothesis.

The interaction between groundwater and surface water as mentioned is an uncertain science in terms of quantifying the actual water inflow rates and volumes. The components that are associated with the interaction processes can be described scientifically and represented with some quantification criteria through numerical modelling, however the range of uncertainties becomes larger as the study area increases due to data insufficiencies and poor quality of data. One component in particular, is the interaction of shallow aquifer water ingress through direct media such as open voids into the deeper groundwater systems and the quantification of the water volumes and rates.

The research question can thus be formulated: Is it possible to quantify accurately the water volumes and rates associated with shallow aquifer water ingress through open mine-related voids leading to the mine workings that directly link with the underground aquifer systems; and can numerical modelling be applied as a tool to model the ingress processes considering both the shallow aquifer and associated water body during rapid recharge events.

1.2 Research aims and objectives.

The aim of the research is to investigate the potential additional volumes of water that could enter open mine voids through shallow aquifer recharge during a high rainfall event where the shallow aquifer recharge gets amplified by flooding rivers and streams.

The objectives to achieve the aims is to implement predictive numerical groundwater modelling as a tool to simulate the inflows into old mine voids situated inside or nearby the shallow aquifer systems during high rainfall events with associated rapid recharge to shallow aquifer systems.

1.3 Research methodology.

This dissertation focused on two main aspects to look at how numerical modelling can aid in quantifying the ingress of water through mine related open voids during rapid recharge events. The first section focuses mainly on the review of literature and research of available data and information related to shallow aquifer ingress through open voids, as well as groundwater studies that has been conducted for the Witwatersrand Gold Fields.

The second section will focus on a case study conducted for the East Rand basin which provides the ideal setting to achieve the objectives of this study. The main objective of the case study is to construct and represent a numerical groundwater model that will be used to simulate a scenario where rapid recharge to the shallow aquifers in the East Rand basin and water ingress during

these rapid recharge events into mine related open voids can be measured and quantified. Site specific data will be required to construct and represent the numerical model and further research and data collection will be conducted to fulfil this requirement.

The following spatial and site-specific data will be gathered during the case study assessment:

- Topographical data and surface drainage network to evaluate the regional topography and surface drainage regime from which a sub-catchment area can be defined that will serve as the model boundary.
- Mapped geology and geological information such a geological structure that forms part of the sub catchment area which will represent the different aquifer systems incorporated into the model boundary at surface and to depth.
- Wetland areas which together with the alluvial deposits along the river systems associates with the shallow aquifer systems that forms the major aquifers that will be assessed during the modelling scenario.
- Rainfall records from weather stations within the sub catchment area that will indicate the flooding events that forms the main driver for the rapid recharge events that will be modelled.
- Groundwater chemistry and more specific Chloride concentrations to determine the recharge ranges that can be applied to the different aquifer systems included in the numerical model.
- Measured groundwater levels within the sub catchment which will form one of the main input parameters to represent the numerical model and illustrate the current state aquifer status of the sub catchment.
- Hydraulic parameters such as hydraulic conductivities that will be applied to the different aquifer systems and adjusted to represent the numerical model.
- The current main mining activities to evaluate the potential dewatering from the different aquifer systems as well as the historic mining footprint and mapped mine related open voids which will be used as the input locations from which the rapid recharge and associated water ingress will be recorded and measured during the scenario simulation.

The data and information gathered as part of the research process will be used to formulate a conceptual model that will describe the purpose of the numerical model and the problem statement that will be addressed by the numerical groundwater model. The conceptual model will also describe the important input parameters and how these will relate and support the

numerical model construction, representation and eventually the scenario simulation to formulate the answers needed to fulfil the research question and hypothesis.

The rainfall data will be evaluated to select a specific period of actual rainfall records that indicates possible flooding events which will be incorporated into the representative numerical model. The scenario simulation will then simulate the rapid recharge applied to the shallow aquifer systems over these recharge events and the simulated inflow rates into the mine related open voids will be recorded and presented as graphs to show how numerical groundwater modelling can be used to quantify water ingress into open voids.

The results from the scenario simulation will be discussed and important observations from the scenario simulation will be noted which could aid in future groundwater assessments related to mine impacted areas. The final stages of the dissertation will include some recommendations derived from the discussion of the literature study and model results.

Chapter 2 Literature review

The first part of the literature review includes studies that focused on the interaction between surface water and groundwater systems, as well as numerical modelling methods that can be applied to better explain and describe the flow dynamics between the two water systems. The second part of the literature review looks at studies conducted for the Witwatersrand Gold Fields in terms of water volumes and rates entering the aquifer systems, and how much water can originate from surface water bodies.

2.1 Modelling the interaction between surface and groundwater systems

The interaction between surface water and groundwater systems has been a long-debated subject from both hydrology and geohydrology disciplines (Tanner, 2015) and (Midgley et al., 1994). The main issue with understanding the interaction between surface water and groundwater systems is the uncertainty of how much water can be contributed by each of these systems and the connection between surface stream flows, shallow purged aquifer systems associated with steams and riverbeds and the connection with deeper hard rock aquifer systems (DWAF, 2006). The typical rationale is that water enters the catchment system through precipitation and drains via streams, rivers and lakes where it then enters the subsurface aquifer systems through recharge (Parsons, 2004). Aquifer systems can also transmit water to surface water bodies through springs, decanting points and as baseflow components from the shallow perched aquifer systems.

The US Geological Survey (Winter et al., 1998) describes the different interactions between surface and groundwater systems in detail with specific reference to how the hydrological cycle and different components (rivers, streams, and lakes) can interact with groundwater systems and aquifers. Although the general understanding of how the two water systems can interact indicates limited confidence in the quantification of actual volumes and rates (Wagener et al., 2001) and (Wagener, 2005).

Numerical modelling could be applied to evaluate the rates and volumes associated with the different components comprising these water systems and their interaction (FEFLOW, 2022). Different modelling approaches exists that can be considered when modelling the interactions and the choice of method is dictated by the different process associated with the groundwater - surface water interactions (Pathare, 2017) and (Baily, 2023). These processes largely depend on

the influences that each of the water systems have on each other (Table 2-1 and Figure 2-1). The groundwater driven processes can be seen when water is abstracted from an aquifer system that relates to a surface water body through a media such as alluvial material or weathered rock material. Surface water driven processes can be in the form of overland flow such as rainfall flowing on surface and through flow where water flows through a shallow aquifer system. Water can also be stored in riverbeds as they widen and deepens as river flow attenuation.

The storage capacity can also be increased during flooding events. Water can also be stored in off stream water bodies such as dams or lakes creating seepage to the shallow aquifer systems that surrounds them. During flooding events a differential gradient can be created as the river rises into its floodplain and recharging the shallow aquifer system as bank storage and over bank flooding can occur when the aquifer systems are fully saturated and exceeds the storage capacity of surface water bodies. These processes often need measurable data during wet and dry conditions and are typically challenging to quantify on a regional scale.

Table 2-1 Ground water - Surface water interaction processes

Ground Water Driven Processes	Surface Water Driven Processes
Stream Depletion: Abstraction of stream water via an aquifer system that is connected to a surface water body due to a fully saturated media	**Overland flow and through flow**: Overland flow or sheet flow incorporates surface flow during rainfall events whereas through flow describes shallow sub-surface flow along the riverbeds or shallow perched aquifer systems.
	River Flow Attenuation: Storage effects created by rivers affect peak flows during rainfall events. The attenuation can be caused by the widening or deepening of the river base
	In-stream Storages and Reservoir Operation: Events that increase the in-stream storage capacity during flooding events
	Off-Stream Storages: Dams or lakes that can contribute to seepage to the aquifer systems
	Bank Storage: During a flooding event a differential gradient can exist between the rising river level and floodplain high conductive shallow aquifers system causing water to move into the shallow perched aquifer system, as the river water level drops then water gets released back into the river over time
	Over-Bank Flooding: Groundwater recharge and soil water exceeds the surface water storage capacity during heavy rainfall events

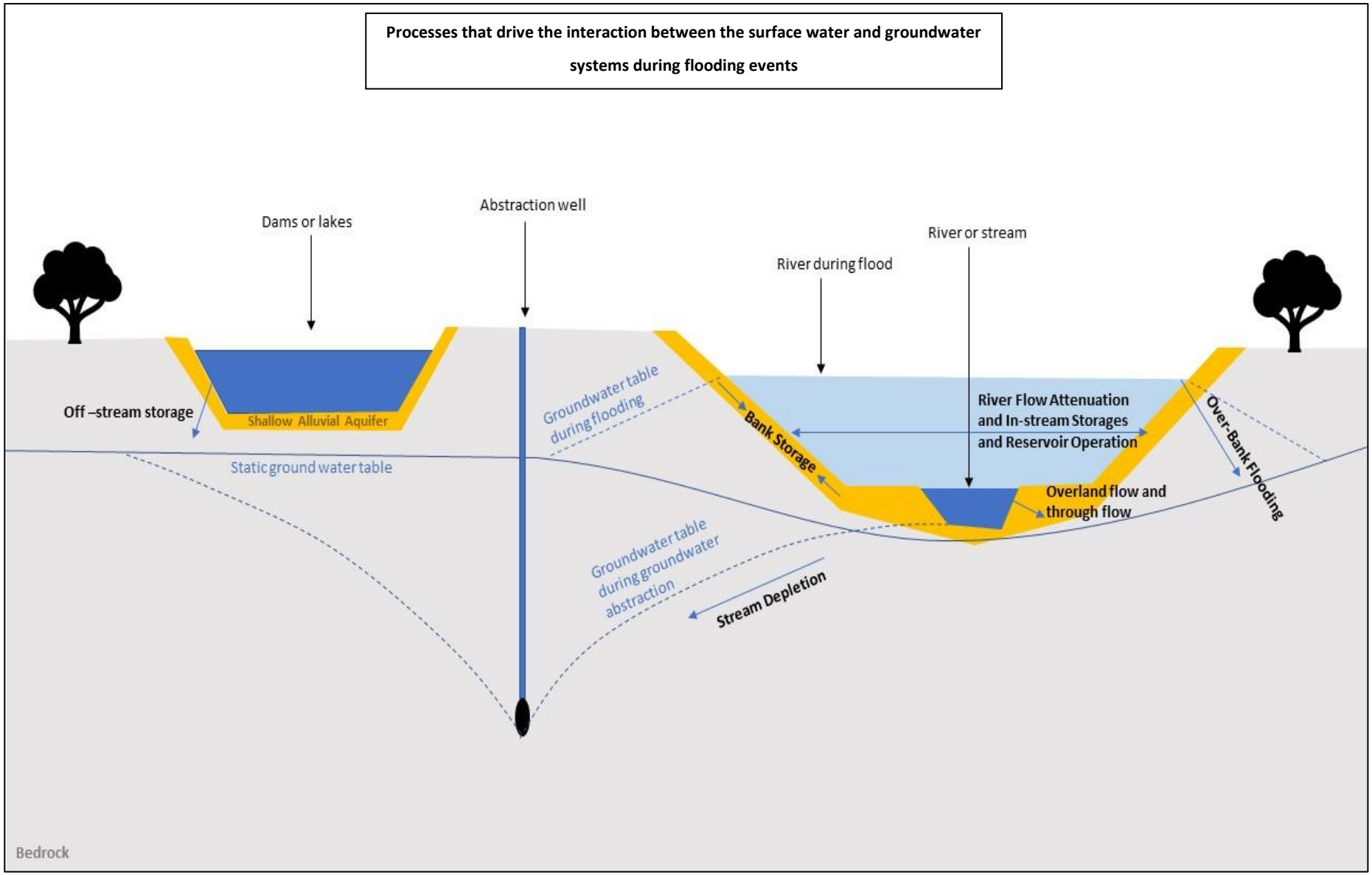

Figure 2-1 Conceptual illustration of the groundwater – surface water interaction processes.

A study conducted by the Water Research Commission (Tanner, 2015) describes the uncertainties related to quantifying the interaction process by looking at regional catchment assessments as part of groundwater reserves determinations in South Africa. The outcome of the study indicated that the lack of field specific data as well as the poor quality of the data that exists from a model input perspective proves to be a major uncertainty to accurately model the interaction between the water systems on a regional scale. The report (Tanner, 2015) also clearly states that the overall hydrology for both surface and sub-surface is an uncertain science due to its variability and non-stationary nature. The lack of accurate data and information are also expressed in the Groundwater Reserve Determination study conducted by (Hobbs et al., 2013) for the Upper Vaal water management area. Despite the limitations numerical modelling might still be efficient to fill gaps where insufficient data and information is not available

2.2 Surface water/groundwater modelling software packages

To date, several software packages is available to conduct numerical water modelling with the specific purpose to model either groundwater or surface water flow. More recent numerical modelling packages were developed to model the interaction between the two media. Numerical software packages that could be applied to model the interactions between surface water and groundwater systems include MIKE SHE integrated numerical modelling software developed by DHI (MIKE, 2022). The MIKE software packages have a wide range of surface water applications as well as the groundwater software package FEFLOW. FEFLOW is a numerical modelling software programme that makes use of the finite element approximation method. The newest version of FEFLOW (7.5) presents the opportunity to link with MIKE SHE through the application of a DFS2 file that includes input such as recharge for improved modelling of groundwater resource management assessments. The integration also includes water quality assessments (mass and concentrations) that can be integrated through the DFS2 file input.

With the release of FEFLOW 7.5 another application FEFLOW piMIKE 1D was also introduced. This application replaced the IfmMIKE11 package and provides a solution to couple with the FEFLOW Fluid Transfer Boundary Condition and a river network file from MIKE 1D (FEFLOW, 2022). FEFLOW 7.5 has also introduced an application that employs the Richards equation (Bonan, 2019) which combines Darcy's law (Whitaker, 1986) with the basic principles of water conservation to estimate the movement of water in soil or the unsaturated zone. This application cloud also be helpful to model the periodic flow through unsaturated media during recharge events however

input data to this application requires additional field measurements and testing for quantification purposes.

Additional modelling programmes that make use of the finite difference approximation method could also be considered such as GSFLOW. Numerical modelling software developed by the US Geological Survey (GSFLOW) is an integrated software package that links the two software packages PRMS-V (Precipitation-Runoff Modelling System) and MODFLOW-2005/NWT (Modular Groundwater Flow Model). GSFLOW is used to numerically model the flow in catchment systems and includes surface flow, subsurface saturated and unsaturated flow and flow within streams and lakes (USGS, 2021).

The software packages and applications available to numerically model the different aquifer systems and interactions between the aquifer systems does present opportunities to quantify ingress rates and volumes however limited information exists that relates to approaches and studies conducted to quantify ingress rates and volumes through open voids. This observation also limits the evaluation on the accuracy and confidence of the recorded inflow rates and volumes. The results usually are presented as ranges which results in further studies having to rely on increased assumptions in the comparison of data and information.

2.3 Groundwater and surface water interaction in the Witwatersrand Gold Fields

Numerous studies have been conducted to understand the water systems, both surface and groundwater, related in the Witwatersrand Gold Fields (DWAF, 2004). A conceptual map (Figure 2-2) taken from (Winde, 2015) of the Witwatersrand Goldfields indicates the major river systems and dams that are associated with the goldfields area on a regional scale with all the major tributaries leading to the Vaal River System (Hobbs et al., 2013). These water bodies have aquifer systems associated with the alluvial deposits that forms the shallow aquifer systems and may intersect the old mine open voids through which water ingress can occur during flooding events. The understanding of how surface water and groundwater interacts could determine the impacts that increased volumes and water quality can have on both water systems (Waal, 2013). Furthermore, the complexity due to the dolomitic (karstic) aquifer systems underlying parts of the gold fields area may be connected to the historic mining infrastructure that left large amount of open mine related voids (shafts and open fissures) scattered over the shallow resource areas (Marè, 2007).

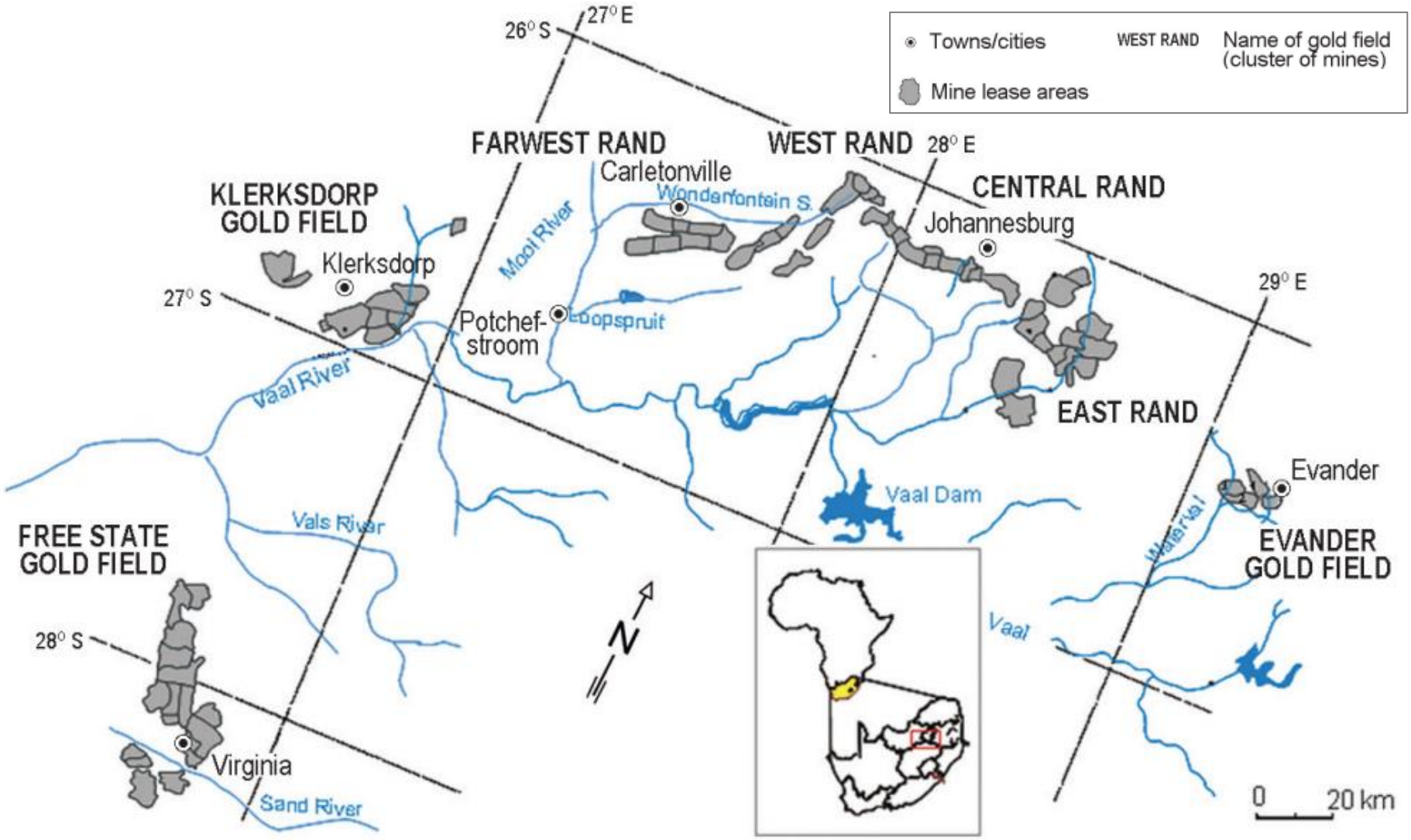

Figure 2-2 Major River systems over the Witwatersrand Goldfields area taken from (Winde, 2015)

The network of historic mine workings referred to as “basins” has a detrimental influence on increased water volumes into the groundwater systems due to the flooding of the decommissioned open mine voids (Coetzee, 2010). There are several ways that surface water can enter the mine workings (Coetzee, 2010):

- Direct rainfall that enters directly through open mine workings.
- Groundwater recharge with associated seepage due to ground disturbances (depressions and subsidence) from the mine workings.
- Surface streams that losses water directly to the open mine voids due to the shallow aquifer systems associated with the streams being close to, or above the shallow mine workings.
- Surface mine workings that directly connects with the underground open voids which creates pathways for water to seep directly into the underground mine voids.
- Mine residue areas (Tailings facilities and Waste rock dumps) causing increased fluxes to the underground mine workings due to increased recharge potential of the waste material.
- Damaged water infrastructure like water supply pipelines, sewerage networks, and storm water reticulation systems that cross the old mine workings and voids can contribute to seepage into the open voids.
- Isotope analysis indicated that groundwater gets rapidly recharged due to possible open voids contributing to surface water ingress and subsequently flows to the shallow aquifer systems.

A study conducted by Itasca Africa (Duthe, 2020) investigated the possible volumes and rates of shallow aquifer water that can ingress into old mine open shafts and mapped open void positions in the Modderfontein area of the East Rand Basin. The potential ingress locations were modelled numerically based on their location in terms of proximity to perennial streams and associated flood plain areas as well as general topography during a flooding event. The study outcome indicated that numerical modelling might be possible to quantify surface water ingress however more site-specific data and information is required to increase the confidence of the results.

The contribution that rapid surface water recharge to the shallow aquifer systems has during flooding events and how open mine voids contribute to overall inflows during such flooding events where the open mine voids are situated near river systems and inside shallow aquifer systems during such flooding events could provide better quantification of volumes entering the

deeper aquifer systems that's connected to the historic workings. The rapid recharge to the shallow aquifer systems during heavy rainfall events and subsequent connection with deeper aquifer systems could play a major role in the dilution of flooded mines as the main driver for Acid Mine Drainage (AMD) at downgradient decanting positions along the major Rivers and streams (McCarthy et al., 2010)

The quantification of water ingress through mine related open voids and rates and volumes that could come from the shallow aquifer recharge may also assist to evaluate the effect on deeper more significant aquifer systems, such as the Malmani dolomite aquifers in terms of stability and where mine-related open voids intersect this dolomite at depth. This applies not just during rapid recharge events, but also during normal recharge according to time dependant recharge applied as per actual historic rainfall records. Studies conducted by (Dippenaar et al., 2018) and , (Danél et al., 2021)and (Winde, 2015) raised concerns on the ingress and decanting potential of the dolomite and karstic aquifer systems in the Wits goldfields and how this can affect the:

1. Stability of the ground conditions with the formation of sinkholes through ingress mechanisms such as rainfall events into open voids and leaking pipelines forming dolines (Dippenaar, 2018). The event densities and occurrence of sinkholes are displayed in Figure 2-3 which shows the large contribution that water ingress makes to sinkhole creation in the west rand alone.
2. Water quality during decanting as groundwater levels rise due to consecutive recharge events and elevated water ingress caused by open voids leading to the mine void. Another aspect to consider is the flooding and re-watering of the mine void once mining stops. The estimated time for the mine voids and dolomitic compartments to fill once mining operations stops ranged between 15 and 30 years (Schrader, 2014)based on numerical modelling methods and estimates, however this period may be less because of the added ingress potential from open mine voids that links the deeper underground aquifer systems to shallow aquifer systems. The decanting potential affects the surface water resources and systems as groundwater gets exposed to atmospheric conditions causing reactive processes, forming acid mine drainage (Van Tonder 2021; Eckart 2016).

The possibility exists that by means of numerical groundwater modelling, the percentages of ingress through open voids that contributes to the overall ingress volumes can be determined and more specifically which open voids can be identified as possible locations that can be capped to minimise the ingress potential.

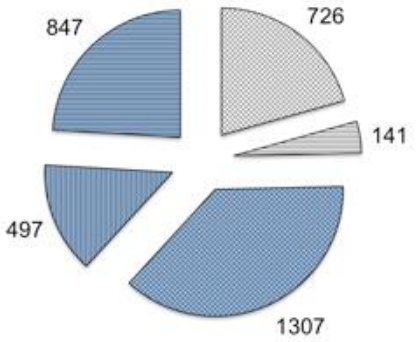

(a) Sinkhole event densities for dewatered and non-dewatered (ingress) areas in Gauteng (blue-shaded – ingress scenario).

Figure 2-3 Sinkhole event densities identified in Gauteng and associated causes as dewatering or ingress (Taken from Dippenaar, 2018)

The literature review looked in detail at the complex interplay between surface water and groundwater systems, particularly within the Witwatersrand Gold Fields. The review indicated the challenges in quantifying the volumes and inflow rates from ingress mechanisms, and their effects on subsurface aquifers, highlighting the uncertainties related to limited site-specific data and the variable as well as dynamic conditions that groundwater systems can present. The integration of numerical modelling methods, and applications presented by software packages like MIKE SHE, FEFLOW, and GSFLOW, offers opportunities to better understand and quantify these interactions.

Studies that focused on the Witwatersrand Gold Fields indicated the significant influences of historical mining infrastructure, such as open voids and shafts, on surface water ingress into different aquifers, and how ingress can impact on stability, water quality, and the potential for acid mine drainage. Additionally, the literature review indicated the complexities of surface water and groundwater interactions and dynamics that supports the need for more site-specific data and refined modelling techniques to confidently address the questions surrounding the interaction and related quantification of water ingress and its effects on both water systems.

Chapter 3 Site characterisation and conceptualisation

The justification of conducting this research can aid in studies relating to water management programs and investigations that incorporates areas with open mine-related voids such as old mine workings and karstic aquifer systems where these voids are exposed to surface. The Witwatersrand have numerous issues concerning acid mine drainage and decanting potential at down-gradient rivers and streams and the increased recharge to the shallow aquifer systems and subsequent deeper aquifer systems through the open mine voids could further influence the potential chemical makeup of the associated groundwater systems. By quantifying the volumes and rates associated with shallow aquifer water ingress during dry and wet periods or rapid recharge events, and the effects that the water ingress has on the sustainability of the aquifer systems, could aid in decision making process on whether to seal, divert or manage shallow aquifer recharge and water ingress into the mine-related open voids.

The quantification of surface water ingress through the old mine workings in the Witwatersrand Gold Fields could be considered due to the effect that the seasonal flooding of the old mine workings has on current mining and dewatering operations as well as management in preparation of future mining activities.

The Witwatersrand Gold Fields extends regionally over a large area and is mostly contained in the Witwatersrand Geological Supergroup (Tucker et al., 2016) (Figure 3-1). The goldfields can be divided into nine known resource areas namely:

- The Evander Goldfields in the north eats of the Wits basin
- The East Rand Goldfields just east of Benoni
- The Central Rand Goldfields just north of Johannesburg
- The West Rand Goldfields, between Klerksdorp and Randfontein
- South Deep Goldfields just southwest of Westonaria
- The Western Areas located in and around Westonaria.
- Carletonville Goldfield located just south of Carletonville.
- The Klerksdorp Goldfields located southeast of Klerksdorp.
- The Welkom Goldfields located in areas around Welkom.

The goldfields originate from Evander in the northeast, extending northwards towards Johannesburg and southwest ward with the most southern resource at Welkom. The Witwatersrand Geological Supergroup which hosts most of the known Wits gold deposits covers an area of approximately 48 000 km².

As mentioned in section 2, a numerical groundwater model could be employed in an attempt to model the ingress potential of shallow aquifer systems into mine related open voids during rapid recharge events. Due to the large area that the Wits goldfields cover, and the amount of input needed to develop such a large numerical groundwater model it was decided to only look at the East Rand Goldfields as a historic mining area to simulate and quantify the ingress rates and volumes from shallow aquifers to the open mine voids.

The East Rand Goldfields covers an area of approximately 530 km² and extends from Daveyton from its northern boundary to Nigel at its southern boundary. The eastern boundary includes Daggafontein, and the western boundary includes parts of Van Dyk Park, Dal Park and Van Eick Park. The East Rand Goldfields and the mining footprint contained within is indicated in Figure 3-2.

The East Rand Goldfields is unique in the sense that it is geologically located in a basin (Waal, 2013) hence referred to as the East Rand Basin, and it is mostly contained within two quaternary catchment areas (C21D and C21E) which implies that recharge into the groundwater systems would mostly be from these catchment areas and the geological setting would support a confined regional aquifer system (Waal, 2013).

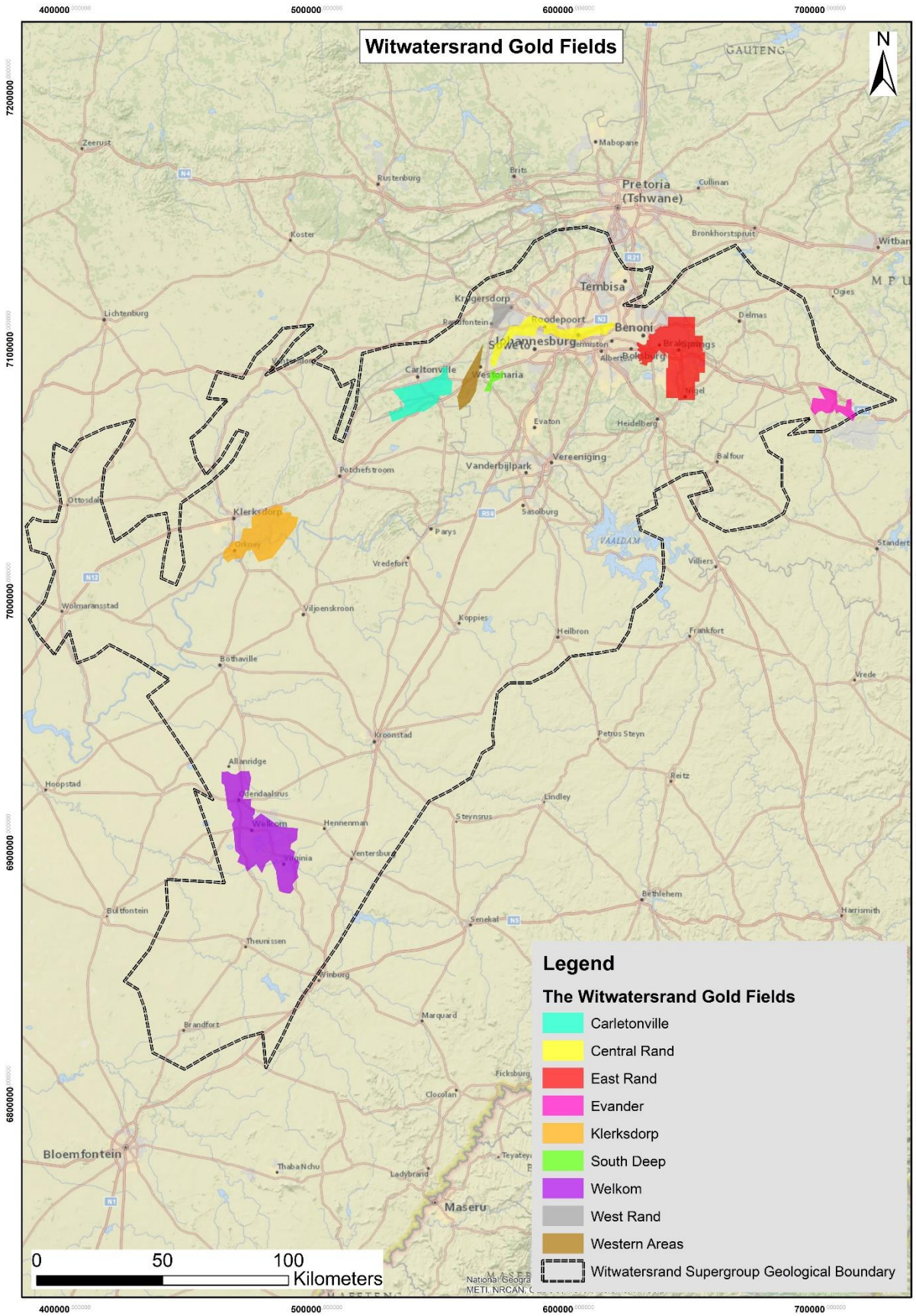

Figure 3-1 The Witwatersrand Gold Fields and the East Rand Basin Boundaries (Taken from Tucker, 2016)

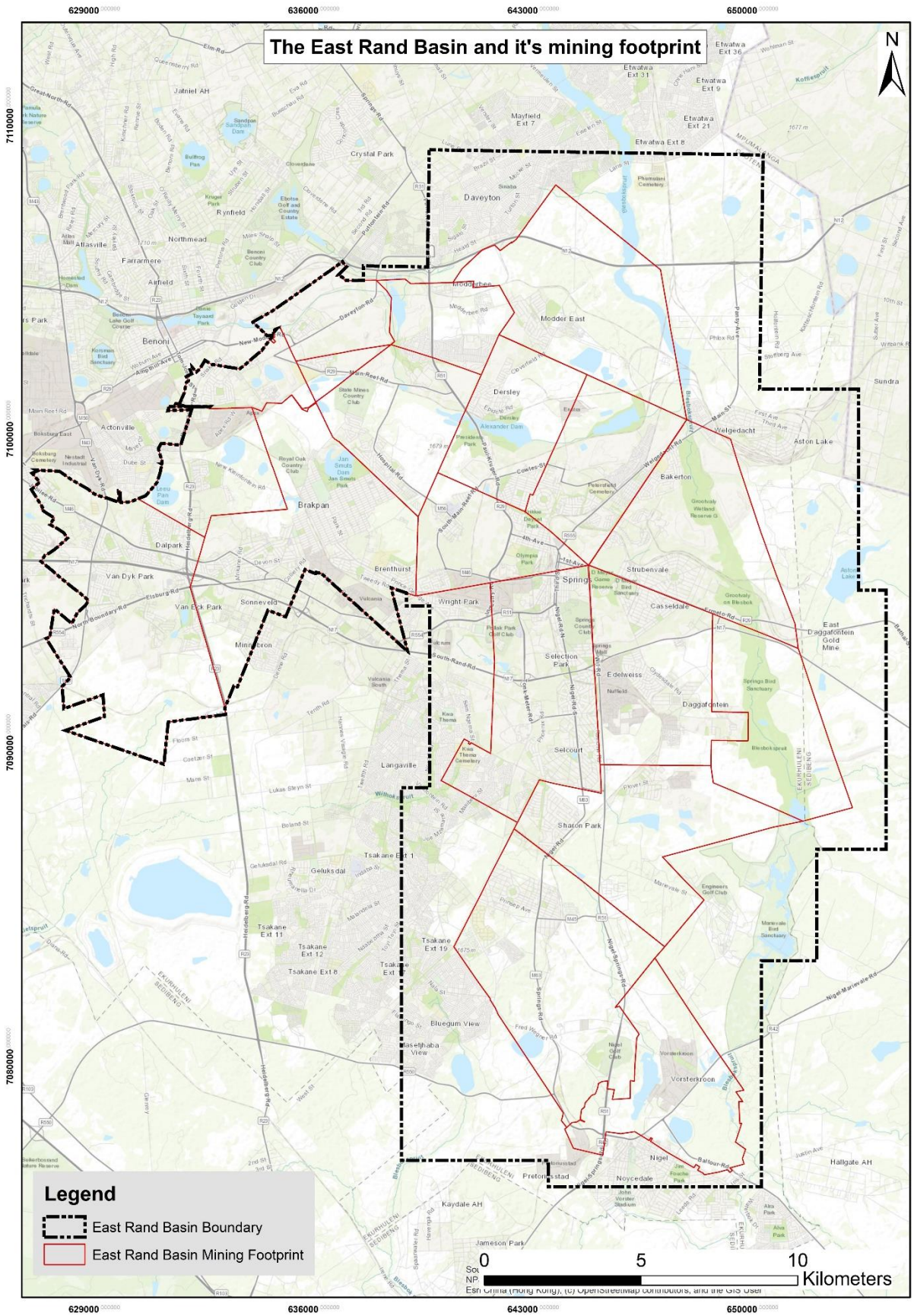

Figure 3-2 The East Rand Basin and mapped Mining Footprint (Taken from CGS, 2018)

3.1 Data review and acquisition

The development of the conceptual model as well as the numerical groundwater model requires spatial as well as site specific data and information. The data required can be divided into different types that will serve different purposes in developing the groundwater model. The different types of data will be integrated in the model during the construction and representation phase. The model input data and sources are summarised in Table 3-1 and described in the sections that follows.

Table 3-1 Model input data and sources

Data	Data source
Topographical data	United States Geological Survey (USGS) Shuttle Radar Topography Mission (SRTM) data developed and issued by the United States National Geospatial-Intelligence Agency (NGA) 30m spacing
Geology data	Council for Geoscience (CGS) of South Africa in digital format for geological map 1:250 000 Geological Map 2628 East Rand, 1986
Wetland areas	Aquifer Dependant Ecosystems (ADE) spatial files index as well as the National Landcover database supplied by the department of forestry of South Africa. Additional wetland areas were delineated from satellite imagery supplied by Arc Map (Esri) as part of the base maps function
Rainfall data	Water Resources of South Africa, 2012 Study (WR2012) internet data base which included 4 rainfall stations that falls within the sub catchment area
Groundwater levels	Local groundwater levels: Supplied by the Department of Water Affairs (DWA), Geodata base for Quaternary Catchments C21D and C21E. Project studies conducted by (Scholtz, 2013), (Koekemoer, 2020) Regional groundwater levels: Data gathered form research papers (Botha, 2018), (Abiye, 2011)
Hydrochemistry: Cl Concentrations and Recharge	Local: Supplied by the Department of Water Affairs (DWA), Geodata base for Quaternary Catchments C21D and C21E. Project studies conducted by (Scholtz, 2013), (Koekemoer, 2020) Regional groundwater levels: Data gathered form research papers (Botha, 2018), (Abiye, 2011) Recharge estimates determined from information supplied by (van Wyk et al., 2011)
Aquifer parameters	Gathered from project reports that included aquifer tests (Koekemoer, 2020) (Scholtz, 2013)
Mine dewatering (Grootvlei mine)	Gathered from "Water management strategies to reduce long term liabilities at Grootvlei gold mine "Irene Lea, Chris Waygood, Andrew Duthie (2001) 8th International Congress on Mine Water & the Environment, Johannesburg, South Africa.
Historic Mine footprint and open voids	Supplied in digital format by Council for Geoscience (CGS) of South Africa

3.1.1 Spatial data

Spatial data will be required to conduct the numerical modelling according to scale that would represent the real-world both in dimension and distances. The spatial data will be used to conduct the following:

- Selection of a model domain or project area according to a surface drainage catchment area on a regional scale.
- Topographical data that together with the surface water drainage patterns will ensure accuracy in selecting the numerical model domain and boundary.
- Geological data that can be plotted and subdivided into the different geological units that will represent the different aquifer systems.
- The surface drainages that are included in the sub catchment area and the alluvial deposits that associates with the drainage and flood boundaries.
- Wetland areas that also holds the potential for shallow perched aquifer systems and associates with the low-lying areas along the rivers and streams.

3.1.1.1 Topography and surface drainage contained in the quaternary catchments

The quaternary catchments as well as the main river systems for South Africa were gathered in digital format as shapefiles form the Department of Water Affairs (DWA) website data base network (DWAF, 2012). The tributaries leading into the main river systems were delineated from Satellite imagery provided as base maps in Arc Map (Esri) and from more detailed satellite imagery in Google Earth. The topographical data set was developed from the United States Geological Survey (USGS) Shuttle Radar Topography Mission (SRTM) data base, developed and issued by the United States National Geospatial-Intelligence Agency (NGA). The data is available in raster format from the internet (Watkins, n.d.) and reworked into a point file format at 30m spacing across the East Rand Basin research area.

The surface drainage, quaternary catchments and topographical data were analysed in Arc Map (Esri) which can be observed in Figure 3-3.

The quaternary catchments contain most of the Eats Rand Basin and includes C21D and C21E. These two catchments were considered to form a sub catchment area which consists of the Blesbokspruit surface drainage that drains the sub catchment from north to south through the two quaternary catchments. The cumulative surface area of the two quaternary catchments is approximately 1073 km².

The East Rand Basin is mainly drained by the Blesbokspruit which has its origins in the Daveyton in the north as well as from secondary drainages flowing from the northwest in the Brakpan area that joins the main Blesbokspruit stream in the central basin close to Welgedacht (Figure 3-2). The Blesbokspruit extends further south and exists the sub catchment near Nigel where it drains into the quaternary catchment C21F further southwards. The smaller tributaries were delineated from satellite imagery which is contained within quaternary catchments C21D and C21E which flows towards the Blesbokspruit from the eastern and western sub catchment boundaries.

The surrounding quaternary catchments to the north of the East Rand Basin includes the Rietvlei and Hennops Rivers that drains quaternary catchment A21A, the Osspruit that drains quaternary catchment B20C and the Koffiespruit that drains quaternary catchment B20B. The Elsburgspruit and Rietspruit drains quaternary catchments C22B and C22C respectively and located east of the East Rand Basin. Quaternary catchments C21A and C21B are drained by the Boesmanspruit southeast of the East Rand Basin.

The topographical data were interpolated in Arc Map (Esri) with the Kriging interpolation method to build a regional raster file. This raster file was clipped to the sub catchment area to evaluate the topographical surface in relation to the surface drainage system included in the sub catchment. The topography indicates the elevation high areas along the northern, western and eastern boundaries from which the secondary drainages flow towards the low-lying central region of the Blesbokspruit. The lowest area (1538 mamsl) is at the exit point of the Blesbokspruit in the southwestern corner of the sub catchment and the highest points (1832 mamsl) is in the northwest section of the sub catchment which supports the general surface flow direction of the Blesbokspruit towards the south. The high ridge bend in the southeast of the sub catchment diverts the Blesbokspruit towards the west. The difference in elevation from the elevation high areas in the north west and southeast to the southwest of the sub catchment is approximately 294 m indicating a relatively low surface gradient sloping towards the south at 1m drop over approximately 140m if an average distance of 40 km from north to south through the sub catchment is considered. (Frimmel, 2019)

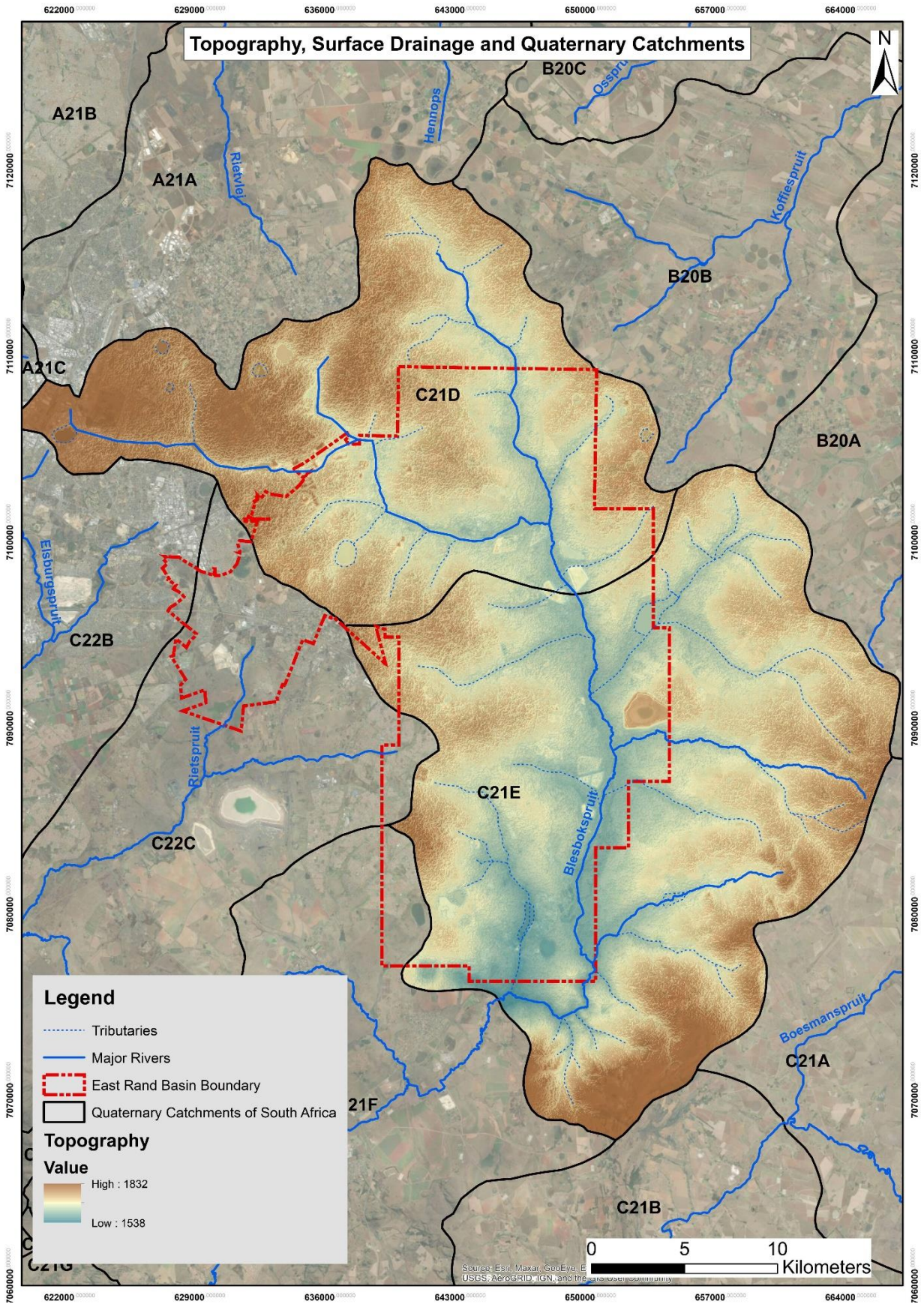

Figure 3-3 Topography and surface drainage of the sub-catchment area

3.1.1.2 Geology

Geological data were provided by the Council for Geoscience (CGS) of South Africa in digital format for 1:250 000 Geological Map 2628 East Rand, 1986. The geological description of the different rock types that are included in the sub catchment as well as the stratigraphic units that they belong to are summarised in Table 3-2. The mapped spatial geology was clipped to the sub catchment area in Arc GIS (Esri) which is indicated in Figure 3-4 and the geological descriptions are indicated in the geological key (Figure 3-5).

The geological description indicated in Table 3-2 provided major rock types that were grouped together and can be considered as major aquifer systems which will be essential in understanding how the groundwater will behave considering the aquifer properties that associates with the different aquifer systems. The different rock types will also play an important role during model construction in terms of lithological successions with depth and varying hydraulic conductivities associated with the deeper rock formations. The following major rock types that can be associated with aquifer units were identified.

- Alluvium which is considered as quaternary deposits and mostly associates with the surface drainage regions.
- Basaltic Lava (Volcanic Rock) as part of the Alberton formation. The basaltic lavas belong to the Klipriviersberg group that falls under the Ventersdorp Supergroup.
- Diabase indicated as an intrusive rock type.
- Diamictite (Sedimentary Rock) belonging to the Dwyka formation and forms part of the Ecca group. The Diamictite also forms part of the Karoo sequence.
- Dolerite dykes also indicated as intrusive rocks that intruded into the Karoo Supergroup.
- Dolomite and Limestone (Sedimentary Rock) belonging to the Malmani subgroup and forming part of the Chuniespoort group. This geology type also falls within the Transvaal sequence.
- Granite and Gneiss (Intrusive Rock) which mainly forms the basement rocks.
- Sandstone and shale (Sedimentary Rock) from the Vryheid formation and also falling under the Ecca group. The sandstone and shale formations form part of the Karoo sequence.
- Quartzite and Conglomerate (Sedimentary Rock) mostly belonging to the Central rand and Chuniespoort groups that falls under the Witwatersrand Supergroup.

- Quartzite and Shale (Sedimentary Rock) that forms part of the Central and West rand groups also belonging to the Witwatersrand Supergroup.

The geological stratigraphy indicates the rock types that falls within the sub catchment area however it is important to understand the succession of the different rock type and associated aquifers with depth (NWU, 2016). This geological succession will determine the numerical model construction and more specifically the layering with depth. The geological successions can be easier explained by referring to Figure 3-6 which indicates the geological units with depth conceptually in section as seen from west to east along a section of the Blesbokspruit. The conceptual model was taken from (Frimmel, 2019) that formed part of a hydrogeological study that focused on the decanting potential of flooded mine water over the East Rand Basin and indicates the orientation of a basin with the geological successions dipping towards the south from the north of the sub catchment.

The geological succession basically indicates the alluvial deposits that associates with the Blesbokspruit and smaller tributaries that drains the sub catchment area. The alluvium deposits form part, and is in some way contained, within the Sandstone and Shale formations that covers most of the sub catchment area and is indicated as the "Karoo" formation in Figure 3-6. The Malmani Dolomites are outcropping in some areas along the Blesbokspruit and dipping towards the south. The Dolomites are also indicated as saturated and may imply that this formation could play a major role in increased seepage and storage of groundwater throughout the sub catchment area making this a major aquifer system. The Diamictite formations forms the contact regions of the dolomite even where dolomite is not outcropping. This relationship can be seen in Figure 3-4 where the green Diamictite surrounds the Dolomite outcrop.

Below the Malmani Dolomites lays the Quartzite formations indicated in Figure 3-6 as the Turffontein, Johannesburg, Jeppestown, Government and Hospital hill subgroups in which most of the minable reefs exists.

The Granite and Gneiss formations forms the basement rocks below the Quartzite formations and protruding from the basement rock would be the intrusive formation like the Diabase, Dolerite Dykes and Basaltic Lavas mostly indicated as isolated features intruding through the Quartzites and Karoo sequences.

Table 3-2 Geological description and stratigraphy

Major Rock Type	Geological description	Legend label	Formation	Subgroup	Group	Super Group	Parent
Alluvium	Alluvium	Q-a					
Basaltic lava	Basaltic lava (porphyritic), tuff (amygdaloidal in places)	Ral	Alberton		Klipriviersberg	Ventersdorp	
	Tholeiitic basalt	Rk			Klipriviersberg	Ventersdorp	
	Lava (mainly andesite and quartz porphyry), shale, quartzite, conglomerate	Rpl			Platberg	Ventersdorp	
Diabase	Diabase	V-di					
Diamictite	Diamictite (polymictic clasts, set in a poorly sorted, fine-grained matrix) with varved shale, mudstone with drop stones and fluvioglacial gravel common in the north	C-Pd	Dwyka		Ecca		Karoo Sequence
Dolerite Dykes	Network of dolerite sills, sheets and dykes, mainly intrusive into the Karoo Supergroup	J-d					Karoo Dolerite
Dolomite and Limestone	Dolomite, subordinate chert, minor carbonaceous shale, limestone and quartzite	Vma		Malmani	Chuniespoort		Transvaal Sequence
Granite and Gneiss	Undifferentiated granite and gneiss	Z23					
Sandstone and Shale	Fine- to coarse-grained sandstone, shale, coal seams	Pv	Vryheid		Ecca		Karoo Sequence
Quartzite and Conglomerate	Quartzite, conglomerate	Rt		Turffontein	Central Rand	Witwatersrand	
	Quartzite, subordinate conglomerate and shale	Vbr	Black Reef		Chuniespoort		Transvaal Sequence
	Quartzite, subordinate conglomerate, shale and amygdaloidal lava	Rjo		Johannesburg	Central Rand	Witwatersrand	
Quartzite and Shale	Quartzite, shale, minor/subordinate conglomerate	Rg		Government	West Rand	Witwatersrand	
	Shale, quartzite, subordinate lava, minor conglomerate	Rj		Jeppestown	West Rand	Witwatersrand	
	Shale, subordinate quartzite	Rbo	Booysens		Central Rand	Witwatersrand	
	Subequal shale and quartzite, minor conglomerate	Rh		Hospital Hill	West Rand	Witwatersrand	
	Fine- to medium-grained quartzite, shale (in middle of formation)	Ror	Orange Groove		West Rand	Witwatersrand	

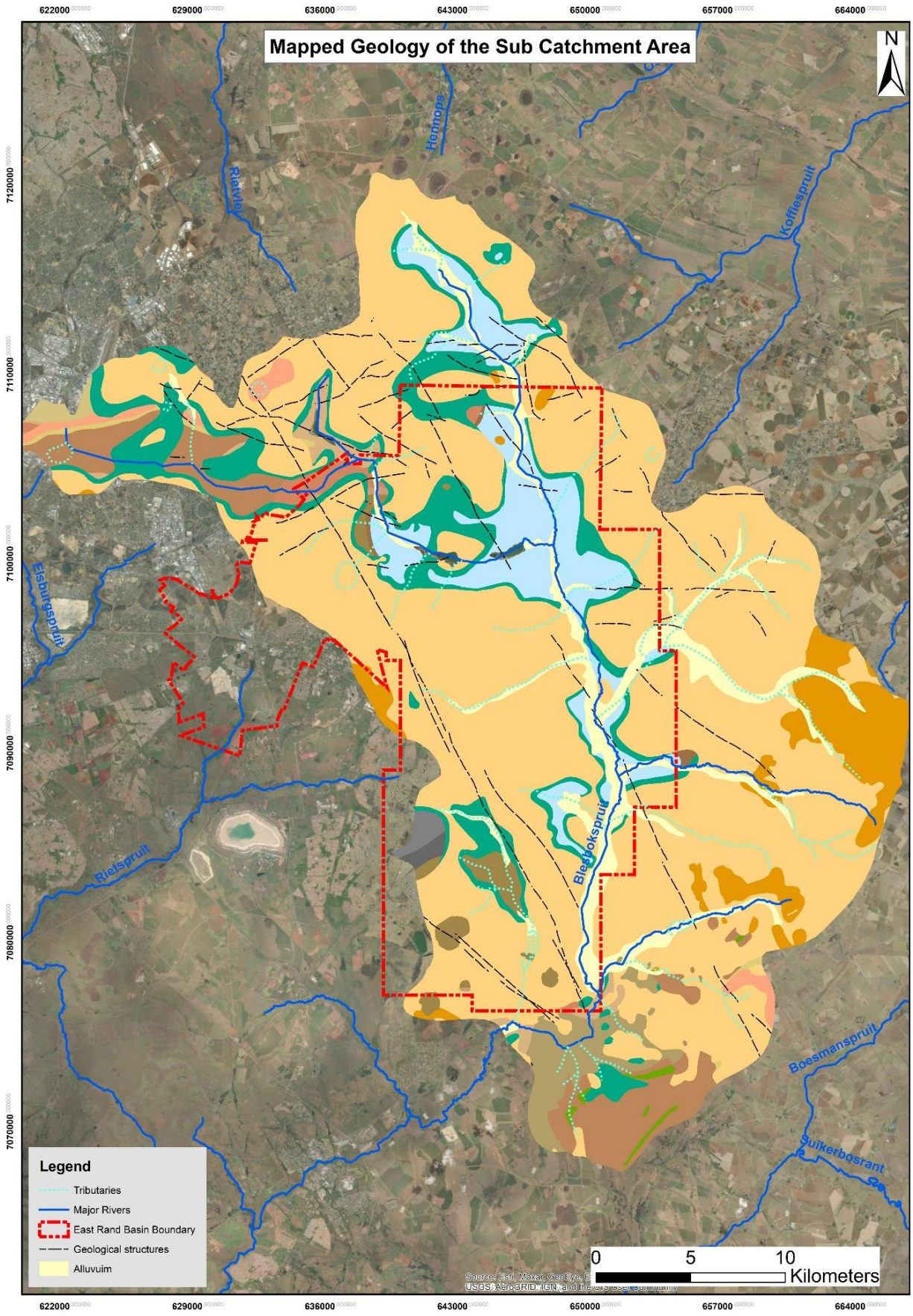

Figure 3-4 Mapped Geology of the East Rand Basin

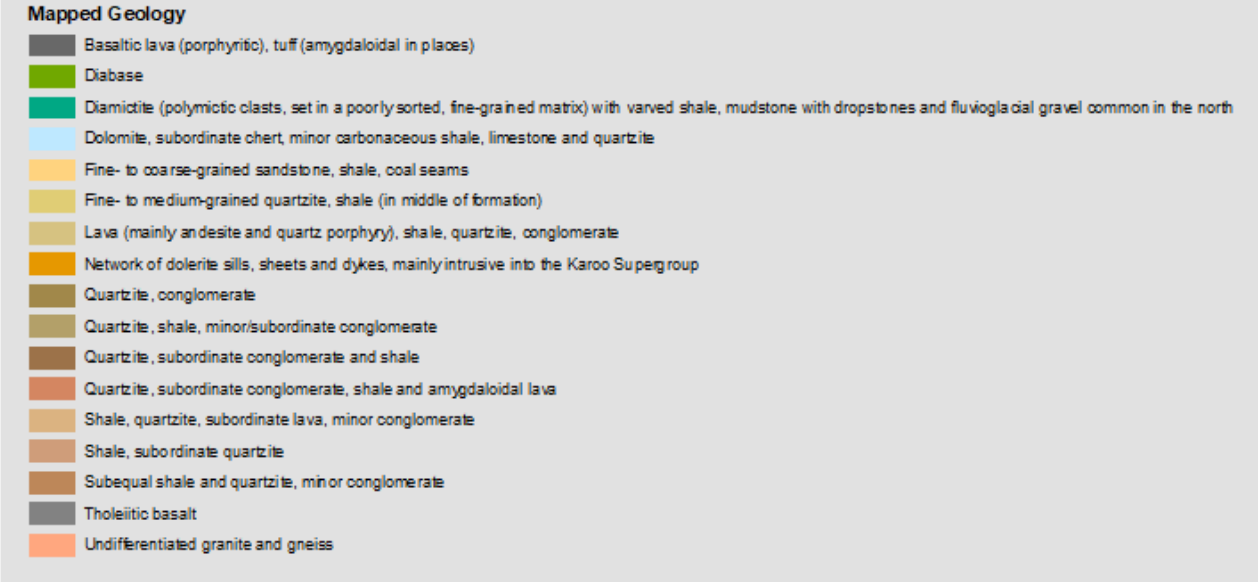

Figure 3-5 Geological key for Figure 3-4

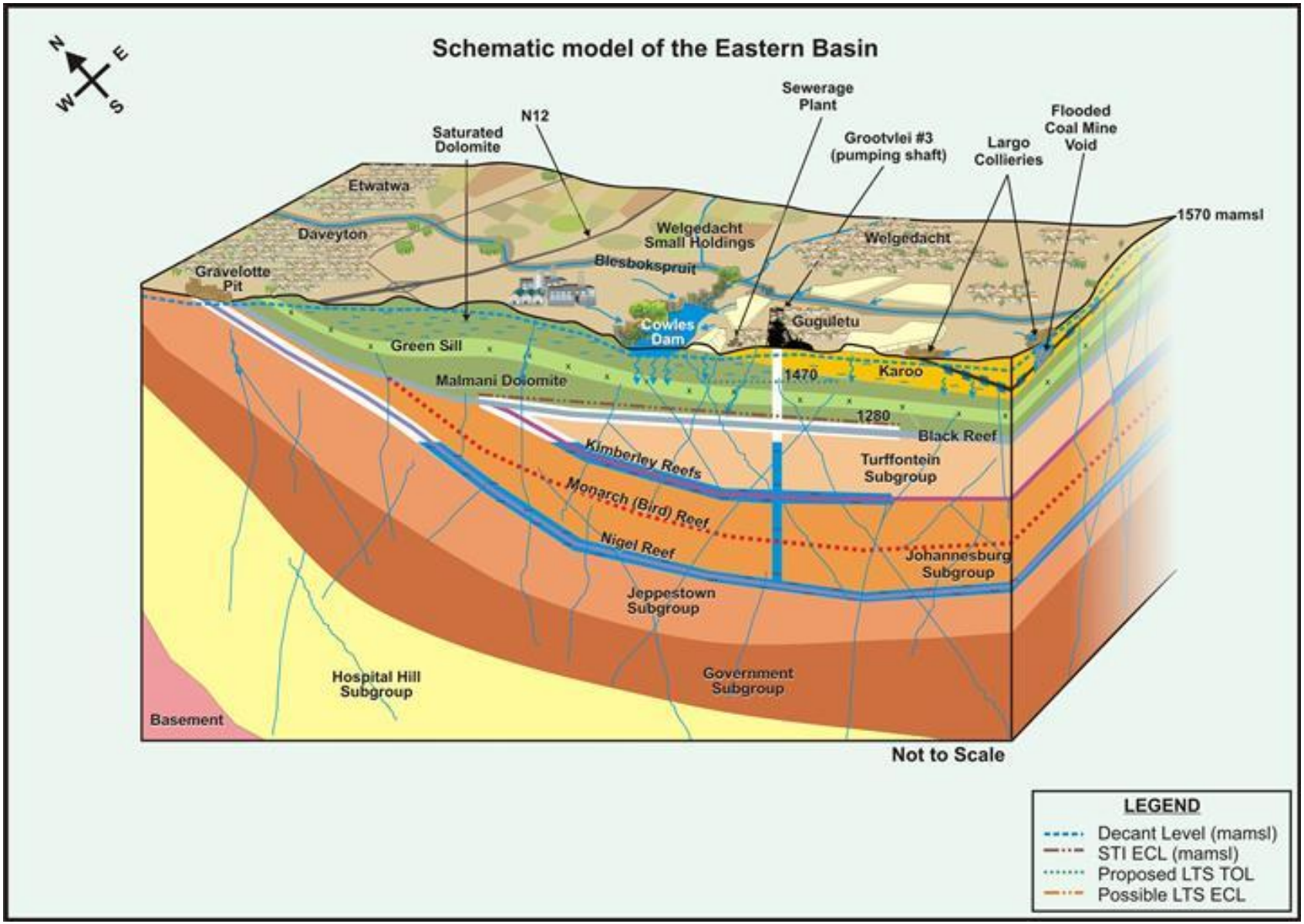

Figure 3-6 Schematic drawing of the sub surface geology of the East Rand Basin (Taken from Frimmel, 2019).

3.1.1.3 Wetland Areas

Spatial files for the wetland areas that fall within sub catchment was gathered from the Aquifer Dependant Ecosystems (ADE) spatial files index as well as the National Landcover database supplied by the department of forestry of South Africa. Additional wetland areas were delineated from satellite imagery supplied by Arc Map (Esri) as part of the base maps function. The three wetland spatial files were integrated to include one spatial file set for the wetland incorporated in the sub catchment.

The wetlands were overlain with the mapped and delineated alluvial deposits as described in section 3.1.1.2 to evaluate the relation that the alluvial deposits have with the wetland areas. The topography and surface drainage were added to indicate the relationship that the wetland areas and the alluvial deposits have with the low-lying topography and associated surface drainages. The spatial plot that indicates the relationship between the spatial files is shown in Figure 3-7.

The main wetland areas follow along the Blesbokspruit and a few tributaries in the northwest as well as in the east that joins the Blesbokspruit. There are isolated wetland areas scattered over the sub catchment that associates with lower depressions and forms pans. The main wetland areas clearly associate with the alluvium deposits that follows along the surface drainages. This observation would imply that the wetland areas and the alluvium deposits form the shallow and perished aquifer systems are mostly dependant on rainfall for recharge during the wet season.

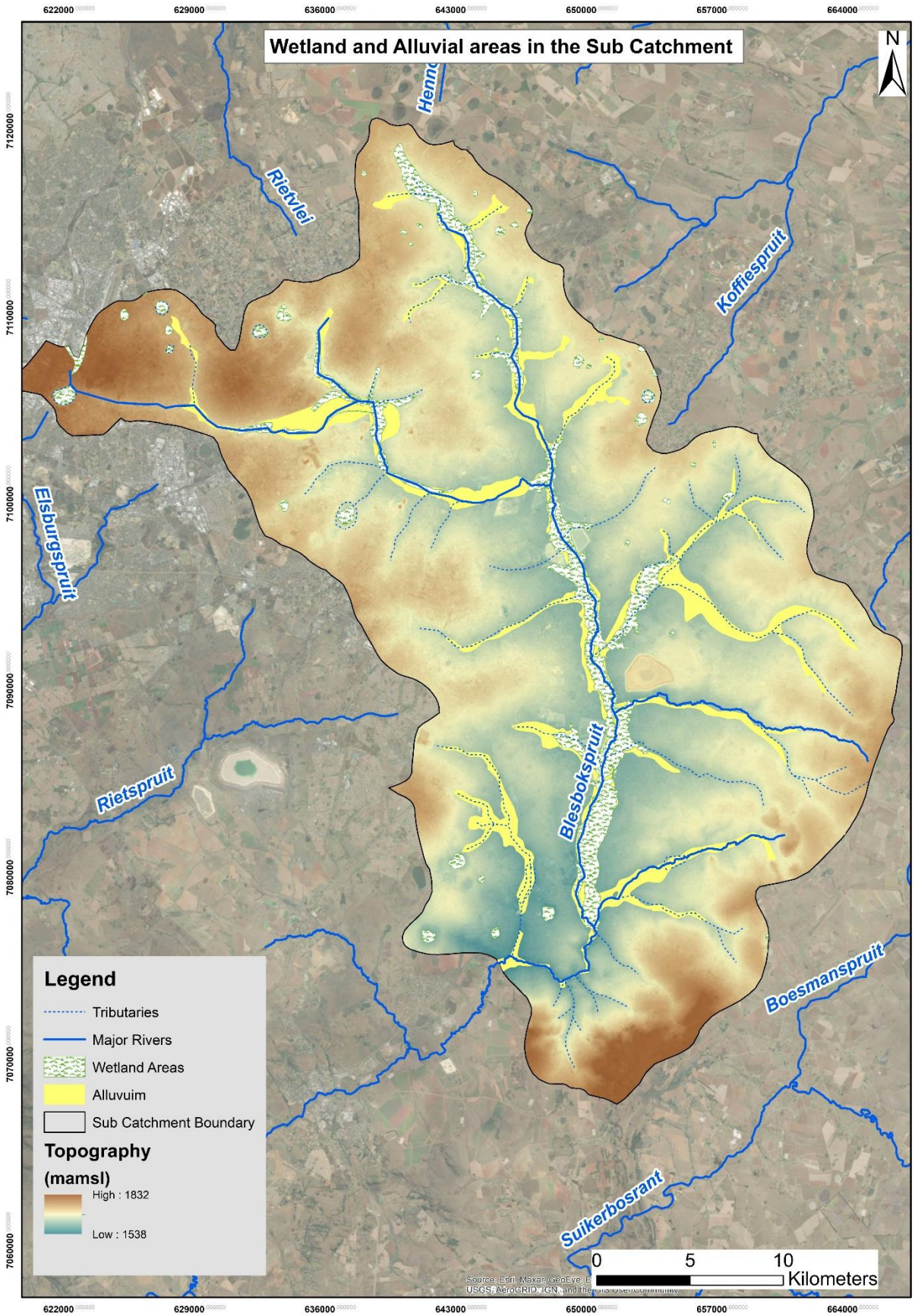

Figure 3-7 Wetland areas in relation to Alluvial deposits along the surface drainages.

3.1.2 Site specific data

The site-specific data and information are required to construct the numerical model for ease of calibration purposes. The site-specific data is usually measured data and information that will serves as input data to calibrate the numerical model and be representative of the actual real groundwater regime and status. The site-specific data will consist of the following:

- Rainfall records of the sub catchment area to determine the mean annual rainfall figure and determine recharge to the different aquifer systems.
- Water quality data specifically Chloride (Cl) concentrations to determine the recharge percentages for the aquifer systems according to the chloride method for recharge determination.
- Measured groundwater levels from existing boreholes that falls within the sub catchment. The groundwater levels will serve as input to represent the current status of the groundwater regime.
- Hydraulic parameters such as hydraulic conductivity determined from aquifer testing conducted on borehole within the sub catchment. The hydraulic conductivities will be assigned to the aquifer systems described in section 3.1.1.2
- The historic underground mining footprint that associates with the subsurface open voids left behind which might have collapsed or were partially backfilled.

3.1.2.1 Rainfall records

Rainfall records were gathered from the Water Resources of South Africa, 2012 Study (WR2012) internet data base which included 4 rainfall station that falls within the sub catchment area. These stations are 0476644W, 0476736W, 0476766W and 0476835W. The full monthly rainfall records are tabulated in Appendix A. The station positions are plotted in Figure 3-8 and indicates three of the stations (0476644W, 0476736W and 0476766W) clustered together on the western boundary of the sub catchment area. Station 0476835W is situated further south almost at the exit point of the Blesbokspruit. The rainfall stations and the years that rainfall was recorded are indicated in Table 3-3. The earliest rainfall records were taken at station 476835W from 1905 and the latest rainfall figures were recorded at 476766W. The station with the longest set of rainfall figures is rainfall station 476736W starting from 1909 to 2003 (94 years). Rainfall station 476766W however has at least 86 years of rainfall records from 1920 to 2006 which is also the most recent rainfall figures. It is for this reason that the data from rainfall station 476766W will be considered for the model calibration and predictive modelling simulation.

Table 3-3 Rainfall station and recorded years

Rainfall station	Year from	Year too	Total years
476644W	1921	1986	65
476736W	1909	2003	94
476766W	1920	2006	86
476835W	1905	1949	44

The rainfall records were analysed, and graphs were generated that indicates the yearly rainfall figures for each of the rainfall stations. The mean annual precipitation (MAP) was also determined as well as the upper 95th and lower 95th percentiles of the yearly totals. The MAP provides a good indication of the average yearly rainfall and associated recharge to the aquifer systems of the sub catchment. The upper and lower 95th percentiles could be used as a tool to assume flooding and drought conditions. Yearly rainfall above the 95th percentile can be considered as a flooding event and below the 95th percentile may represent a drought period.

The MAP from all 4 rainfall stations range between 682 mm/a and 735 mm/a. The MAP for the rainfall station clustered on the eastern boundary of the sub catchment does not differ that much from the station situated to the south which indicates that the rainfall figures are homogeneous over the sub catchment area. The rainfall records from all the rainfall stations show different flooding and drought periods.

The rainfall stations (476736W and 476766W) with longer and more recent rainfall records will be more suitable to evaluate the flooding and drought conditions. Both rainfall stations indicated flooding conditions during 1986, 1995 and 1999. The drought conditions from these two rainfall stations were during 1945, 1965 and 1982. Rainfall station 476766W indicated at least 5 flooding events and 5 drought events over the 86 year period.

The most extreme climatic events seem to have occurred during the period from 1980 to 2006 (26-year period) with numerous flooding and drought events. For predictive modelling a 10 year rainfall set can be used over this period to ensure that a flooding and drought period are included in the simulation.

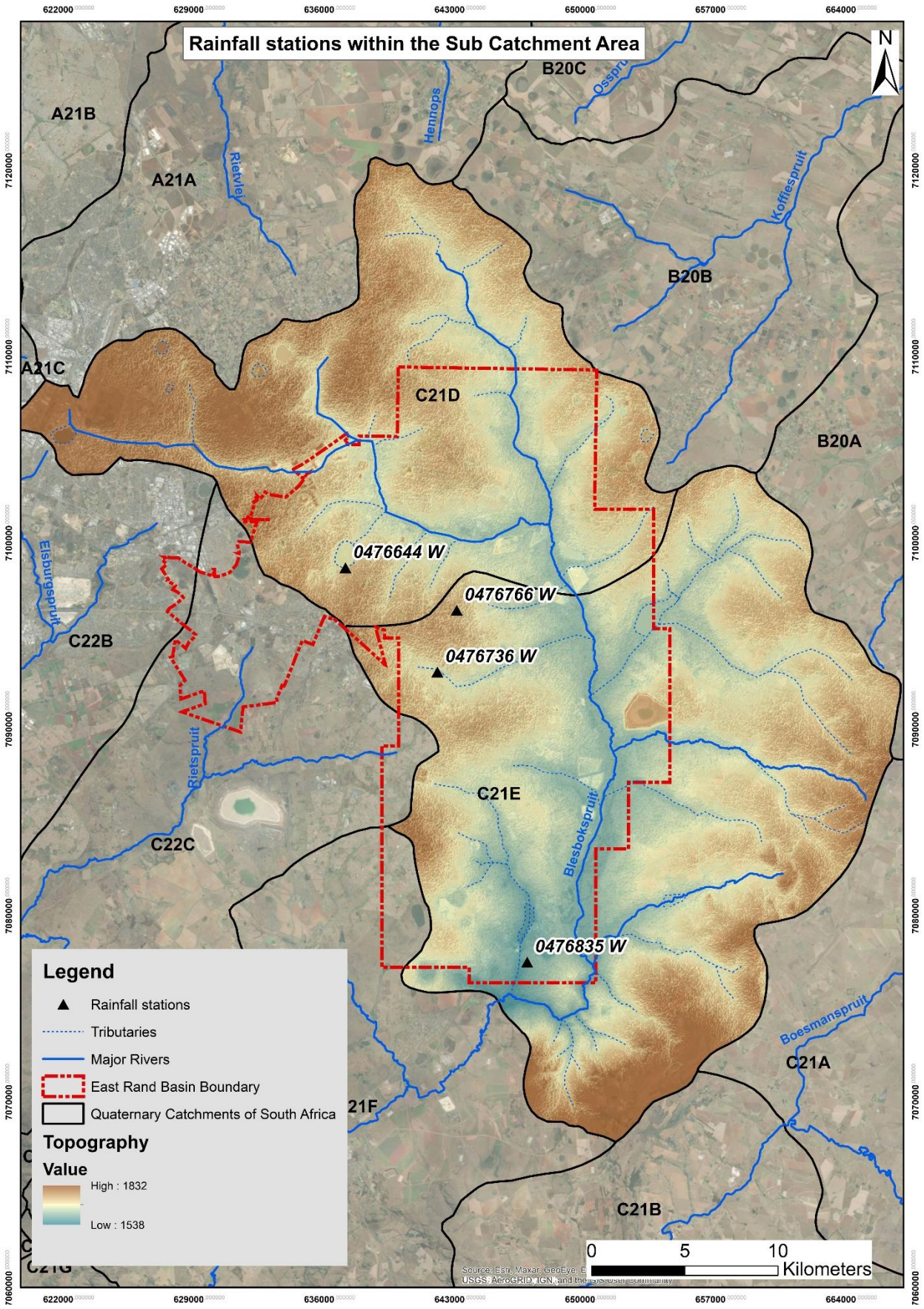

Figure 3-8 Rainfall Station within the sub catchment area

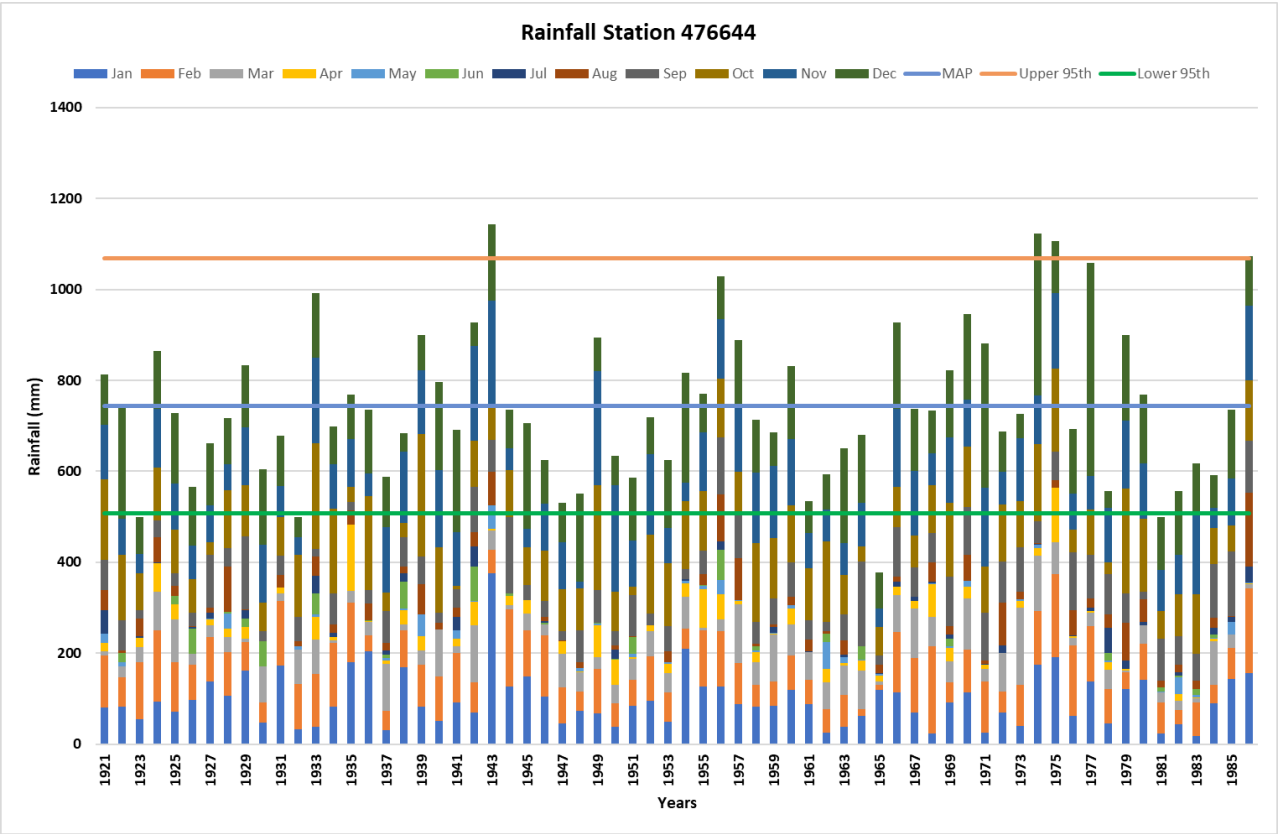

Figure 3-9 Rainfall records for station 476644.

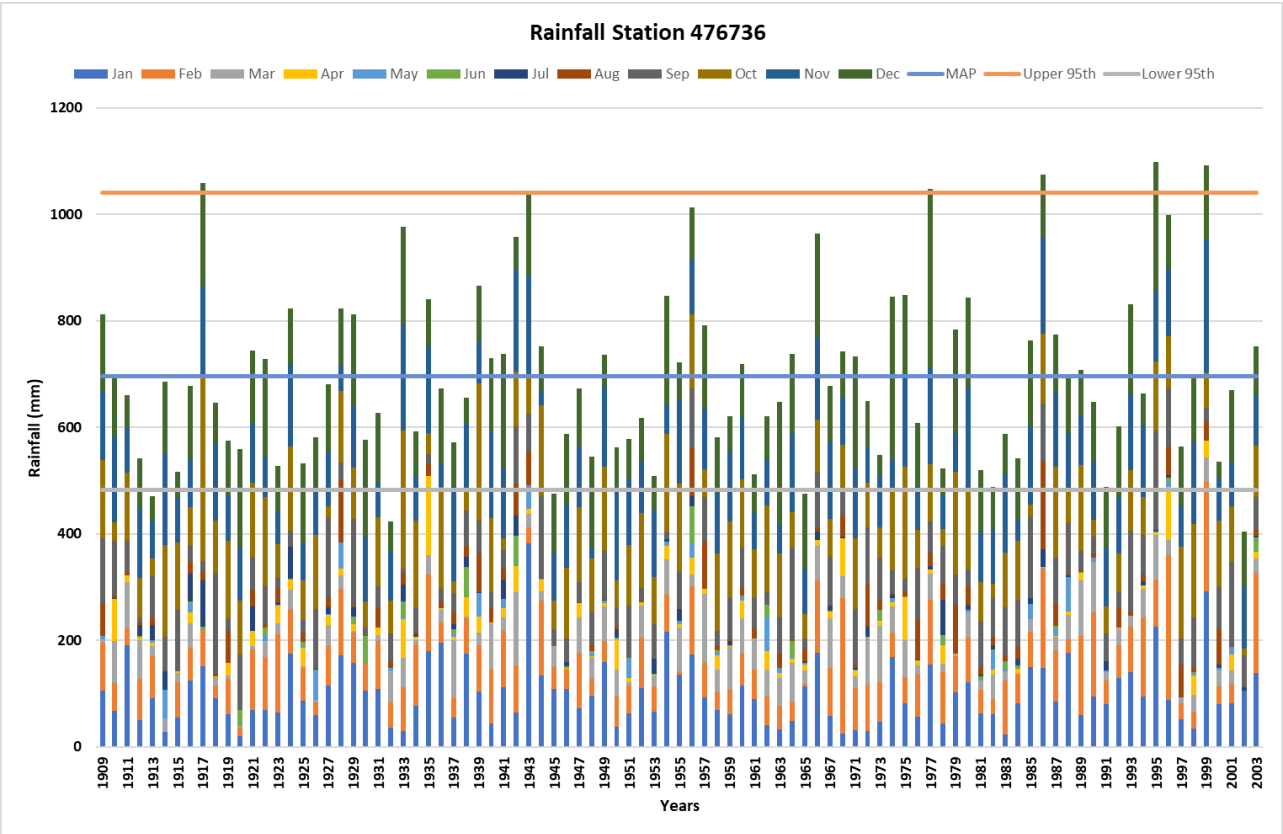

Figure 3-10 Rainfall records for station 476736.

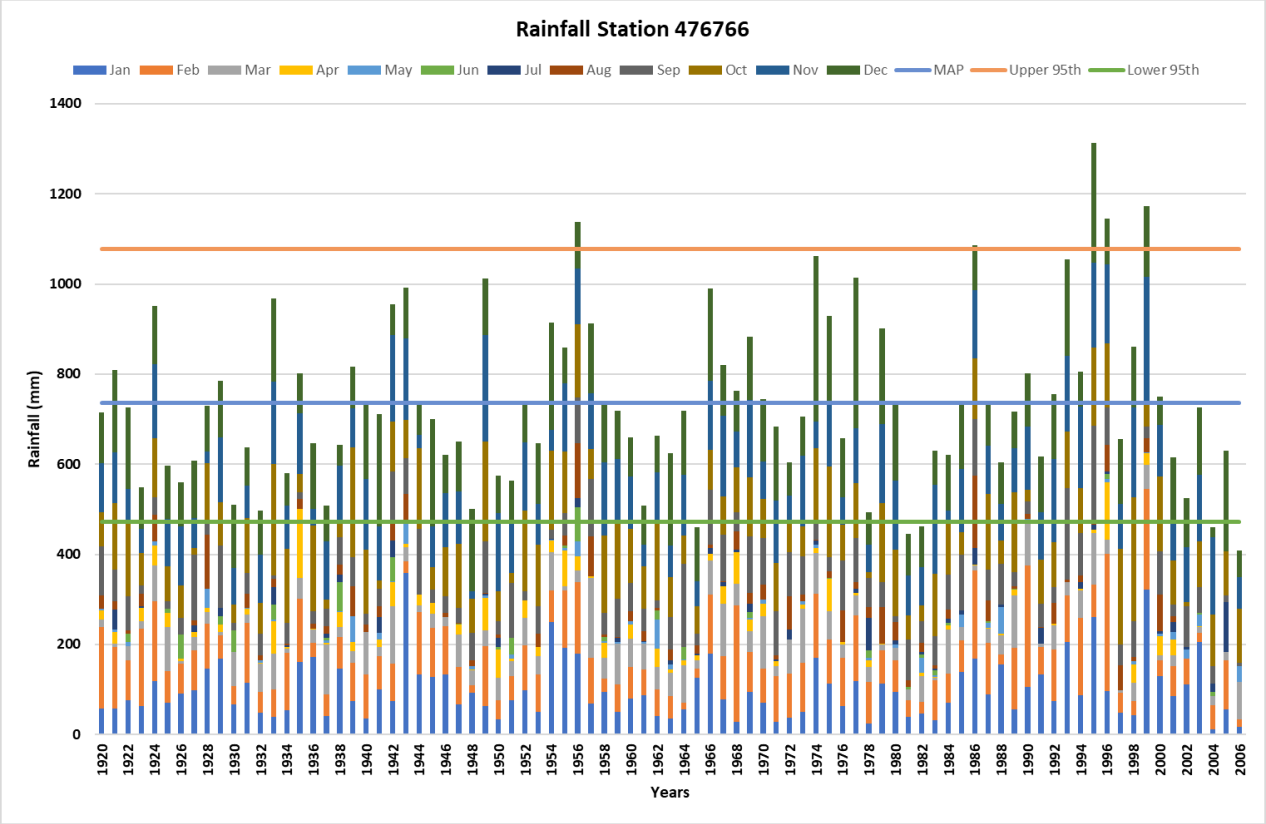

Figure 3-11 Rainfall records for station 476766.

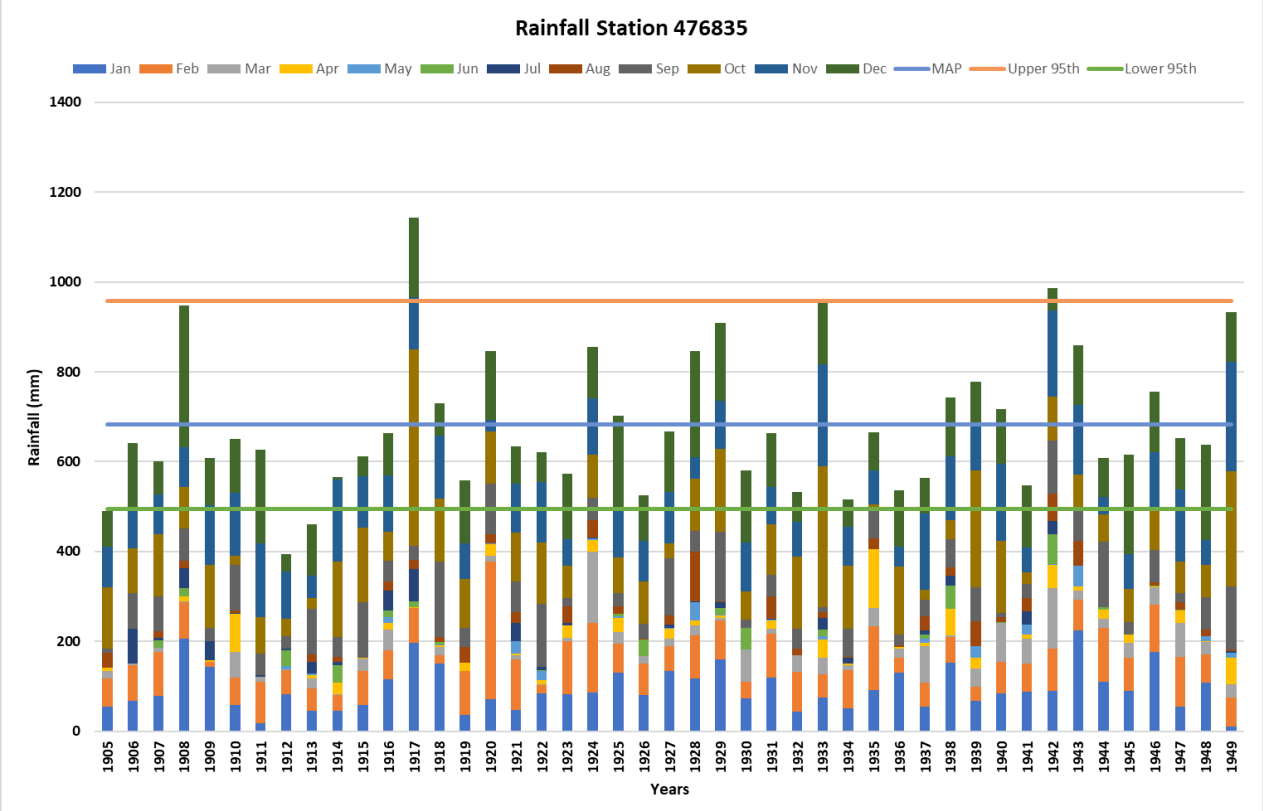

Figure 3-12 Rainfall records for station 476835

3.1.2.2 Groundwater Chloride Concentrations and Recharge

The ground water chloride concentrations were sourced from the Department of Water Affairs (DWA), Geodata base for Quaternary Catchments C21D and C21E as well as project reports (Scholtz, 2013), (Koekemoer, 2020) and research paper (Abiye, 2011) , (Botha, 2018). The ground water quality data were integrated to represent a full set of chloride concentrations which is presented in Appendix B. A total of 167 groundwater quality samples could be gathered that included Cl concentrations for groundwater. The groundwater Cl concentrations can be used to determine the recharge potential for the different aquifer systems (Marei et al., 2010). The chloride method for determining recharge potential could be applied and the recharge percentages assigned to the different aquifer systems will serve as input to the numerical model.

A spatial bubble plot of the Cl concentrations can be seen in Figure 3-13 which shows the samples that falls within the sub catchment area as well as samples near the sub catchment. Most of the samples that were analysed and presented in the research paper (Abiye, 2011) are located regionally across the Witwatersrand Goldfields, however samples that are near the sub catchment area also provides a good indication of the recharge potential for related aquifer systems that falls outside of the sub-catchment area. The samples that are located within the sub catchment area are located mostly towards the north, east and central parts with a few samples further south in the sub catchment and towards were the Blesbokspruit exits the sub catchment.

The bubble plot indicates Cl concentrations ranging from 2 mg/l to 90 mg/l for samples along the northern and eastern part of the sub catchment. The samples in the central part indicate higher concentrations that can range from 462 mg/l to 7437 mg/l. These increased concentrations may be due to historical, as well as current active mining operations in these areas. The samples indicating concentrations above 900 mg/l and within the sub catchment are situated just south of the Grootvlei Mine (GROOTVALLEY (DUP NAME 22680) and just north of the Geduld Proprietary Mines (G10D and G23D). The proximity to the mining activities would imply possible seepage to the groundwater systems within the mining areas and increased Cl concentrations. The samples further south within the sub catchment mostly indicate Cl concentrations ranging from 91 mg/l to 462 mg/l.

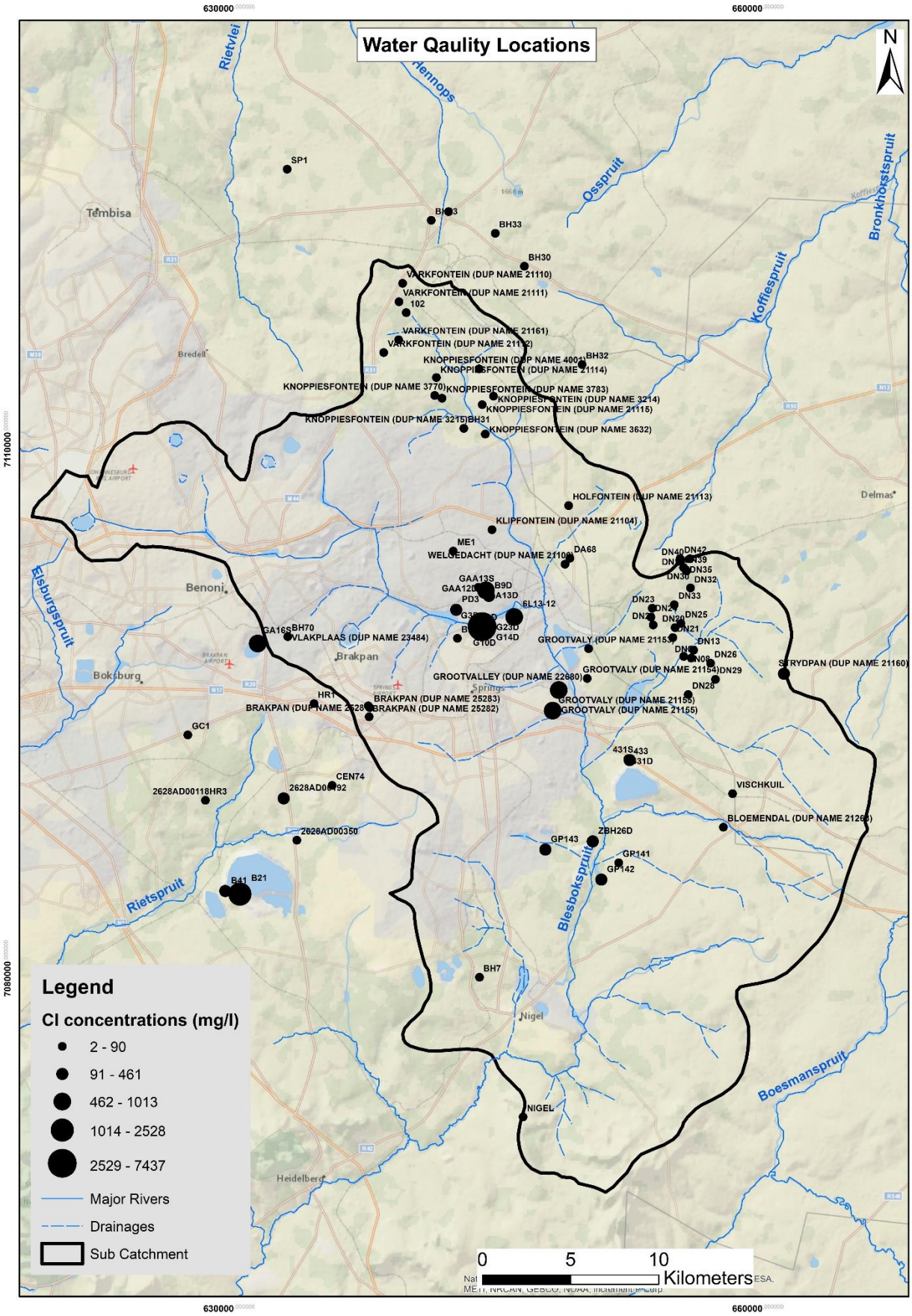

Figure 3-13 Chloride concentrations in and around the sub catchment

Recharge to the different aquifer systems can be determined through the chloride method by using the MAP for the associated area and the groundwater Cl concentrations (Conrad et al., 2004) and (Van Dyk, 2006) The groundwater samples that had increased Cl concentrations due to mining activities were not considered for the recharge estimations.

The Chloride method makes use of the chloride concentrations in groundwater, the mean annual rainfall as well as the chloride concentrations in rainwater for the specific area. The chloride mass balance for determining recharge can be described by Equation 3-1, where R represents Recharge in mm/a, P represents Precipitation (mm/a), Cl (GW) represents Chloride concentrations in groundwater and Cl (RW) represents Chloride concentrations in rainwater.

The potential chloride concentrations in rainwater can best be described by looking at the Urban Highveld Cl concentrations in rainwater during early, peak and dry tier intervals of semi-arid regions in South Africa (van Wyk et al., 2011) which is indicated in Table 3-4 as 0,6 mg/l for early, 0,3 mg/l as peak and 1 mg/l during dry periods. The three tier chloride concentrations are also represented in **Figure 3-14** for the Pretoria region as 0,7 mg/l during early periods, 0,3 mg/l at peak conditions and 1 mg/l during dry periods (van Wyk et al., 2011).

$$R = P * \frac{Cl\ (RW)}{Cl\ (GW)}$$

Equation 3-1 Chloride mass balance to determine recharge potential.

Table 3-4 Rainwater chloride concentrations for South Africa Taken from (van Wyk et al., 2011)

Attribute	Karoo Region[1]			Savanna Region[2]			Ghaap Plateau[3]			Urban Highveld[4]			Bushveld Region[5]			Kalahari Sandveld[6]		
Anions:	**mg·ℓ$^{-1}$**																	
Cl^-	0.8	**0.7**	1.3	0.9	**0.8**	1.0	0.7	**0.4**	1.0	0.6	**0.3**	1.0	1.0	**0.7**	2.0	0.7	**0.3**	0.8
SO_{42-}	0.1	**0.8**	1.1	3.6	**2.7**	1.1	1.3	**1.0**	1.5	1.6	**1.4**	5.0	0.1	**2.2**	4.1	2.4	**0.6**	1.6
NO_{3-}	0.9	**0.2**	1.4	1.1	**0.7**	j	0.1	j	1.6	1.4	**0.4**	0.5	0.1	**0.1**	0.1	0.9	**0.3**	1.6

[1] *Beaufort West area (northeast), towards the Nuweveld Escarpment, Western Cape – wildlife reserve*
[2] *Stella area, Vryburg District (south), Northern Cape – stock farming and dryland irrigation*
[3] *Catchment of the Kuruman A-Eye at Kuruman (south), Northern Cape – wildlife reserve*
[4] *Pretoria East (Lynnwood-Garsfontein), Gauteng (semi-humid region) - urban residential*
[5] *Taaiboschgroet area in the Alldays District (southwest), Limpopo – wildlife reserve*[6] *Van Zylsrus area (west), Gordonia District, Northern Cape – wildlife reserve j Not detected, concentration level probably <0.05 mg·ℓ$^{-1}$*

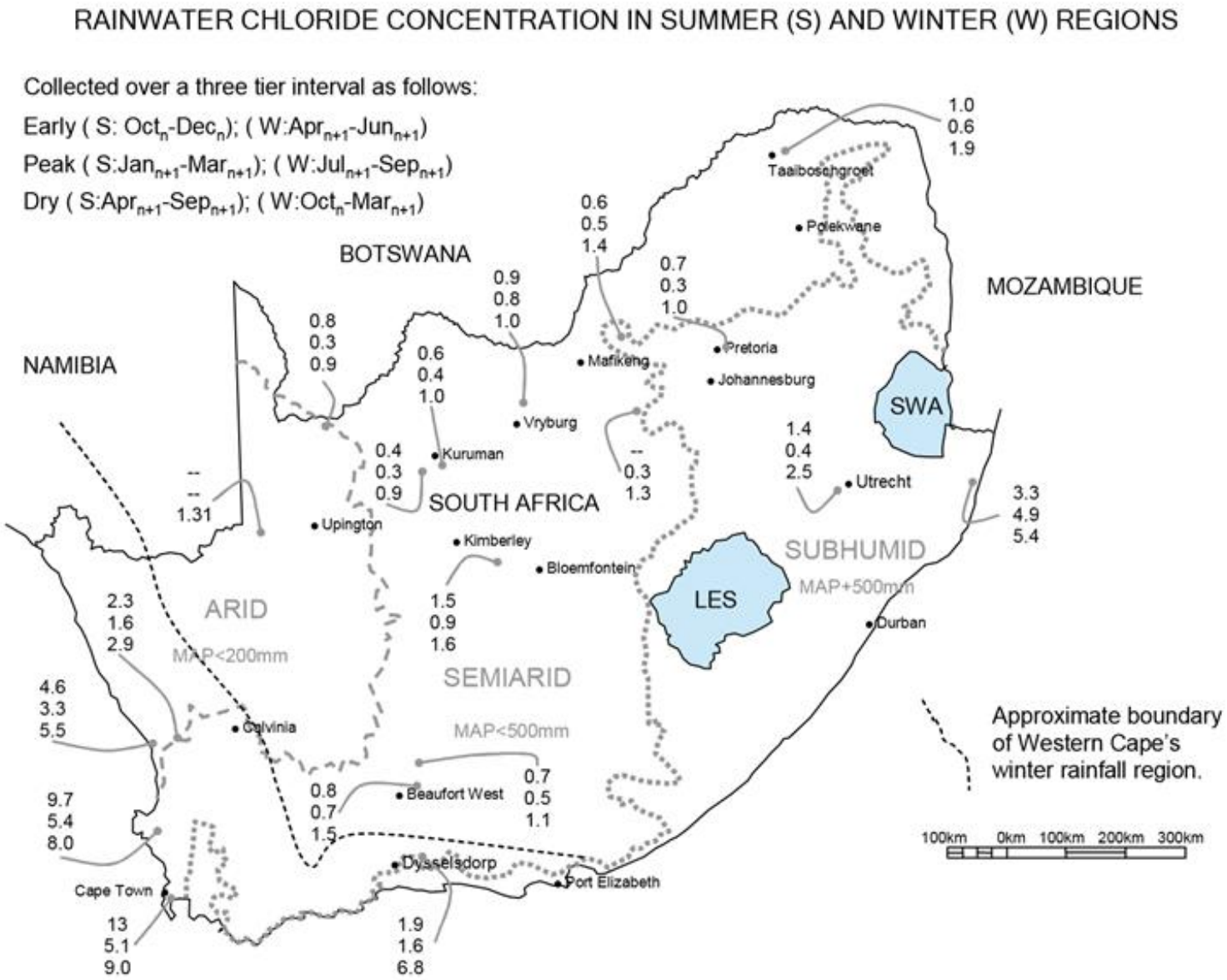

Figure 3-14 Figure indicating the rainwater chloride concentrations over South Africa Taken from (van Wyk et al., 2011)

The potential recharge estimations from using the chloride mass balance equation and assuming the peak conditions for chloride concentrations as indicated above together with the groundwater chloride concentrations from the samples are summarised in Appendix C. The assumptions for samples that could be influenced by mining activities as well as concentrations that were at the detection limits were not considered for the recharge estimations.

The minimum recharge potential was calculated at 1,8 mm/a (0,2%) and the maximum at 509,7 mm/a (69,3%). The average recharge was calculated at 82,6 mm/a (11,2%). The recharge potentials indicate a wide range of possible recharge to the different aquifer systems and potential additional influences from contaminant sources on a regional scale.

The potential recharge estimations for the sample locations within the sub catchment area were plotted against the geology to evaluate the potential recharge for the associated aquifer systems in terms of geology types. The bubble plot indicated in Figure 3-15 shows that recharge percentages for the different geology types and associated aquifer systems varies over a wide range. The recharge potential and related geology for the sample locations in the sub catchment are summarised in Appendix D with the following that needs to be noted:

- Recharge to the alluvial deposits and shallow aquifer systems can range from 3,9% to 14,4% of MAP.
- Recharge to the Diamictite formations and associated hard rock aquifer systems can range from 0,2% to 17,6% of MAP.
- The Dolomitic and karstic aquifer systems which predominantly underlies the shallow aquifer and alluvial deposits has recharge ranging from 0,6% to 29,5% of MAP.
- The sedimentary Sandstone and Shale aquifer systems that covers most of the sub catchment area indicated recharge ranging from 0,5% to 40% of MAP.
- The high recharge percentages from the sedimentary aquifers may also be influenced by external factors.

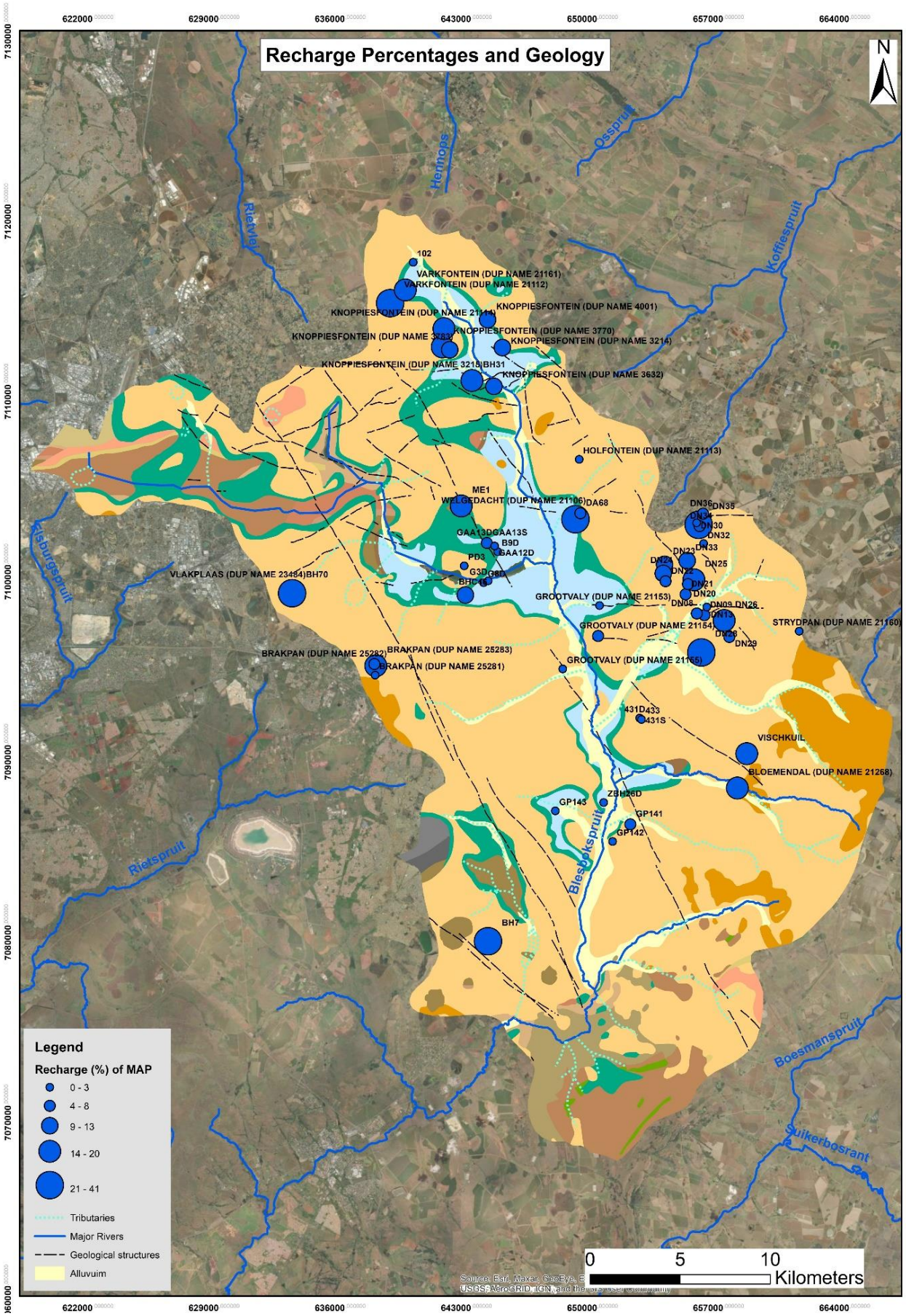

Figure 3-15 Recharge percentages and Geology for the Sub Catchment

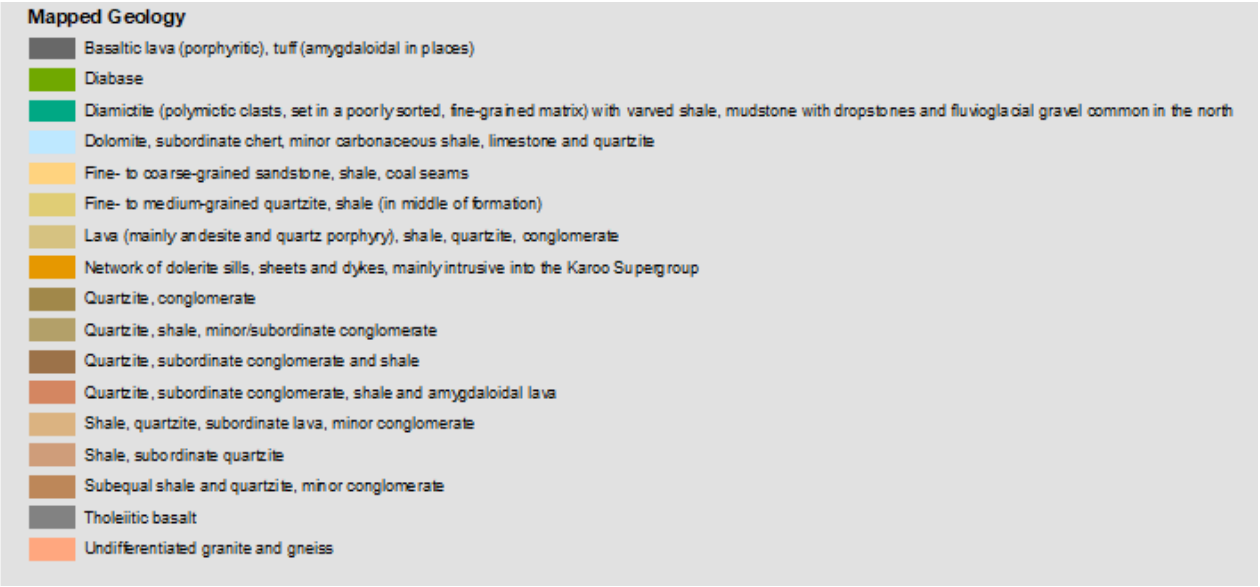

Figure 3-16 Geological key for Figure 3-15

3.1.2.3 Groundwater levels

Groundwater levels from at least 112 regional boreholes could be gathered from Department of Water Affairs (DWA), Geodata base for Quaternary Catchments C21D and C21E as well as for the same project reports (Scholtz, 2013), (Koekemoer, 2020) and research papers (Abiye, 2011) and (Botha, 2018). Limited data regarding recent groundwater levels for the sub catchment area could be sourced, however, it is believed that with the active mining and dewatering from the mines that exit in the sub catchment area that there will probably be more groundwater level data available, and this information might be of a sensitive nature which will require special permission to be used for research purposes.

The groundwater levels are summarised in Appendix E which indicates the regional groundwater levels for the sub catchment area and surroundings. The measurements dates for the research papers and project reports range from 1984 to 2023. The groundwater level data sourced from DWA have at least four boreholes (C2N1113, C2N1114, C2N0890 and C2N0893) that were measured within the last four years with two sites (C2N0890 and C2N0893) that were measured in January 2023. The oldest measurements dates to 1984 and 1989 for boreholes C2N0113 and C2N0888 respectively which may imply that these boreholes do not exist anymore. The shallowest groundwater level measurement was measured at 0,3 mbgl and the deepest at 169 mbgl. This observation indicates that the aquifer system could be influenced by dewatering and abstraction that causes the wide range of water level depths. The average water level depth was estimated at 32,9 mbgl.

The groundwater positions the falls within the sub catchment area and associated hydraulic heads were plotted against topography (Figure 3-17) to look at the correlation between hydraulic head and elevation. Generally, a good correlation between measured hydraulic head and topography would be represented by at least 90% and above however in this case for the sub catchment, the correlation is around 8% which would imply a large influence from groundwater abstraction at some of the boreholes and subsequent water level drop during abstraction. The regional groundwater level could also be influenced by dewatering from Grootvlei mine. The 45-degree angle line does indicate some correlation for specific boreholes and that the general trend show that water levels are below topography as all the holes plot above this line.

A spatial plot of the regional groundwater level positions in and around the sub catchment and their respective water levels depths represented as bubble plots are presented in Figure 3-18. The groundwater levels that's in close proximity to the drainage systems generally indicated shallower

groundwater levels (0,3 to 7 mbgl) and could be due to the baseflow component that surface water presents to the groundwater systems from the drainages and related shallow alluvial aquifers. This is also evident from the boreholes (BH41 and BH21) located to the east of the sub catchment and next to the lake along the Rietspruit. The boreholes that are situated along the Rietvlei River to the north of the sub catchment indicated groundwater levels as deep as 169 mbgl and its possible that these holes may be used for irrigational purposes for farming activities or water supply to the local municipalities.

The groundwater level positions provided by DWA, all fall within the sub catchment area and are mostly concentrated along the northern and north-eastern boundary of the sub catchment. The boreholes located along the northeastern boundary of the sub catchment area indicates deeper groundwater levels (77-169 mbgl) which also may imply abstraction from groundwater resources for mining and agricultural purposes. The EnviroServe Holfontein Landfill site is adjacent to a mining activity and C2N0113 (138.4 mbgl), C2N1113 (49.57 mbgl) and C2N1113 (48.95 mbgl) is situated almost on the boundary of this mining facility.

The groundwater level positions clustered along the eastern boundary of the sub catchment indicated groundwater levels ranging from 3,5 mbgl (DN08) to 100,5 mbgl (DN57). The shallow water levels in this area may also be due to the shallow aquifer systems although the deeper water levels may be influenced by farming and irrigational purposes.

The hydraulic heads from the groundwater positions that falls within the sub catchment were contoured to evaluate the groundwater flow regime locally (Figure 3-19). The correlation between hydraulic head and topography implies an aquifer that is readily influenced by groundwater abstraction and this observation is reflected when looking at the contours in relation to the sub catchment topography. At this stage it is difficult to say what the groundwater regime and flow direction is however some indication in the northern part of the sub catchment shows groundwater flow to be towards the Blesbokspruit and form east and west trending tributaries and then a general southwards flow direction towards the exit point of the Blesbokspruit.

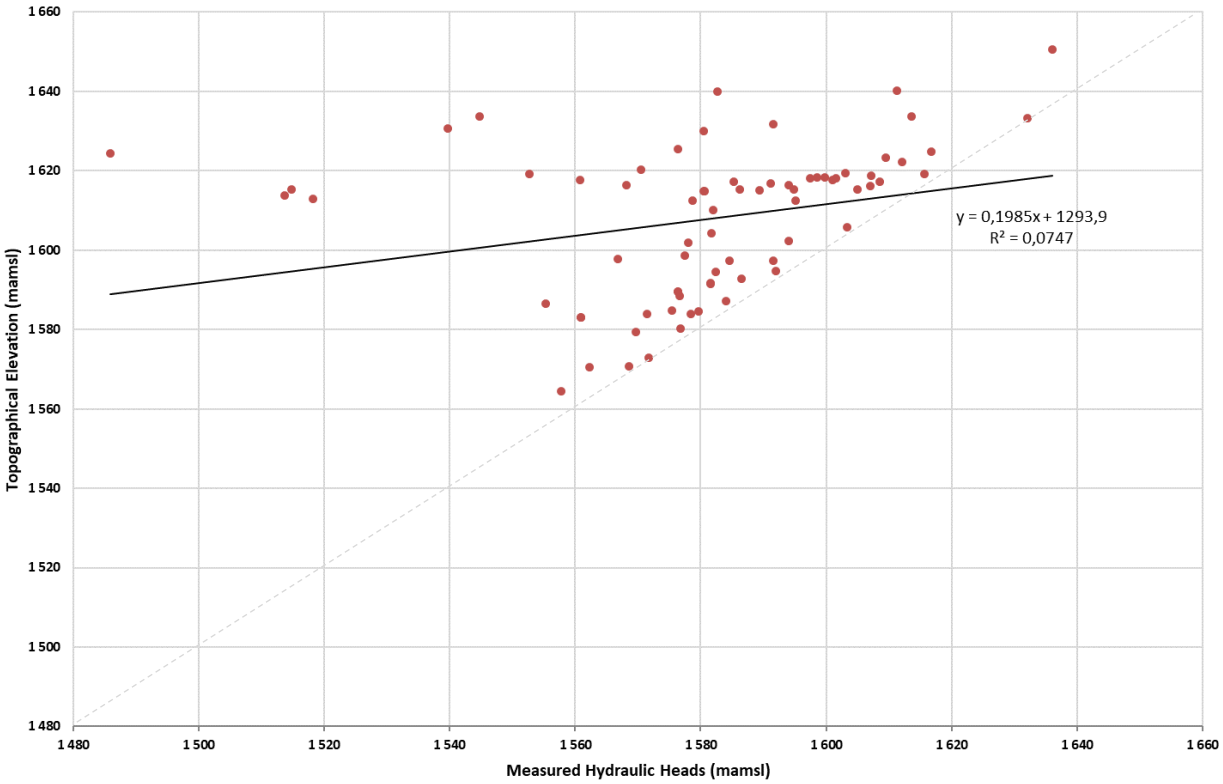

Figure 3-17 Correlation between measured hydraulic head and topography.

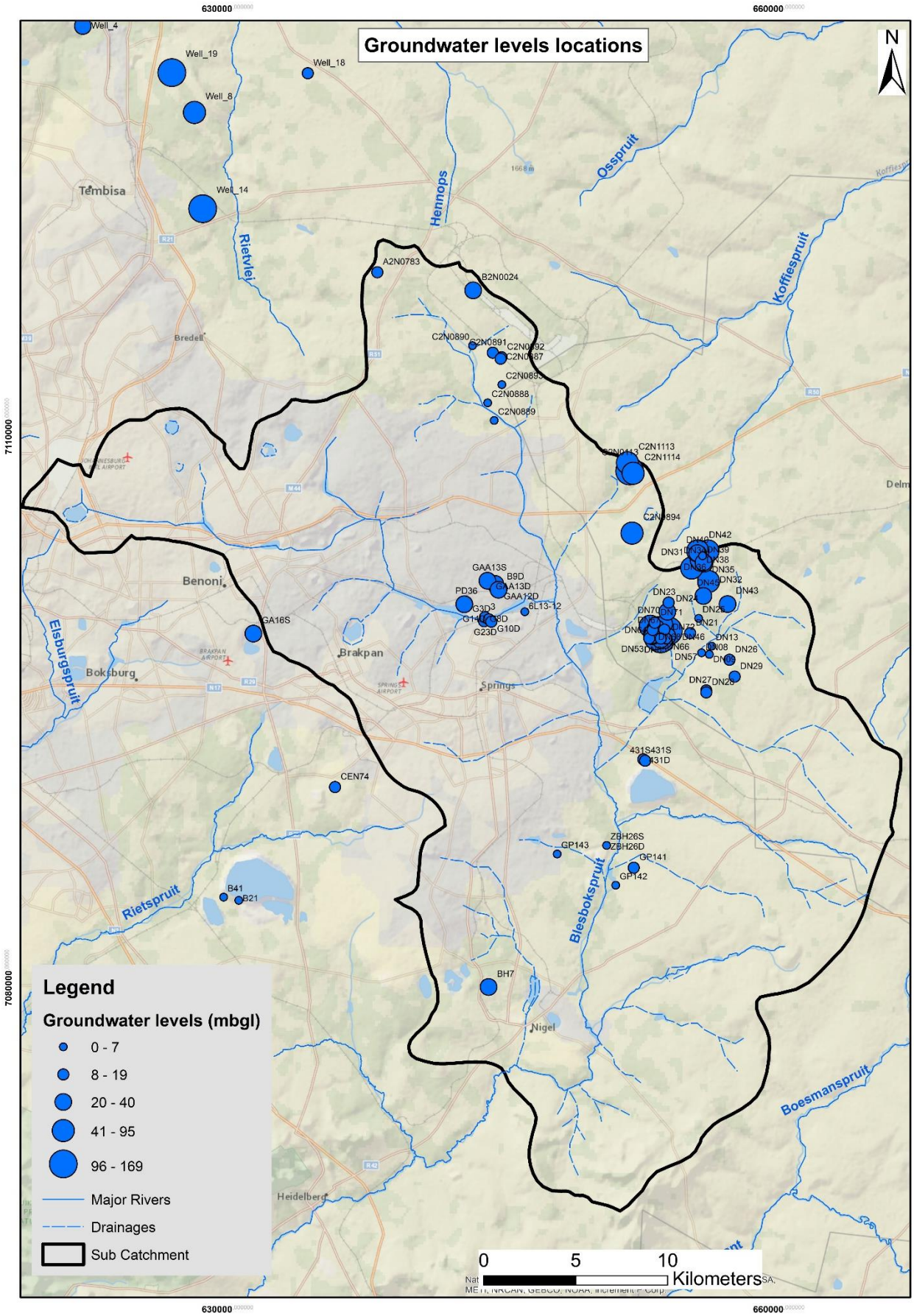

Figure 3-18 Groundwater levels in and around the sub catchment area

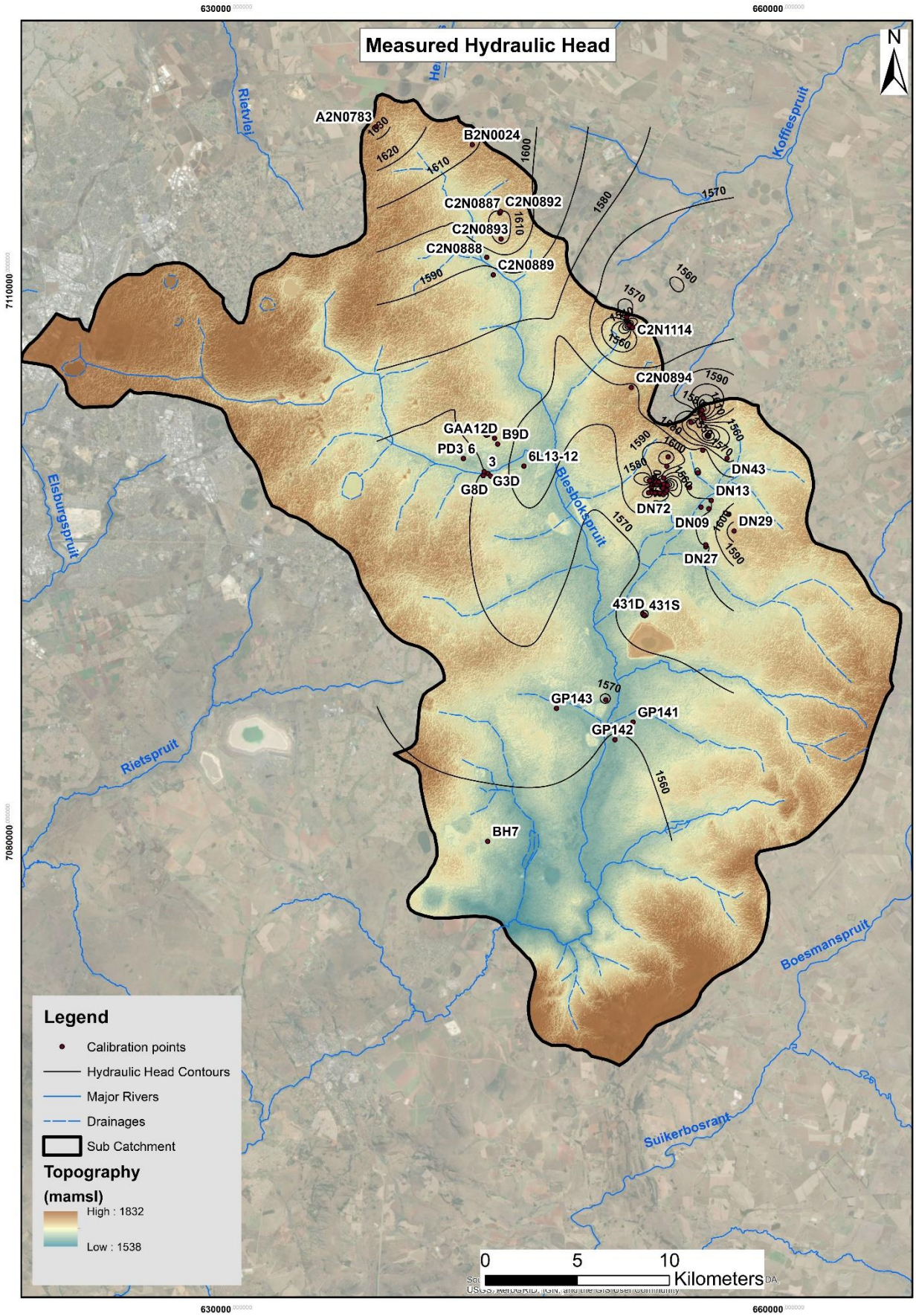

Figure 3-19 Measured Hydraulic Head as interpolated from the reported groundwater levels

3.1.2.4 Hydraulic Parameters

The hydraulic parameters that could be gathered for the sub catchment area mainly included aquifer tests conducted on boreholes for the project studies (Scholtz, 2013) and (Koekemoer, 2020). The pump test data were analysed to determine hydraulic conductivities and transmissivity values for the different type of aquifers associated with the project sites.

The project study conducted by Shangoni Aquiscience (Scholtz, 2013) listed the types of aquifers associated with the boreholes that got tested as well as the hydraulic conductivities and transmissivities values which are indicated in Table 3-5. Three different aquifers were identified namely:

- The shallow unconfined zone which may represent the weathered and semi weathered profile above the fresh bedrock,
- The fractured Karoo aquifer systems that may represent the fractured bedrock and,
- The dolomitic confined aquifer systems that mainly consists of the dolomite and karstic formations.

The pump tests analysis indicated hydraulic conductivities ranging between 0,009 m/d to 0,05 m/d for the shallow unconfined aquifers. Equally the transmissivities range between 0,045 m^2/d to 0,25 m^2/d for this aquifer system. The fractured Karoo aquifer system indicated hydraulic conductivity and transmissivity of 0,049 and 3,9 respectively. The dolomitic aquifer systems were described as high yielding (10 -20 l/s) and indicated a transmissivity value of 372 m^2/d which are usually associated with dolomitic and karstic aquifer system due to chemical weathering and the formation of dolines and cavities.

The aquifer parameters for the different geology types are summarised in Table 3-6 which shows hydraulic conductivities for the soil and clay between 0,023 m/d and 0,049 m/d for the sandstone formation. The Malmani dolomite have hydraulic conductivity that can range from 0,1 – 10 m/d and Storage values of 0,01. The storage value for the sandstone formation were estimated at 0,0005.

Table 3-5 Aquifer parameters determined from (Scholtz, 2013)

Borehole ID	Hydraulic Conductivity (m/d)	Transmissivity (m^2/d)	Aquifer type
DN08	0.009	0.045	Shallow unconfined zone
DN09	0.05	0.25	Shallow unconfined zone
DN13	0.01	0.05	Shallow unconfined zone
DN21	0.049	3.9	Fractured Karoo aquifer
DN22		372	Dolomitic confined aquifer

Table 3-6 Aquifer parameters summarised for the different aquifer systems (Scholtz, 2013)

Aquifer	Type	Geology	K (m/d)	T (m²/d)	S
Shallow perched	Unconfined (primary)	Quaternary Soil /Clay	0.023	0.115	-
Weathered/fractured	Semiconfined	Karoo Sandstone (Ecca)	0.049	3.9	0.0005
Karstic/fractured	Confined	Malmani dolomite	0.1-10	372	0.01

The project study conducted by (Koekemoer, 2020) for the mining development at the West Wits Mine located approximately 20 km west of the East Rand Basin provided additional aquifer parameters that can be considered as model input parameters. The geology types and associated aquifer systems in which these boreholes were drilled are the same as for the East Rand Basin which includes the Johannesburg, Orange Grove and Turffontein Subgroups and mainly consists of Quartz Conglomerate and Quartz Shale formations.

The pump tests conducted on four boreholes provided data that were analysed and indicated hydraulic conductivities ranging from 0,0013 m/d to 0,0025 m/d. The transmissivity values for the same formations range from 0,0066 m²/d to 0,1 m²/d. The aquifer parameters from this study indicates lower permeability in the Quartz formations than the sedimentary sandstone aquifer systems as reported in (Scholtz, 2013).

Table 3-7 Aquifer parameters analysed for boreholes at the West Wits Mine (Koekemoer, 2020)

Borehole	Transmissivity (m²/d)			Hydraulic Conductivity (m/d)		
	Constant Rate	Recovery	Average	Constant Rate	Recovery	Average
BH1	1,08E-01	2,44E-02	6,62E-02	2,13E-03	4,79E-04	1,30E-03
BH2	1,28E-01	8,44E-02	1,06E-01	2,97E-03	1,96E-03	2,47E-03
BH3	1,31E-01	2,47E-02	7,79E-02	3,18E-03	6,01E-04	1,89E-03
BH4	1,16E-01	4,82E-02	8,21E-02	2,23E-03	9,26E-04	1,58E-03

3.1.2.5 Historic mining footprint and open voids

The historic mining footprint was delineated from georeferenced maps supplied by the Council of Geoscience (CGS) for the historic mining activities in the East Rand Basin. The delineated historic mining footprint is indicated in Figure 3-20 which shows section of mining assumed to sub surface areas that has either been mined out or backfilled to an extent. These mined out sections could imply open or semi open underground voids left from the historic mining activities which could

either be flooded or partly flooded. These sub surface open areas could also act as pathway for groundwater flow creating an interactive network of voids in the sub surface environment. Shallow aquifer ingress can also be directly linked to these areas in terms of rapid recharge that can directly enter the groundwater systems during heavy rainfall events.

The historic mining footprint covers most of the northwestern and western parts of the sub catchment area with isolated areas situated southwest of the sub catchment. The bulk of the mining footprint are located west of the Blesbokspruit. The wetland and associated shallow aquifer systems that maybe influenced by the historic mining footprint are the tributaries leading from the northwestern section of the sub catchment towards the Blesbokspruit.

The CGS also provided mapped historic mine shaft locations as well as potential surface ingress locations mostly situated over the northwestern historic mining footprint. These mapped shafts and potential surface water ingress locations can act as possible conduits for surface water to enter the shallow aquifer systems along the wetland areas increasing groundwater flow towards the deeper aquifers which is linked to the historic mining footprint. Although the historic shafts and ingress locations that were supplied only cover the northwestern mining footprint its quite certain that more historic shafts and surface ingress locations exists over the western and southwestern historic mining footprint that still needs to be mapped.

The east rand basin currently experiences dewatering from the Grootvlei mine to keep the mining basin dry for deep mining operations (Lea et al., 2001). The dewatering is believed to aid in dewatering the deep hard rock aquifer system for the deeper mining operations to continue. This dewatering practice has limited effect on the regional shallow aquifer systems that is mostly recharge dependant. The dewatering rate was reported (Lea et al., 2001) on average to be in the region of 75 000 m^3/d maintaining the water level at approximately 740 mbgl (± 843 mamsl). The dolomitic aquifer contributes roughly 30 000 m^3/d (Scott, 1995) with seepage from the Blesbokspruit reported to be between 2000 to 3000 m^3/d (Lea et al., 2001).

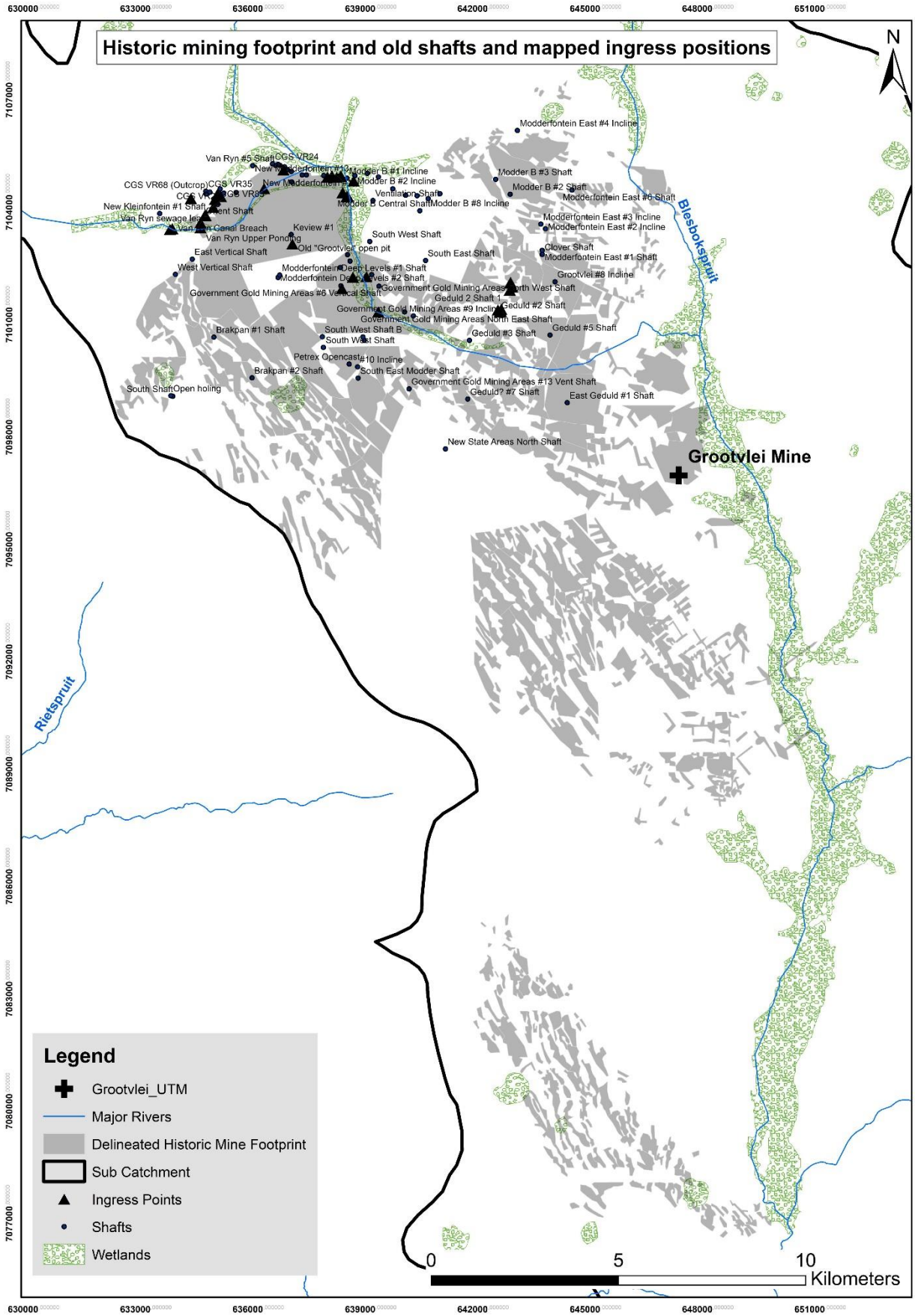

Figure 3-20 Historic Mining footprint as well as mapped shafts and ingress positions.

3.2 Conceptual model

The conceptual model is a representation and understanding of the numerical modelling problem statement and the current groundwater status and regime of the modelling area and domain in terms of aquifer units and input included to model the desired outputs needed to answer the problem statement. The conceptual model also explains the expected outcomes of the numerical modelling assessment and approach that needs to be followed to conduct the numerical model.

For the purpose of this case study the conceptual model will look at the following aspects to aid in developing the understanding of what needs to be modelled, the different components that needs to go into the numerical model such as geological units and related aquifer systems and in particular the shallow aquifer systems related to the surface drainage areas where alluvium makes up most of the subsurface, surface drainage systems, and factors that has an influence on the groundwater systems currently. For the East Rand Basin these factors will be mostly mining related in terms of mine dewatering decreasing the hydraulic head regionally and mine storage facilities such as tailings and waste rock facilities having an increased recharge component causing the mounding of the hydraulic head locally within these storage facilities. The hydraulic influence that the mining activities could have on the hydraulic head regionally will also determine the groundwater regime and gradient across the East Rand Basin.

To develop the conceptual model for this case study the following components needed to be included and described:

- The modelling problem statement which is to quantify the ingress rates and volumes of the shallow aquifer systems into mine related open voids during rapid recharge events.
- The historic mine workings and extent over the East Rand Basin with specific reference to the connection with the mine related open voids like old shafts.
- The surface drainage systems for the East Rand Basin and how it relates the shallow aquifer systems as alluvial deposits along the flood plains and wetlands.
- The geological units and related aquifer systems for the deeper hard rock geology
- How the shallow aquifers get rapid recharge during rainfall events and how ingress into the mine related open voids occur during the recharge events.

The conceptual model could be better explained by looking at a cross section from west to east through the Blesbokspruit and sub catchment as illustrated in Figure 3-21 and Figure 3-22. The

aim of the conceptual model is to explain how the shallow aquifer systems promote ingress into the historic mine related open voids when rapid recharge events occur.

The cross section in Figure 3-21 indicates the limited ingress expected when the groundwater systems is in static conditions and the following needs to be noted:

- The groundwater level is at static levels and may be at the base of the Furrow and canal systems that flows from the west towards the Blesbokspruit.
- Equally the groundwater levels will be at the base of the Blesbokspruit.
- The alluvial deposits associated with the tributaries and rivers are mostly unsaturated when static conditions prevail.
- The deeper aquifer systems, and in this case the Dolomite, Sandstone and Diamictite aquifers will only be influenced by the exiting mining activities.
- The mine related open voids from historical mining infrastructure will have limited ingress from the alluvial aquifers during static conditions.

The aim of the numerical model representation will be to represent the numerical model according to the static conditions according to site specific data and information. The cross section from Figure 3-22 indicate how rapid recharge could increase water ingress into the historic mining infrastructure and the following needs to be noted:

- When a large rainfall event occurs then the alluvial deposits associated with the rivers and tributaries gets rapid recharge causing the groundwater level to potentially render the alluvial deposits completely saturated
- During this rapid rise in groundwater level and complete saturation, ingress into the historic mine related open voids will increase.

The aim of the numerical groundwater model simulation will be to measure the inflow rates during these rapid recharge events and quantify the inflow rates at peak flooding.

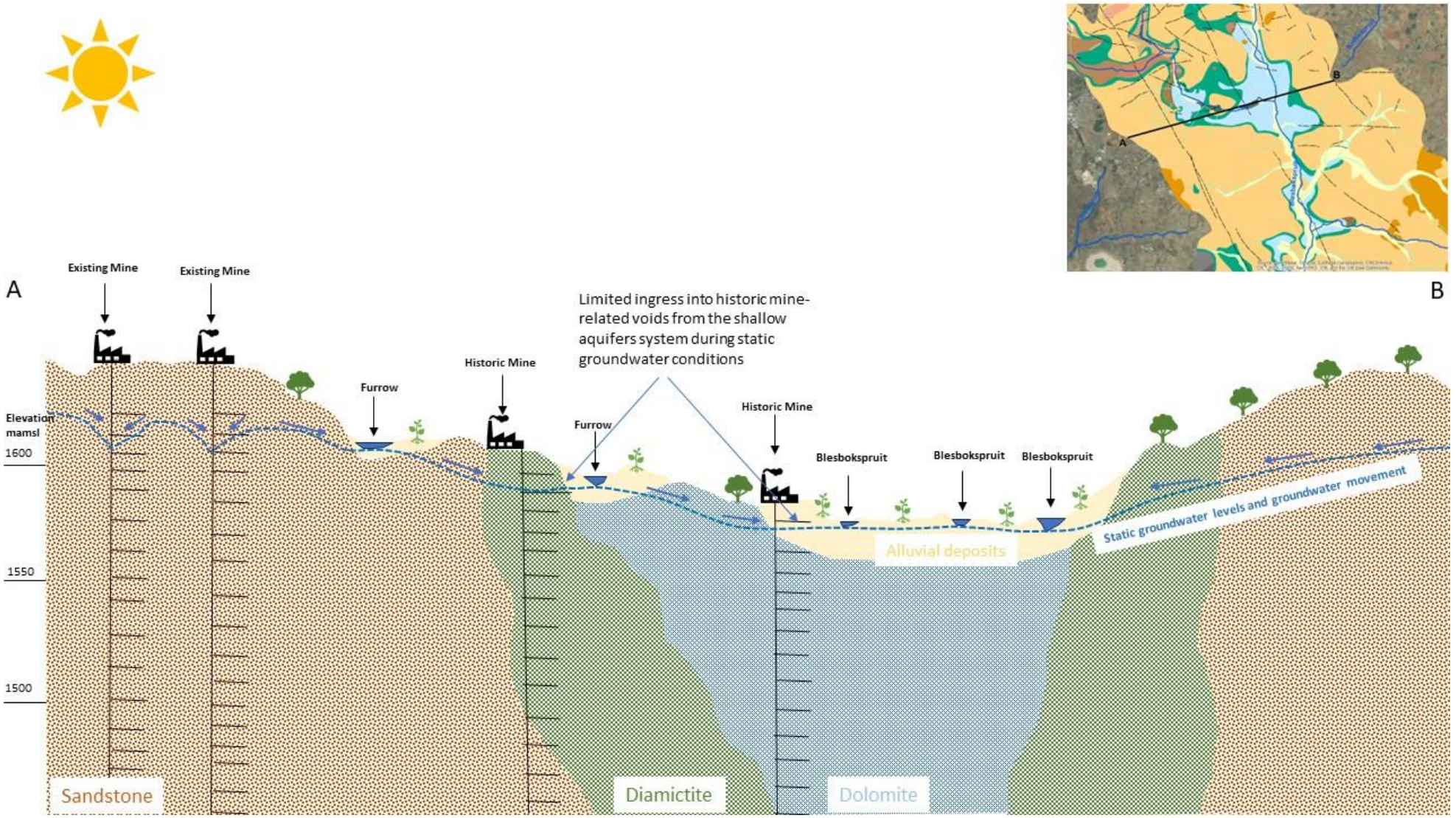

Figure 3-21 Limited ingress into mine related open from shallow aquifers during static conditions (not to scale)

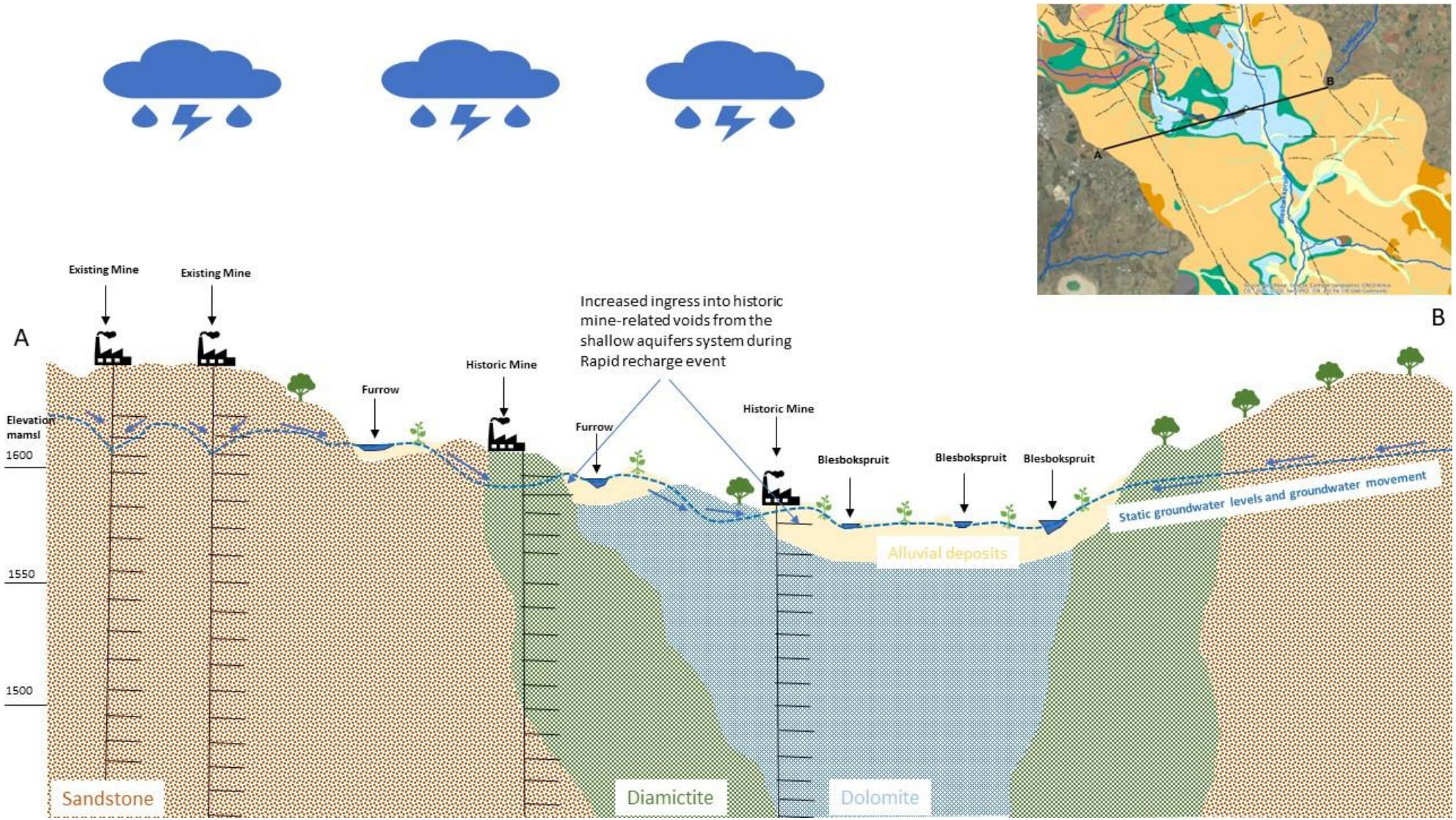

Figure 3-22 Ingress into Mine related open voids during rapid recharge events (not to scale).

Chapter 4 Numerical Groundwater Flow Model

The conceptual model paved the way for the numerical groundwater model construction and calibration as well as the scenario simulation that will inform the quantification of water ingress from the shallow aquifers into the mine related open voids during rapid recharge events. The conceptual model describes in theory how the groundwater static conditions may be influenced by rapid recharge events and to take the theoretical description from a conceptual representation to a real world representation will be the focus of the numerical groundwater model.

The data and information gathered and described in section 3.1.1 were used as the basic building blocks for the numerical model construction and to establish the model domain and dimensions as well as formulate the wireframe of the model domain. The data and information from section 3.1.2 were used to calibrate the numerical model to represent the current real world groundwater status of the sub catchment.

The calibrated model was then used to simulate the scenario described in Figure 3-22 where the shallow aquifer systems are allowed to get saturated during rapid rainfall events and the water ingress from the shallow aquifer systems can be recorded.

4.1 Model construction.

The numerical model was constructed using FEFLOW groundwater modelling software developed by DHI (FEFLOW, 2022). The software package is specifically developed to model groundwater flow and has applications in contaminant transport modelling however for the purpose of this model the groundwater flow application was used.

The numerical model construction included the sub-catchment area as the model domain. The model domain and mesh included a 3D finite element wireframe and was developed from mesh polygons adopted from the spatial data gathered and indicated in Section 3.1.1. The finite element array is developed by constructing triangles, each representing an element and the corners of the elements representing nodes. The geological units and associated aquifer systems, the tributaries and major rivers formed the basic building blocks for the mesh polygons and the topography represents the surface of the 3D domain.

The numerical model super mesh is indicated in Figure 4-1 which shows the length, width, and depth of the model domain. The 3D model domain is made up of 6 layers and 7 slices which

includes the top layer at 10 m thick to represent the unconsolidated profile for the alluvial deposits followed by a 30 m thick layer to represent a layer for the historic underground mining footprint. The third and fourth layers were included as 100 m thick layers to represent probable borehole depths where abstraction could take place. The fifth layer and particularly slice 6 represents the elevation (843 mamsl) at which Grootvlei mine is dewatering currently. The final layer and slice 7 represent the basement rock at an elevation of 500 mamsl (± 1130 mbgl).

The numerical model domain has a surface area of ±1073 km² and a volume of ±1198 km³. The total number of nodes and elements are 283 675 nodes and 481 890 respectively. The tributaries can also be seen in Figure 4-1 and correlates with the topographical depressions.

The model setting included an unconfined aquifer system and constrained at the top and bottom of the model domain. This setting ensures that the shallow aquifer gets modelled in unconfined conditions during the calibration stage and transient modelling process. The initial input to the constructed model in terms of recharge were assigned according to the rainfall records supplied and specifically the MAP from rainfall station 476766W that were used to assign recharge estimates to the different aquifer systems on the top layer. The recharge estimates that were estimated for the different aquifer systems according to the chloride mass balance as indicated in Appendix C and D were applied.

Similarly, the hydraulic conductivities that were gathered in section 3.1.2.4 were used to allocate aquifer parameters for the different geological units and associated aquifer systems.

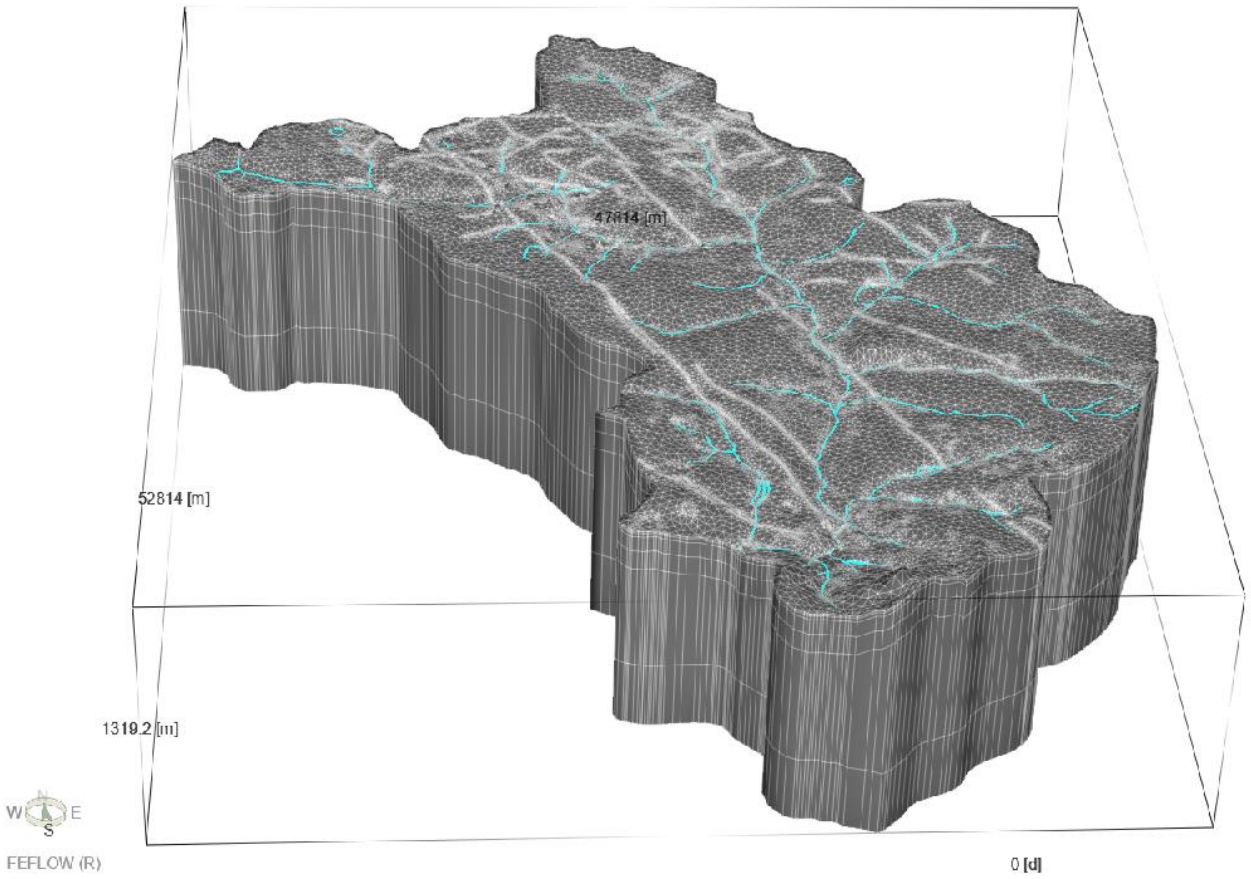

Figure 4-1 Horizontal and vertical finite element discretisation of the model domain, showing the surface features included (rivers, structures and mining outlines)

4.2 Model evaluation.

Model representation was conducted using the input parameters gathered from the site-specific data as indicated in Section 3.1.2. The model representation was done in steady state assuming static conditions over the sub-catchment area. The model input parameters for recharge and hydraulic conductivities are indicated in Table 4-1.

The alluvial deposits were assigned a recharge potential of 8% of MAP, while the sandstone and shales were assigned a recharge potential of 3% of MAP. The dolomite and limestone aquifers were assigned a recharge potential of at least 10% of MAP as these are major aquifer systems that could form karst formations and associates with high recharge potentials. The consolidated geology units and basement rock outcrops were assigned recharge potentials between 1% and 2,5% of MAP. The geological intrusions that may represent aquicludes (dolerite and diabase intrusions) were assigned a recharge potential of 0,5% of MAP and the faults structures 8% of MAP.

The hydraulic conductivities were assigned differently for some of the layers and are also indicated in Table 4-1. The alluvial deposits were only included in the first layer with a hydraulic conductivity of 1,6 m/d. The historic mining footprints were included only in the second layer and were assigned an assumed hydraulic conductivity of 0,4 m/d due to uncertainty of the underground voids being open or backfilled. The possibility that the historic underground workings may have collapsed also exists which implies lower hydraulic conductivities along the tunnels.

The sandstone and shale formations were assumed to only extent to layer 4 (roughly 250 mbgl) with an assigned hydraulic conductivity of 0,16 m/d. The dolomitic aquifer systems extend from surface to layer 5 and were assigned a hydraulic conductivity of 0,48 m/d. The consolidated geology units were considered to extend to layer 5 with hydraulic conductivities ranging from 0.08 m/d to 0,24 m/d. The granite and gneiss formations that forms the basement rock extends to layer 6 and were assigned a hydraulic conductivity of 0,016 m/d and the dolerite and diabase intrusions also extend to layer 6 with hydraulic conductivities of 0,072 m/d. The fault structures were also considered to extend to layer 6 and were assigned a hydraulic conductivity of 0,64 m/d.

The storage and compressibility input were considered to decrease with depth and were determined as a function of layer thickness for each consecutive layer. The top layer storage was assigned as 1,00E-04 decreasing to 2,00E-08 for layer 6.

The model calibration input parameters are represented visually in Figure 4-2, which shows the hydraulic conductivities assigned for each layer accordingly in the top insert and the recharge input in the bottom insert. The hydraulic conductivities that were assigned to the historic mining footprint on layer 2 are indicated in the top insert of Figure 4-3.

The Blesbokspruit and tributaries were assigned hydraulic head boundary conditions on the nodes associated with the rivers and tributaries to act as drainages at the specific elevations once the hydraulic head reaches these nodes. Similarly, nodes on slice 6 were assigned to act as drains at the location of the Grootvlei mine at elevation 843 mamsl to represent the dewatering component as indicated in Lea (2001). The dewatering component was calibrated at 27 000 m^3/d which is slightly lower than the reported average in (Scott, 1995) at 30 000 m^3/d that could come from the dolomitic aquifer system. The hydraulic head boundary conditions assigned to the nodes associated with the tributaries and the Grootvlei underground pump station are indicated in Figure 4-3 in the bottom insert.

Table 4-1 Numerical Model Input Parameters

Model geology	Hydraulic conductivity (m/d)	Storativity	Recharge (%)	Recharge (mm/a)
Layers one (unconsolidated geology)				
Alluvium	1,60E+00	1,00E-04	8,0%	58,8
Sandstone and Shale	1,60E-01	1,00E-04	3,0%	22,1
Basaltic lava	8,00E-02	1,00E-04	1,0%	7,4
Diamictite	1,20E-01	1,00E-04	2,5%	18,4
Dolomite and Limestone	4,80E-01	1,00E-04	10,0%	73,5
Quartzite and Conglomerate	2,40E-01	1,00E-04	2,0%	14,7
Quartzite and Shale	2,40E-01	1,00E-04	1,0%	7,4
Granite and Gneiss	1,60E-02	1,00E-04	1,0%	7,4
Diabase	7,20E-02	1,00E-04	0,5%	3,7
Dolerite Dykes	7,20E-02	1,00E-04	0,5%	3,7
Faults	6,40E-01	1,00E-04	8,0%	58,8
Layer two (Consolidated geology)				
Sandstone and Shale	1,60E-01	5,00E-06		
Basaltic lava	8,00E-02	5,00E-06		
Diamictite	1,20E-01	5,00E-06		
Dolomite and Limestone	4,80E-01	5,00E-06		
Quartzite and Conglomerate	2,40E-01	5,00E-06		
Quartzite and Shale	2,40E-01	5,00E-06		
Granite and Gneiss	1,60E-02	5,00E-06		
Diabase	7,20E-02	5,00E-06		
Dolerite Dykes	7,20E-02	5,00E-06		
Faults	6,40E-01	5,00E-06		
Historic Mined Out/ Backfilled Areas	4,00E-01	5,00E-06		
Layer three and four (Consolidated geology)				
Sandstone and Shale	1,60E-01	1,10E-06		
Basaltic lava	8,00E-02	1,10E-06		
Diamictite	1,20E-01	1,10E-06		
Dolomite and Limestone	4,80E-01	1,10E-06		
Quartzite and Conglomerate	2,40E-01	1,10E-06		
Quartzite and Shale	2,40E-01	1,10E-06		
Granite and Gneiss	1,60E-02	1,10E-06		
Diabase	7,20E-02	1,10E-06		
Dolerite Dykes	7,20E-02	1,10E-06		
Faults	6,40E-01	1,10E-06		
Layer Five (Consolidated geology)				
Basaltic lava	8,00E-02	5,26E-07		
Diamictite	1,20E-01	5,26E-07		
Dolomite and Limestone	4,80E-01	5,26E-07		
Quartzite and Conglomerate	2,40E-01	5,26E-07		
Quartzite and Shale	2,40E-01	5,26E-07		
Granite and Gneiss	1,60E-02	5,26E-07		
Diabase	7,20E-02	5,26E-07		
Dolerite Dykes	7,20E-02	5,26E-07		
Faults	6,40E-01	5,26E-07		
Layer six (Consolidated geology)				
Granite and Gneiss	1,60E-02	2,00E-08		
Diabase	7,20E-02	2,00E-08		
Dolerite Dykes	7,20E-02	2,00E-08		
Faults	6,40E-01	2,00E-08		

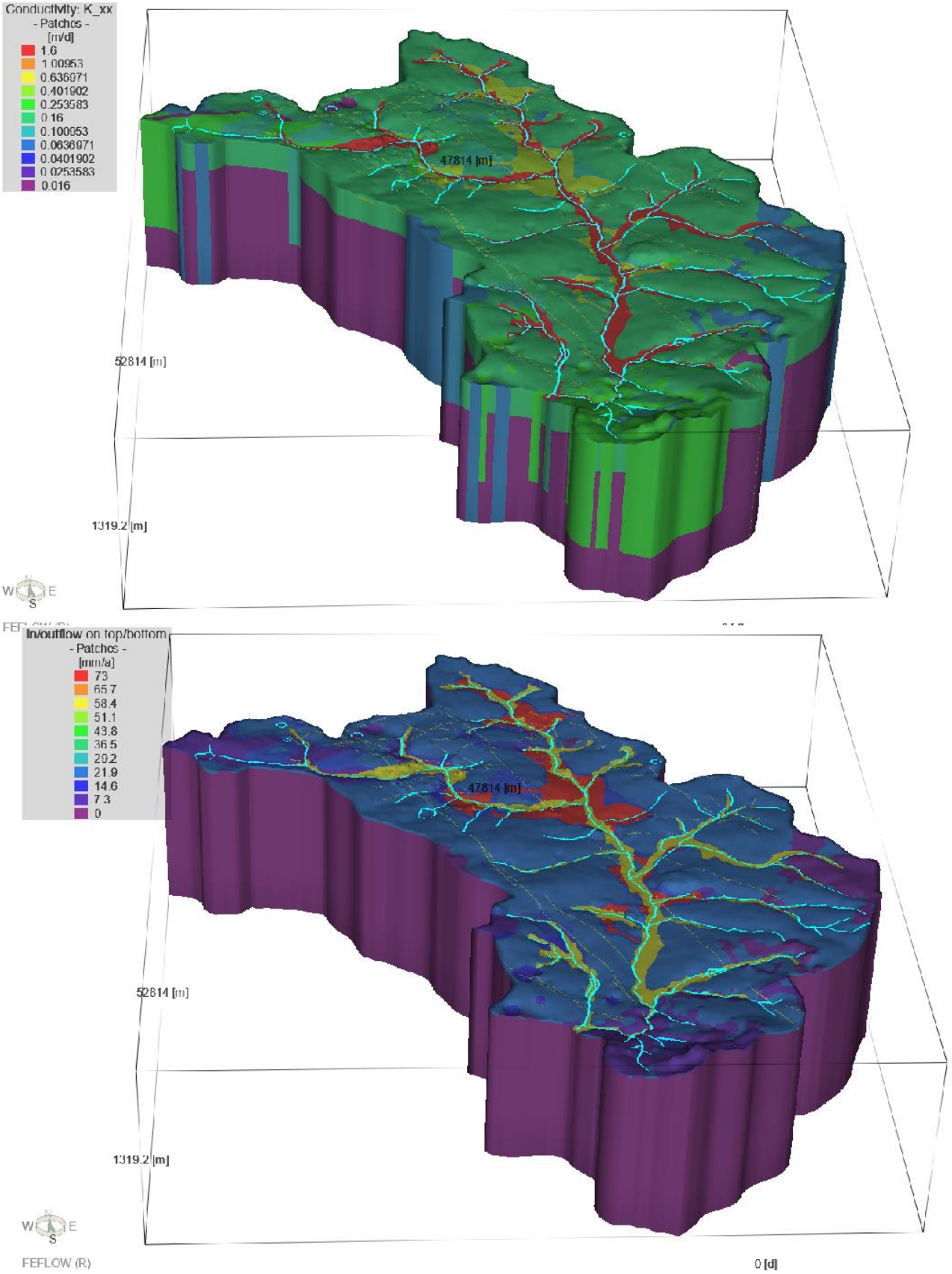

Figure 4-2 Model calibration input parameters: Hydraulic Conductivity and Recharge

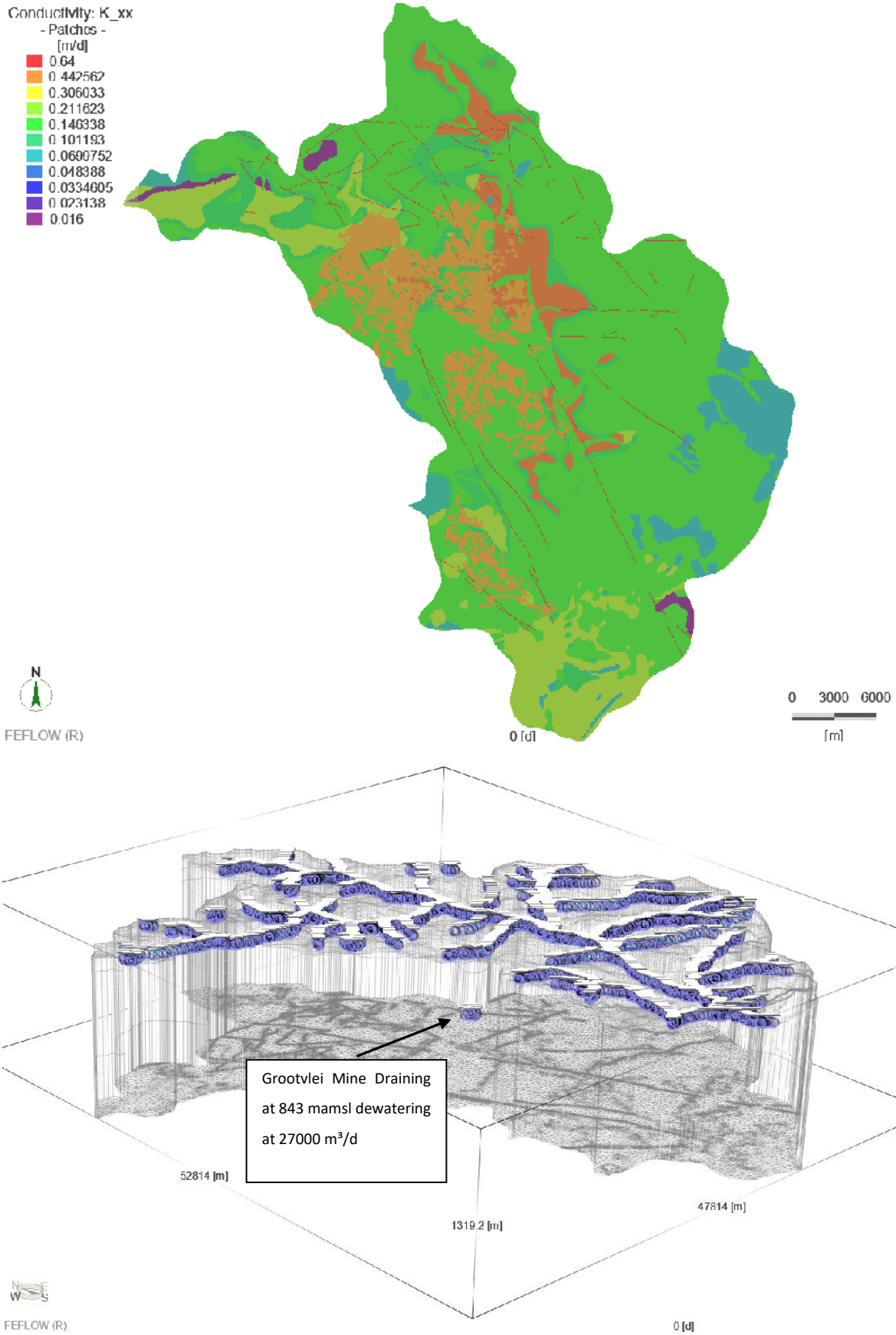

Figure 4-3 Model representation input: Historic Mine hydraulic conductivity and Hydraulic Head Boundary Conditions

To represent the steady state numerical groundwater in terms of groundwater flow regime it is required to include site-specific data and information such as measured groundwater levels and compare it to the simulated hydraulic head. The groundwater levels indicated in Section 3.1.2.3 were used for this purpose. The groundwater positions which are included in the sub-catchment and model domain indicated a correlation between measured hydraulic head and topography of only 8% and as mentioned may be due to dewatering and groundwater abstraction creating a dynamic aquifer system rather than a static aquifer system. This observation may cause difficulty in calibrating a groundwater flow model as the hydraulic head can be in a different status at any given moment.

For the purpose of this numerical model and the study objective it would be required to simulate the hydraulic head to represent as close as possible the measured hydraulic head even though the measured hydraulic head indicates a dynamic aquifer system for the sub-catchment. The correlation between the measured hydraulic head and simulated hydraulic head are indicated in Figure 4-4, with a correlation of only 9%. The correlation between topography and measured hydraulic head were estimated at around 8% indicated in Section 3.1.2.3 which implies a dynamic aquifer system influenced by groundwater abstraction and or dewatering from mining activities.

Due to this observation the representation and associated correlation between the simulated and measured hydraulic head would also indicate the dynamic nature of the aquifer and influences from abstraction and dewatering practices within the East Rand basin. The 45-degree line also indicates how some point correlate well with a few outliers. The simulated hydraulic head was plotted against measured hydraulic head and is indicated in Figure 4-5. From this graph it is clear which of the groundwater positions are causing the low correlation coefficient. These are C2N0113, DN70, DN71, DN57, DN46, DN31, DN30, DN38 and DN32.

The outlier locations were looked at individually and 8 out of the 9 measured water levels indicated deep measurements (between 66 and 138 mbgl) except for DN38 which had a shallow water level of 1.2 mbgl. This shallow water level may be an incorrect measurements or faulty input during the capture stage. The geographic setting of these boreholes also indicated that at least 90% of the deeper observations are located within farming areas and are probably used for water abstraction to farm steads. C2N0113 are located next to mining complex and may be used for water supply purposes for mine processing water. The possibly exists that measurements were taken before static water level conditions were reached after abstraction from these boreholes. The outliers were removed to evaluate the correlation between simulated and measured

hydraulic head as indicated in Figure 4-6 and Figure 4-7 and the correlation percentage improved to around 45% indicating the impact that a dynamic water from a few observation points can have during the model evaluation phase. The simulated hydraulic head compared to the measured hydraulic head also improved with the majority of simulated hydraulic heads below the measured hydraulic head to ensure the worst case in terms of surface to groundwater levels.

The calibration process has thus been applied to this modelling application, but due to the data-limitations, the model should not be considered “calibrated”. However, for the research purposes, the use of an “idealised” model is still deemed appropriate.

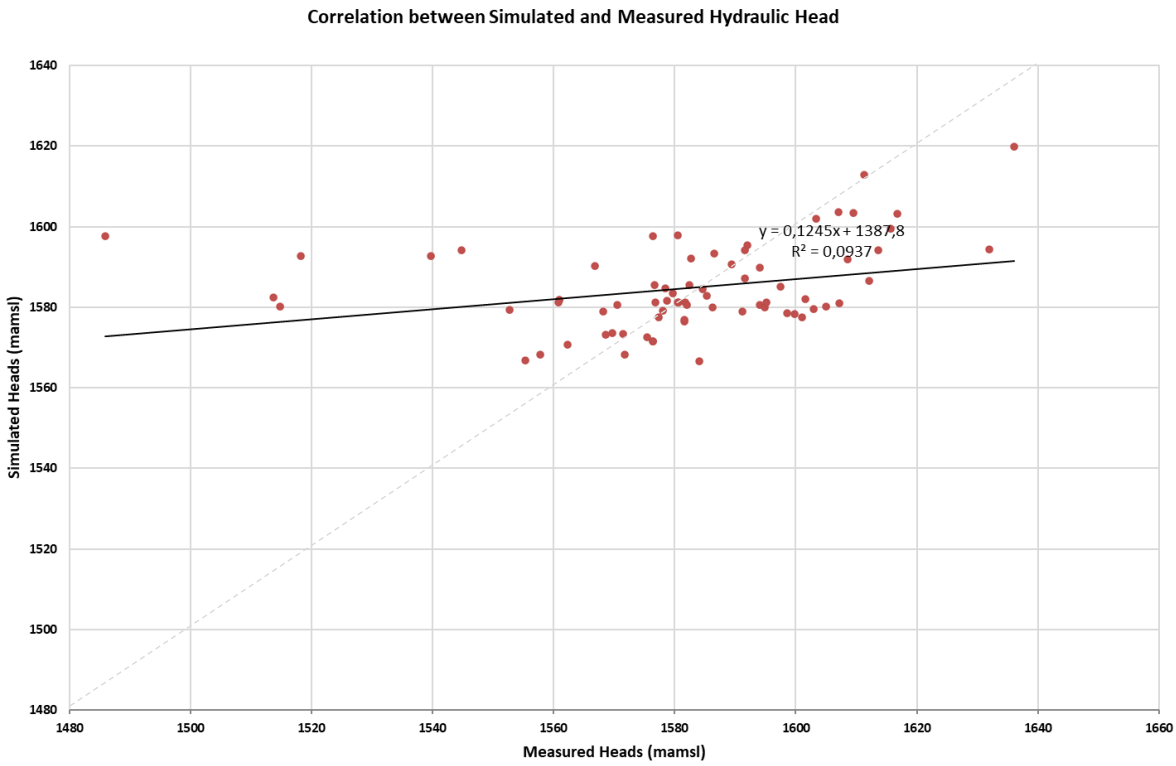

Figure 4-4 Correlation between measured and simulated hydraulic head.

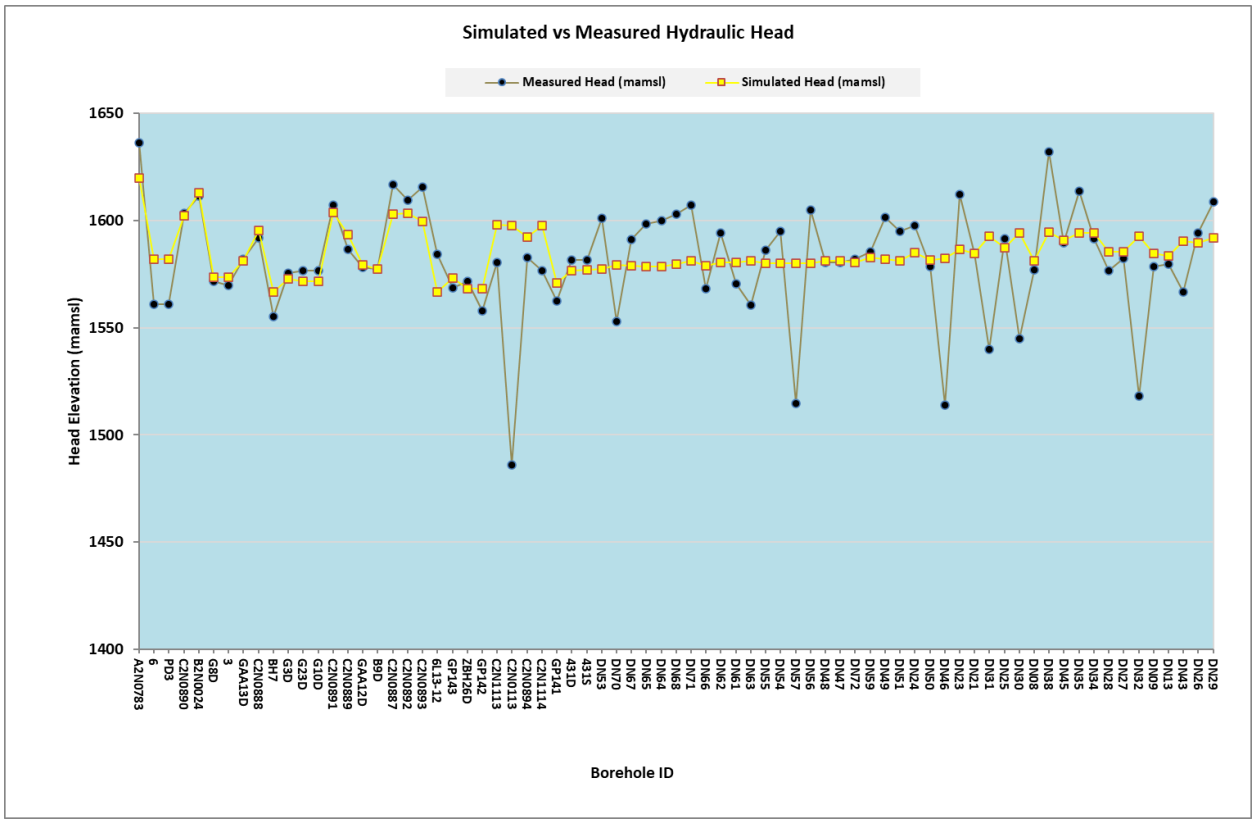

Figure 4-5 Measured vs Simulated Hydraulic Head

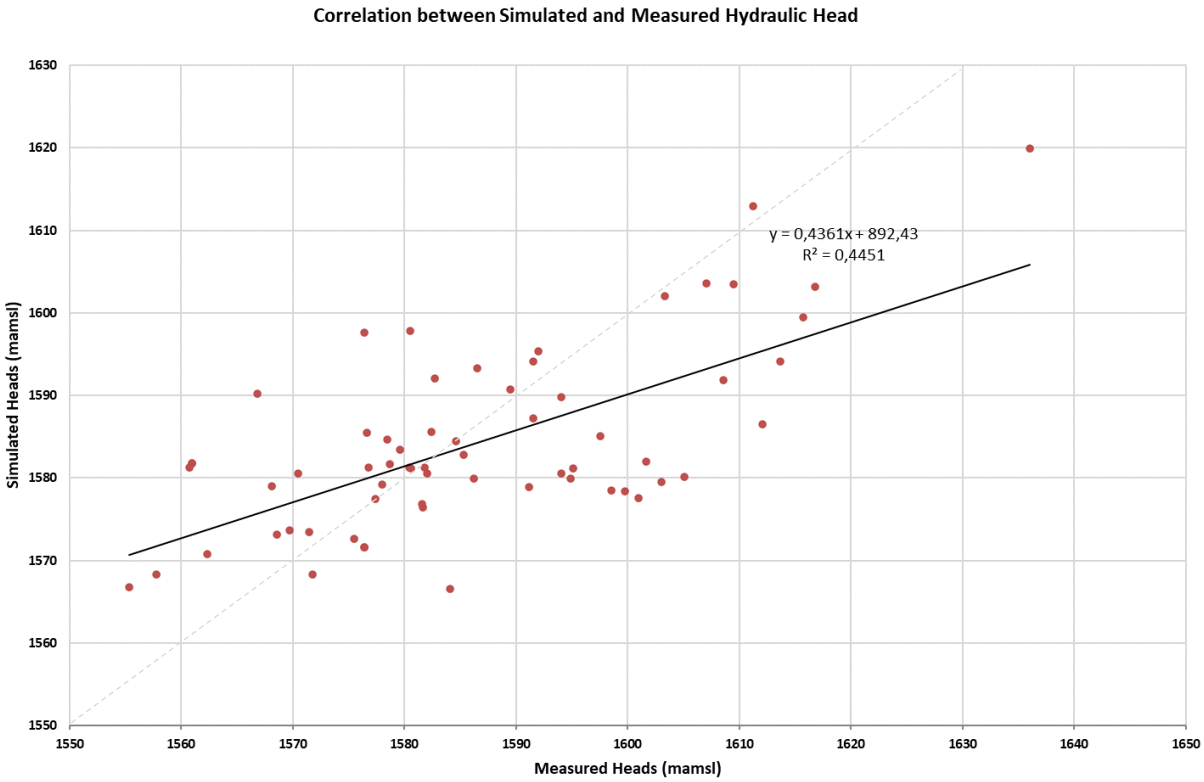

Figure 4-6 Correlation between simulated and measured hydraulic head excluding outliers.

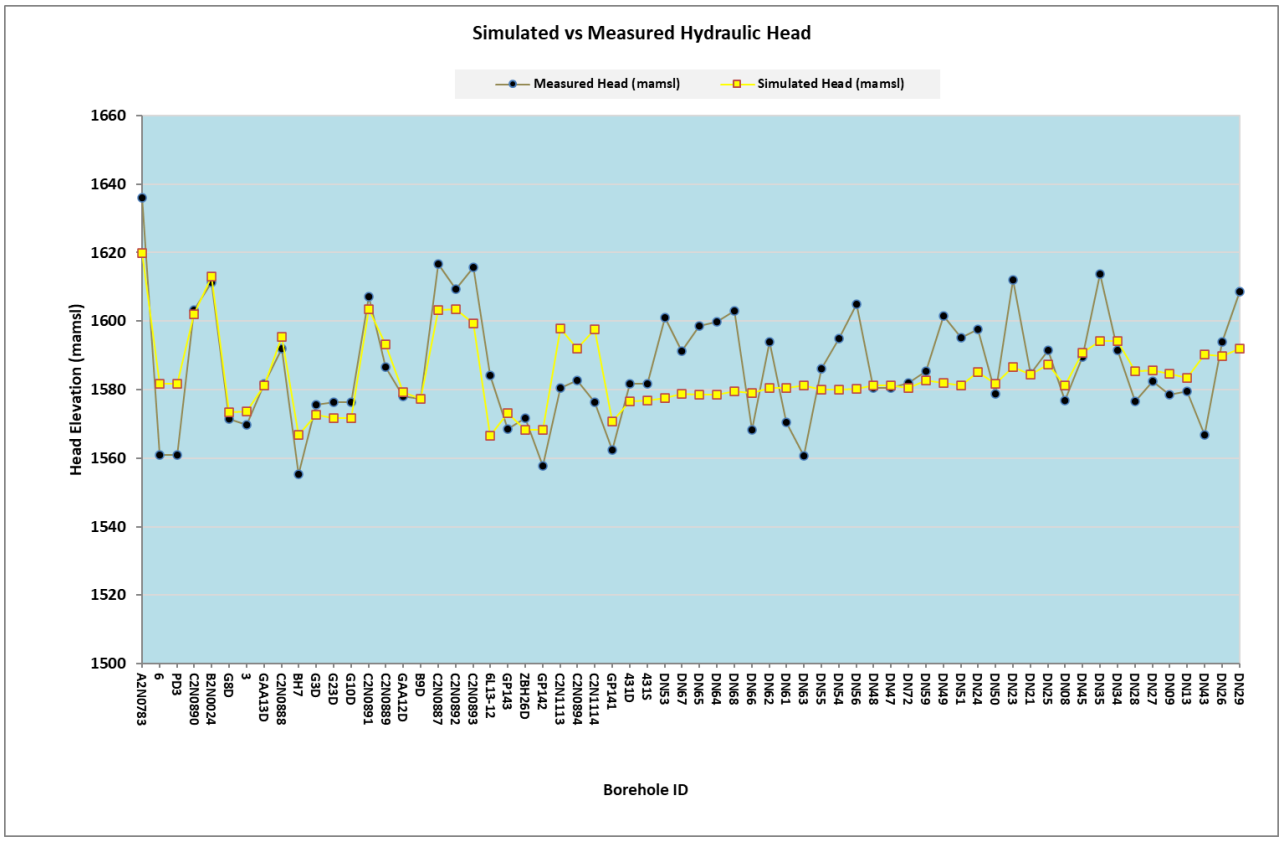

Figure 4-7 Measured vs Simulated Hydraulic Head excluding outliers

4.3 Simulation results

The simulated hydraulic head for the sub catchment area is indicated in Figure 4-8, indicating the hydraulic head distribution and contours. For the purpose of this model, and the fact the sub-catchment is mostly made up of dynamic aquifer systems, the simulated hydraulic head indicated in Figure 4-8 are considered sufficient for the current research purposes.

The simulated hydraulic head follows the surface drainage pattern regionally along the tributaries leading to the Blesbokspruit with increased hydraulic heads to the north and east of the sub-catchment. The lower hydraulic head follows along the Blesbokspruit with the lowest hydraulic head towards the south and where the Blesbokspruit exits the sub catchment. The hydraulic depression created by the deep dewatering from the Grootvlei mine indicates the hydraulic head to be around 1550 mamsl (± 30 mbgl) which is also indicated in Figure 4-8.

The simulated hydraulic head is compared with topography to ensure that the groundwater table is below topography for the regional area over the sub-catchment. To evaluate the surface to groundwater depth, a spatial calculation was conducted whereby the hydraulic head is subtracted from the topography at each node. The evaluation is indicated in Figure 4-9, which shows that isolated areas along the Blesbokspruit flood plain are above elevation which can be expected due to the hydraulic boundary conditions that were assigned to the main river system. The regional hydraulic head are below topography which is representative of the sub-catchment water table.

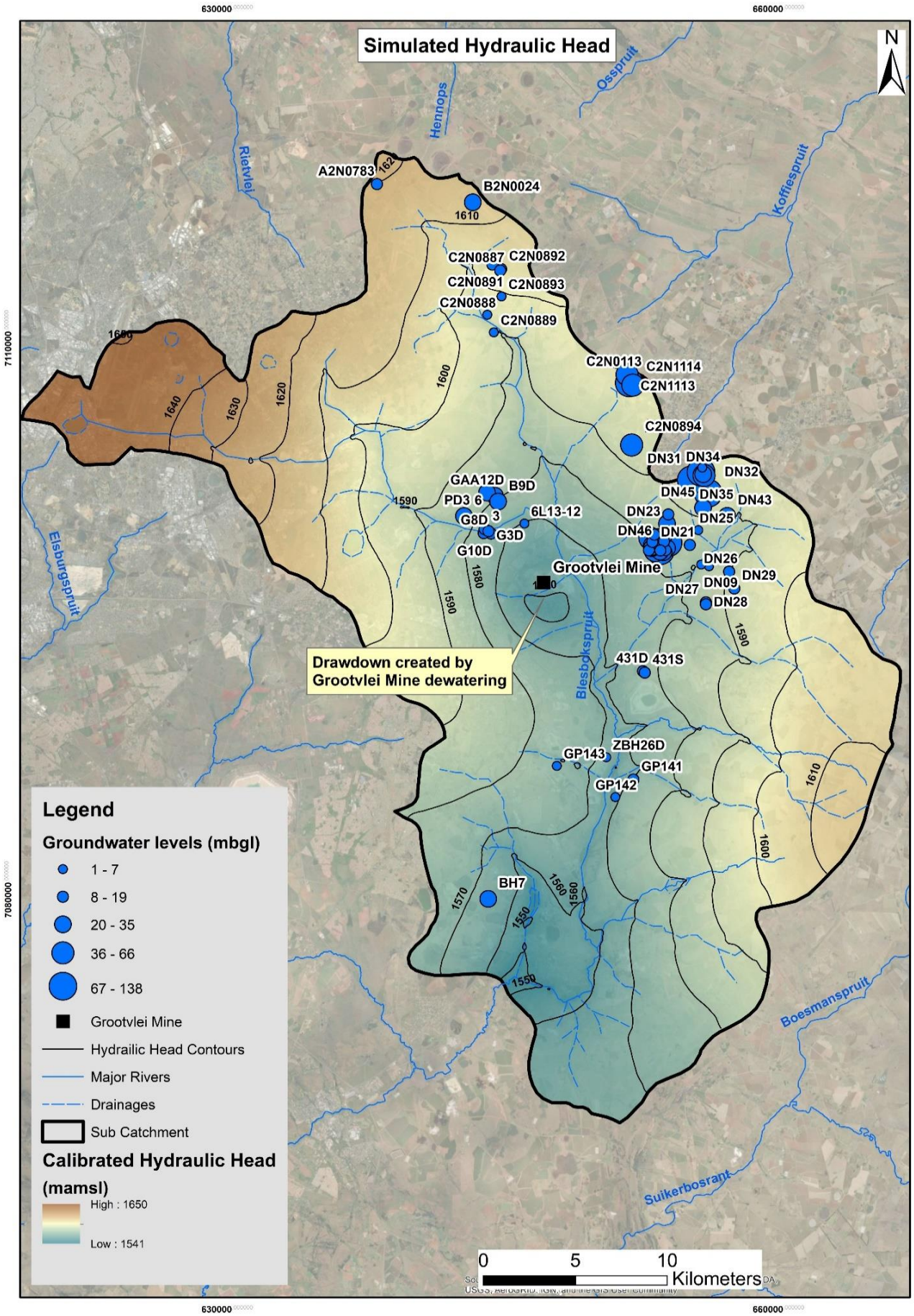

Figure 4-8 Simulated Hydraulic Head to represent the static groundwater conditions

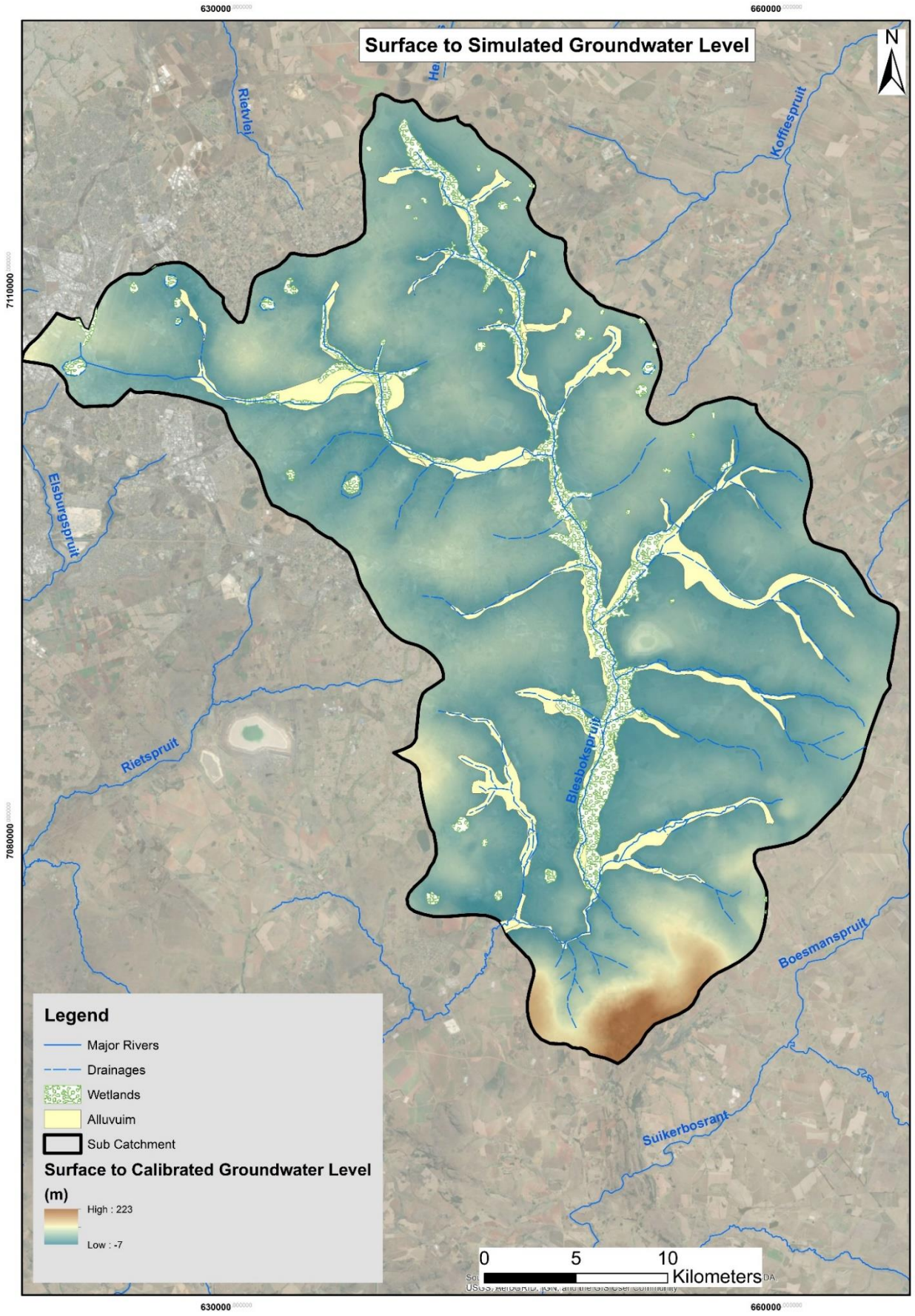

Figure 4-9 Simulated Surface to Groundwater Level to evaluate that hydraulic head is below topography

4.4 Model application: Shallow aquifer ingress into mine related open voids.

4.4.1 Numerical model application and model input

The modelling application was conducted to evaluate the possible ingress of water through the shallow aquifer systems to the mine related open voids located within the shallow aquifers during rapid recharge events to the shallow aquifer systems during heavy rainfall periods.

In order to achieve the transient modelling objective, the following input would be required:

- The areas that can be considered as shallow aquifer systems along the main tributaries and the Blesbokspruit and could potentially get flooded during heavy rainfall events.
- Mine related open voids like historic shafts or mapped surface voids caused by historic mining activities that falls within the shallow aquifer areas and may receive influx of shallow aquifer groundwater during the rapid recharge events.
- Rainfall record of the project area to evaluate possible flooding events over a few years (at least 3 years)

The areas that were considered as the shallow aquifers for the transient simulations was a combination of the wetlands and alluvial deposits described in earlier sections (3.1.1.2 and 3.1.1.3) The wetlands and alluvial deposits were combined to represent areas that may receive rapid recharge when the major tributaries and Blesbokspruit flood.

The available mine related open voids described in Section 3.1.2.5 that falls within the shallow aquifer systems were selected to the combined alluvial and wetland areas which are indicated in Figure 4-10. The total number of mine related open voids from the acquired data set that falls within the shallow aquifer systems were estimated at 33 and mostly located along the furrow stream that leads east towards the Blesbokspruit. The mine related open voids were assigned to the first layer as discrete features which are described by (FEFLOW, 2022) as being finite element objects of dimension that's lower than dimensional elements of the model. Discrete features can be added to an existing FEFLOW mesh to represent a 1 or 2 dimensional features such as tunnels, pipes, drains, faults and in this case the mine open voids. The discrete features were assigned to mesh edges located at the specified open mine voids with assigned cross sectional areas assumed at 1 m^2 and hydraulic conductivities assumed at 100 m/d to represent an open void to semi open void as some of the old mining tunnels may have collapsed or backfilled.

The rainfall records that were considered for the transient simulation was taken from station 476766W as indicated in section 3.1.2.1. Rainfall records from January 1994 to December 1996

were taken as the time dependant rainfall and associated recharge for the transient simulation. The recorded rainfall over the 3-year period indicated relatively high rainfall figures compared to the overall recorded years and a possible flooding event in February 1996.

The same percentages that were applied during the steady state calibration process for the different aquifer systems were used to determine the time dependant recharge from the actual monthly rainfall which is tabulated in Appendix F.

4.4.2 Model application criteria.

The transient simulation time was assigned over a three-year period and the modelling time steps set as daily time steps to accommodate for rapid rainfall over a one-day period. Monthly time periods were considered at 30 days. The 3-year rainfall record indicated close to, or above 100 mm/month for at least 14 months. As daily rainfall data is not available it was assumed that the rapid rainfall and associated rapid recharge to shallow aquifer systems would happen at daily time steps associated with a 30 day rainfall period.

A selection of nodes was made over the shallow aquifer area and the elevations for these nodes were used to add 0.2 m to 1 m to the surface elevations for each node. These increased surface elevations were assigned to the nodes representing the saturation of the shallow aquifer system at a specific time step for a one-day period to increase the hydraulic head. The reasoning behind this approach is to raise the hydraulic head within the shallow aquifer areas to between 0.2 m to 1 m above the surface elevation of the shallow aquifer system and ensuring that the shallow aquifer systems get saturated for the one-day flooding event. During this flooding event as the shallow aquifer system gets saturated then water will flow into the mine related open voids which has been assigned as discrete features and the inflow rates can be recorded over the one-day flooding event and during the recovery period after the flooding event has occurred as the groundwater system returns to static.

A rainfall event below 150 mm/month were assigned an increase head elevation of 0,2 m and 0,4 m for rainfall event that had more than 150 mm/month. The same sequence was applied for 0,6 m and 0,8 m at rainfall events lower than 250 mm/month and over 250 mm/month respectively. The major rainfall event in February 1996 were assigned an increased hydraulic head elevation of 1 m. The dates, rainfall, time steps and hydraulic head lift at each step are summarised in Table 4-2.

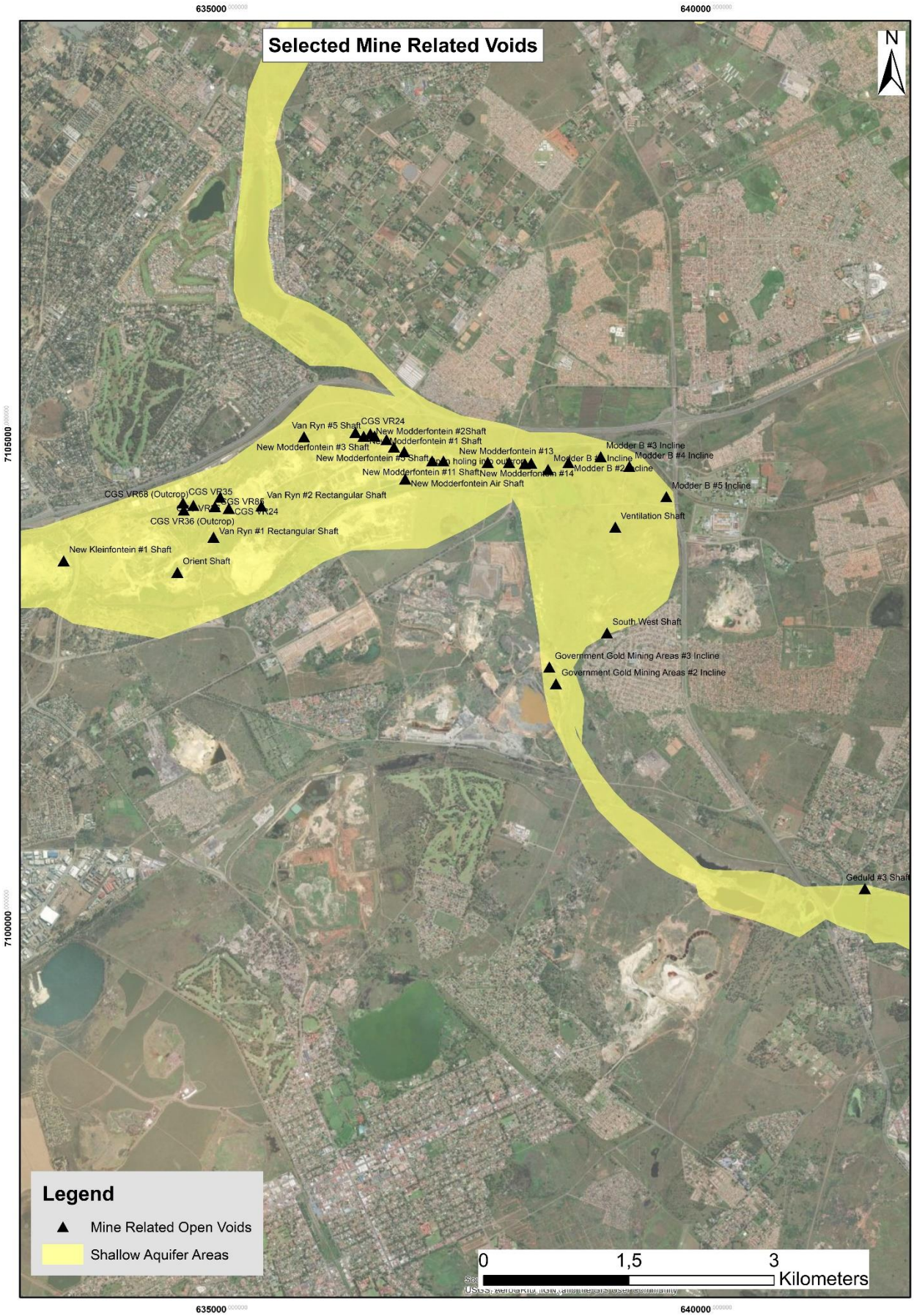

Figure 4-10 Selected mine related voids to the shallow aquifer systems.

The hydraulic head lift over the shallow aquifer systems were deactivated after the one-day time step were complete and the original hydraulic drains over the tributaries and main rivers were activated again to represent the normal surface draining from the model drainages. The simulation was then allowed to continue until the next rapid recharge event and associated hydraulic head lift until the final simulation time of 1050 days was achieved.

Table 4-2 Time steps at which hydraulic head needs to be raised during elevated rainfall.

Date	Rainfall (mm/month)	Time step (day)	Assumed hydraulic head lift above elevation (m)
Feb-94	172,7	30	0,4
Oct-94	99,7	270	0,2
Nov-94	181,5	300	0,4
Jan-95	261	360	0,8
Mar-95	114	420	0,2
Sep-95	217,2	600	0,6
Oct-95	173,3	630	0,4
Nov-95	189,4	660	0,4
Dec-95	265,3	690	0,8
Feb-96	305,3	750	1
Apr-96	126,6	810	0,2
Oct-96	142,8	990	0,2
Nov-96	174,2	1020	0,4
Dec-96	101,3	1050	0,2

4.4.3 Model application results.

The transient simulation results included the hydraulic head increases as the rapid recharge events occur as well as recorded inflow rates at the different mine related open voids located within the shallow aquifer system.

The hydraulic head increases at each of the mine related open voids are indicated in Figure 4-11 that shows the hydraulic head plotted over time. The static groundwater levels ranged between 1594 mamsl and 1616 mamsl. When the shallow aquifers get saturated during the rapid recharge event then groundwater levels can increase between 15 m to 20 m. The gradual return to static groundwater conditions after each rapid recharge events is also indicated during the dryer parts of the year however during the wet seasons static conditions are not achieved as consecutive rapid recharge events could steadily increase the over hydraulic head yearly. This observation may imply decanting potential over a number of years however wet periods followed by dry periods may also reduce the yearly hydraulic head rise for conditions to return to original static state and even lower than normal hydraulic head levels. Rising groundwater levels were reported

at the Sub-Nigel No. 1 Shaft at a rate of 0.3 to 0.4 m/d (Waal, 2013) and the consecutive ingress from rapid recharge could contribute to this rise in groundwater levels.

The recorded shallow aquifer seepage rates during the rapid recharge events are indicated in Figure 4-12. The inflow rates were plotted as logarithmic values to better illustrate the peaks during the rapid recharge events. During static conditions inflows to the mine related open voids can range between less than 0.5 m^3/d to ± 10 m^3/d. When the shallow aquifers get saturated and rapid recharge increase seepage to the open voids, the inflows can increase to between 900 to just over a 1000 m^3/d over a short period until the rain events stops. The gradual return to static seepage rates also happens in a short period (less than a day) which supports the observation and assumption that a sudden event occurred.

In order to compare the modelled results with similar ingress rates reported in similar studies focusing on ingress quantities from surface sources such as the Blesbokspruit, Leeupan, Cowles Dam, Van Rhyn Channel, Gravelotte, Largo, and West Pits are a good indication of the ingress potential during different climatic conditions into the East Rand basin are indicated in Waal (2013) and summarised in Table 4-3. The combined ingress of water from the surface water sources to the mine void indicated in Table 4-3 shows that during average precipitation periods approximately 82 000 m^3/d can flow into the mine void.

The numerical model results indicated 54 655 m^3/d that can flow from the shallow aquifer system to the mine void. This implies that roughly 64% of water ingress from surface sources can come from the shallow aquifer system and interaction with the deep aquifer systems as well as the direct link with the mine void. The reported ingress rates during extreme wet conditions indicated in Table 4-3 are approximately 108 000 m^3/d and the modelled ingress from the shallow aquifer systems during a flooding event indicated ± 145 000 m^3/d. The modelled ingress rates are 36 % higher than the reported ingress during the wet conditions and may imply that the shallow aquifer systems when saturated could yield higher ingress rates.

The cumulative ingress rates are indicated in Figure 4-13 which shows the total ingress rates from the mine related open voids. A maximum of ± 12 000 m^3/d can ingress into the mine related open voids during a flooding event. This figure relates only to the 33 mapped voids and there could be more un-surveyed open voids along the entire Blesbokspruit and associated shallow aquifer systems.

This observation implies that approximately 8 % of water ingress could come from less than 50 % (69 total indicated mine related open voids (Figure 3-20) of the mapped shafts and ingress positions located in the northern part of the east rand basin and this percentage could be higher once more ingress positions are identified and mapped.

Table 4-3 Water ingress during different climatic conditions for the east rand basin (Waal, 2013)

Rainfall	MAP (mm)	Change in MAP (%)	Predicted ingress (ML/d)	Change in ingress (ML/d)
Average	727	0	82	0
Dry	452	-37,83	77	-6,1
Wet	990	36,18	87	6,1
Extremely Wet	1439	198,07	108	31,7
Climate Change	**1100**	**40**	**90**	**9,8**

The hydraulic head increase during each rapid recharge are spatially indicated in Figure 4-14 which shows how the groundwater levels rise in the shallow aquifer systems during the flooding event with rainfall >300 mm. The increased hydraulic head is more evident over the mine related open voids located along the northern part of the furrow channel that leads towards the Blesbokspruit. The anticipated hydraulic head rise in close proximity to the Grootvlei Mining area could also be influenced by the drawdown created from the underground dewatering, however, the direct connection and associated flow between the shallow aquifer systems and the deeper bedrock aquifer may be not as sudden during the rapid recharge event.

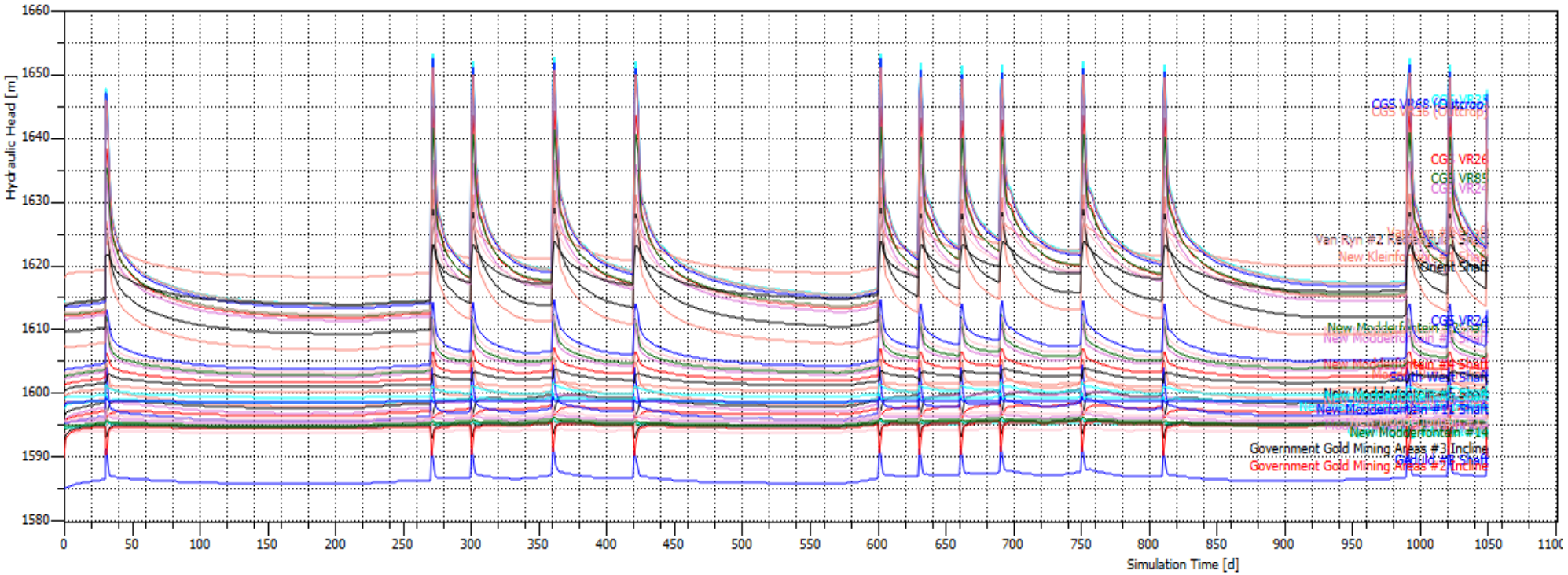

Figure 4-11 Hydraulic Head increases during the rapid recharge event.

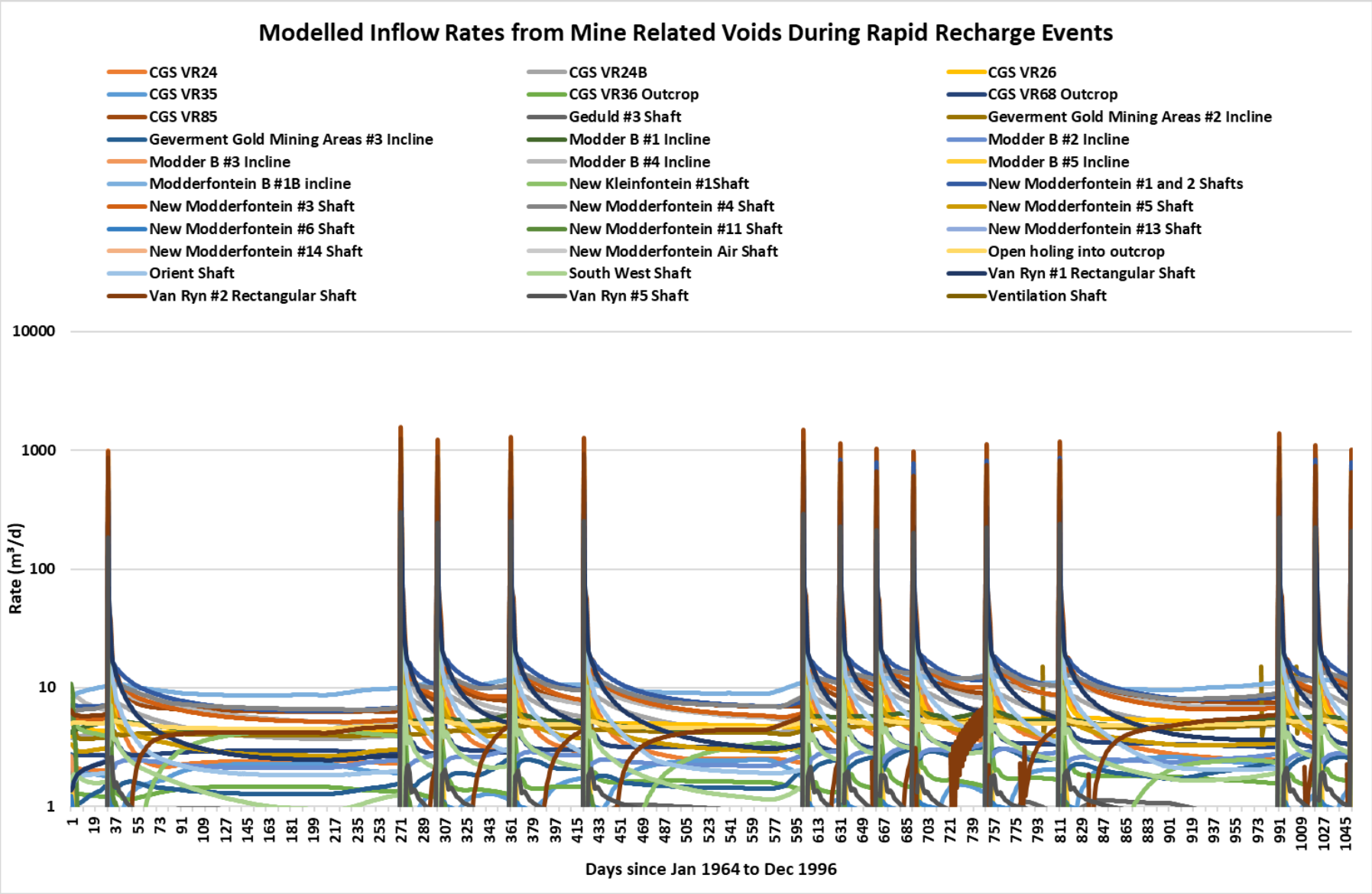

Figure 4-12 Estimated inflows rates during the rapid recharge events.

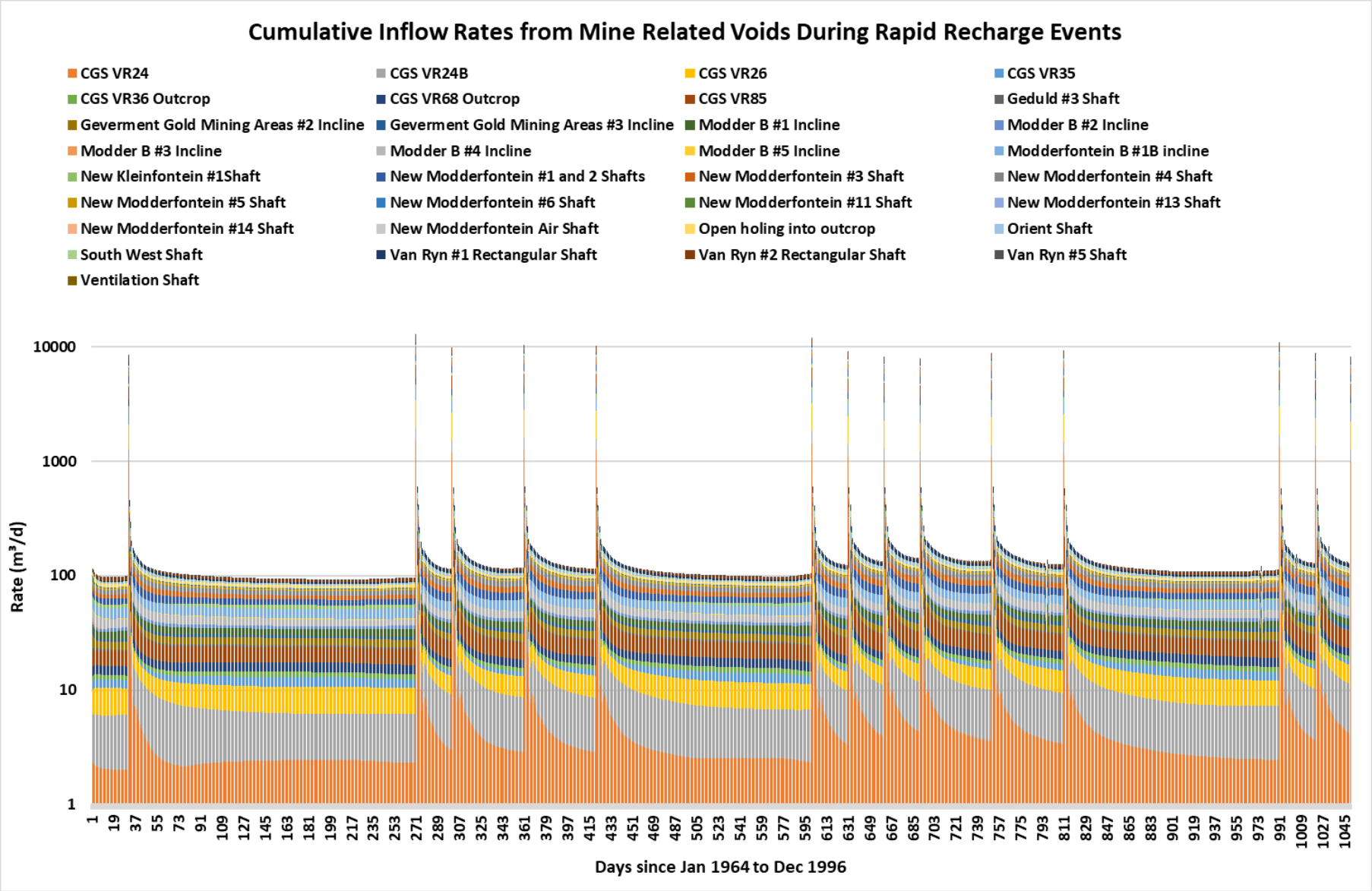

Figure 4-13 Cumulative inflow rates during the rapid recharge events from the mine related open voids.

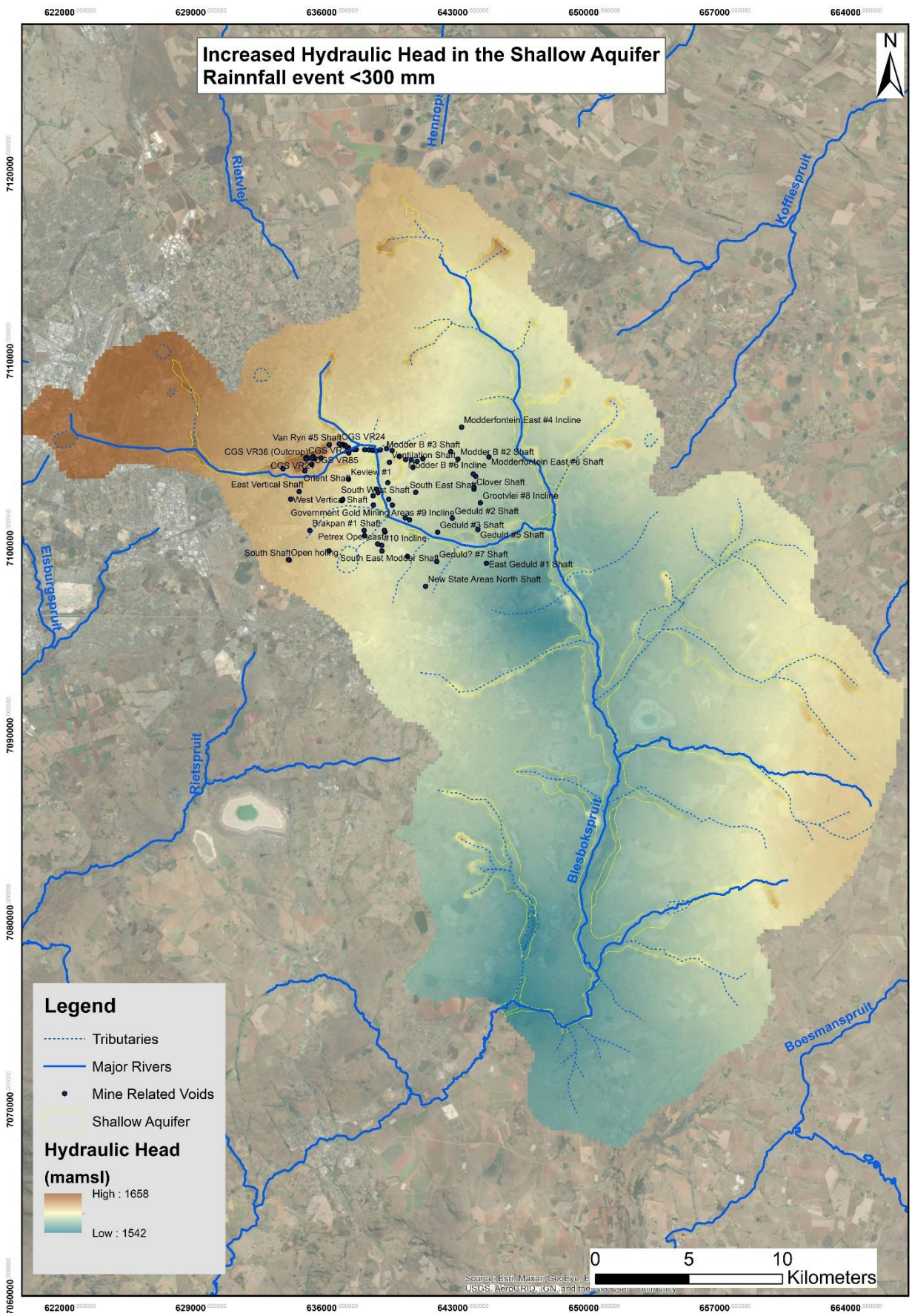

Figure 4-14 **Hydraulic head increase during rainfall events: Rainfall event >300 mm.**

Chapter 5 Discussion of Numerical Groundwater Modelling as a Tool to Quantify Shallow Aquifer Water Ingress through Mining-Related Open Voids

The research question stated that is there a possibility to employ groundwater modelling as a tool to quantify water ingress rates and volumes into mine related open voids through shallow aquifer systems during rapid recharge events. The case study conducted as part of the research and to address the research question may in part answer this question.

A groundwater model was constructed and simulated according to spatial and site-specific data to represent the actual real groundwater conditions. The representative groundwater model was used to simulate the rapid recharge events to the shallow aquifers and the ingress into the mapped mine related open voids during the rapid recharge events were recorded. The shallow aquifer systems were identified by means of a GIS operation that combined the alluvial deposits and the wet land areas along the main rivers and streams and the mapped open mine related voids that fell within the shallow aquifer systems were identified also with the GIS operations.

To accurately simulate the ingress through these open mine related voids it was required to saturate the shallow aquifer systems during an increased recharge event. In order to simulate the scenario that best represent the rapid recharge to the shallow aquifer systems, a rainfall record that indicated possible flooding events were required and this rainfall record were applied as time dependent recharge to the numerical model. The open mine related voids were assigned as discrete features to represent an open area that extends through to the historic mine workings and footprint and act as conduits for water flow from the shallow aquifer systems.

The approach to record the ingress volumes and rates was to identify the possible flooding events from the rainfall record and applied time dependant recharge to saturate the shallow aquifer by raising the hydraulic head at specific elevations above the surface over the shallow aquifers during the increased recharge event. This approach would represent the rapid recharge of the shallow aquifer system and the inflows into the mine related open voids could be recorded during the rapid recharge event as well as the return to static once the rapid recharge event occurred.

The scenario simulation was able to record the inflow rates during the rapid recharge events. The open voids represented as discrete features were selected individually and the inflow rates were

extracted for the simulation period. The results indicated the rapid increase at each open void that fell within the shallow aquifer zones and compared to ingress rates reported in a similar study conducted by (Waal, 2013), which at this stage are the only study available for reporting quantified ingress rates for the East Rand basin. The numerical model and modelling approach were able to quantify ingress rates for each of the mine related open voids that fell within the aquifer system (33 out of 69 mapped positions) and indicated that a maximum of 12 000 m^3/d could come from less than 47 % of the mapped mine related open voids. The inflow rates for the individual open voids ranged from 900 m^3/d to 1000 m^3/d. Compared to the ingress rates reported by Wall (2013), shallow aquifer ingress through the mine related voids can contribute almost 16% of water from surface water ingress sources and this rate is from less than 50% of the mapped open voids.

In addition, groundwater level rise during the rapid recharge event could be recorded at the mine related open voids, with the observation that consecutive rapid recharge events could lead to surface decanting over a longer period that was modelled for.

The numerical model constructed for the case study was constructed and simulated according to data and information gathered from literature and groundwater studies conducted in the East Rand Basin, which are mainly available in the public domain. The represented hydraulic head were considered sufficient for the purpose of the modelling approach even though the aquifer conditions are in a dynamic state regionally. It is important to note that due to the lack of insufficient groundwater level data and outdated measurements that the calibration process could only be as accurate as the data and information presents itself. The purpose of this groundwater model, which is to indicate that numerical groundwater modelling can be used as a tool to quantify water ingress and make use of an idealised numerical groundwater model, as long as the uncertainty is accounted for in the analyses.

The acquired data and information limit the accuracy and confidence in the numerical model output, however comparable ingress rates as indicated in Section 4.4.3 showed that the model outputs and results are within range of studies conducted previously in terms of ingress volumes and rates.

The following model limitations and assumptions needs to be noted:

- The topography data used were only available at 30 m spacing and more recent detailed topographical data can be used to add confidence in the numerical model elevations.

- The limited groundwater levels gathered from the different sources creates clusters on focused areas which if considered in a regional sense indicates the low correlation between hydraulic head elevation and topography. The model is limited to be calibrated according to these clustered groundwater levels and assumes the highly dynamic nature of the regional groundwater regime.
- The model was calibrated according to out-dated data such as groundwater levels and rainfall. The current state of the aquifer system for the sub-catchment area may look much different today compared to when the data was recorded. The model assumes the steady state calibration conditions to represent historic groundwater conditions.
- The limited information of active mining operations in the sub-catchment area may also influence the groundwater regime. The model assumes dewatering from the Grootvlei Mine only at the reported dewatering rates and was calibrated accordingly. Additional mining activities in the sub-catchment area could imply increase drawdown depressions in hydraulic head over a wider area which may influence the recovery periods and hydraulic head increases from the observed mine related open voids.
- The model only assumes groundwater abstraction from the Grootvlei mine and as mentioned additional mining activities can also change the how the groundwater regime looks like currently, however privately owned boreholes that supplies water for irrigational and domestic purposes were not included and this additional groundwater abstraction component could also influence the groundwater system.
- The modelling approach to simulate the saturation of the shallow aquifer system assumes an unconfined aquifer system and represents the saturated zones below surface. The Richards equation mentioned in section 2.2 can be employed to simulate the unsaturated zone above the water table to see the effect of saturation during flooding, however this approach would require a lot of additional input data for calibration purposes and the transient simulation.
- Research conducted for similar type studies that indicates quantified rates and volumes only yielded one (Waal, 2013), which could be used to compare the modelled output. The assumption that the modelled results are within range of the reported rates and volumes from (Waal, 2013) may limit the validity of the observations.

Apart from the numerical modelling limitations and assumptions there are certain more general limitations and assumptions that also need to be considered in terms of the research approach

and available literature on similar studies that looked at quantifying ingress rates through open voids.

The literature study conducted for similar studies that focused on quantifying rates and volumes through open voids as well as approaches and methods to conduct such studies are limited and only indicating general rounded figures on a regional scale rather than focusing on individual open voids (Coetzee, 2022). The limited literature information and accessible information on modelling methods to determine the individual ingress rates into an open void make it difficult to compare the approach followed and validity of the results. One way to confirm this approach would be to consult with the software package developers and associated hydrogeologists to validate and confirm the approach as part of standard protocol to determine ingress through open voids.

At this stage the ingress rates and volume were based on a saturated level at an assumed elevation for the shallow aquifers that indicated ingress rates that's relatively within the range indicated by (Waal, 2013). The model scenario can be simulated in terms of sensitivity analysis and calibrated to inflows compared to surface water flows from surface water studies conducted for the Blesbokspruit catchment area and associated flooding rates and volumes by raising the hydraulic head at levels that correlates to the surface water study results. The comparable ingress rates will then provide more accurate inflows through the open voids once the shallow aquifer is saturated during flooding.

The current understanding of the interaction between the shallow aquifers systems and surface water are vague, which needs more characterisation especially in the flood plain areas along the rivers and streams. The same applies for the interaction between the Blesbokspruit and the dolomite (Malmani dolomites) formations where surface water may ingress directly to the deeper aquifer systems.

The case study has proven that ingress rates from the shallow aquifer systems through mine related open voids can be quantified individually during rapid recharge events as well as during static conditions for voids on a regional scale. The quantified rates are comparable to ingress rates formulated by similar studies conducted for the East Rand basin.

The conducted case study represents a contribution in addressing the research question regarding the application of groundwater modelling as a tool to quantify water ingress rates into mine-related open voids during rapid recharge events. The simulation approach whereby spatially, site specific data and a representative groundwater model were employed to quantify ingress rates

and volumes into shallow aquifer systems during dynamic and static conditions motivates the opportunity to this approach. The results indicated the substantial contribution (up to 16%) from shallow aquifer ingress through mapped mine-related voids, gives better perspective on a critical aspect of water dynamics within the studied area. By offering a quantitative understanding of ingress rates on a regional scale, this research not only confirms previous findings but also provides a methodological framework and modelling approach to accurately assess and monitor water ingress from shallow aquifer systems into mine-related voids. This comprehension holds immense relevance for both hydrogeological studies and the management of groundwater resources, particularly in regions affected by historic mining activities, contributing significantly to the broader understanding of groundwater-surface water interactions.

Chapter 6 Conclusions and Recommendations

The research conducted for the dissertation indicated that limited studies have been conducted to quantify the ingress of water from aquifer systems into open voids on a regional scale. Additionally, limited studies have been done in terms of modelling approaches to look at the effect that the direct link between rapidly recharged aquifer systems and associated water quantity and quality could have on deeper aquifer systems or mined out areas. The main limiting factor in applying a modelling approach for conducting studies related to water ingress driven by rainfall events and rapidly recharging shallow and perched aquifer systems is data availability, data accuracy and lack of site-specific information.

There are numerous software packages that area available to conduct numerical modelling approaches and simulate water ingress scenarios with constant improvements on applications and methods of applying interactions between surface and groundwater systems. However, one major issue is the application of the open voids to such groundwater models especially on a regional scale.

The research aims and objectives were met through the case study and the numerical model assessment conducted for this dissertation which indicated that groundwater modelling methods can be used as a tool to simulate the ingress of water from shallow aquifer systems into mine related open voids. The research data and information available for the case study were used to construct and represent a numerical groundwater model and a scenario simulation were conducted with site-specific data that produced quantified inflow rates from the shallow aquifer systems through the mine related open voids during consecutive increased rainfall events that can infiltrate the subsurface aquifer systems and, in this case, a large majority of ingress towards the historic mine workings. The location and setting of the East Rand basin and the historic mining history creates the ideal conditions to conduct an assessment to look at the possibility of using numerical modelling as a tool for the desired objective, which was achieved.

The numerical modelling assessment also implies that the same approach may be employed to look at inflow rates and volume to other aquifer systems and open voids in general that intersects the sub-surface aquifers at depth.

The quantification of inflow rates through open voids and especially during heavy rainfall events can be used in further studies related to:

- Water quality and how the shallow aquifer water can affect the dilution properties of groundwater.
- Decanting potential in terms of locality and outflows as well as the impact on environmental and social receptors.
- Identification and prioritisation of specific open voids that can be capped to reduce the increase inflows during heavy rainfall events and subsequent effects.
- Improve on stability investigations for karstic aquifer systems that may be affected by the increased weathering potentials from excessive groundwater inflows by capping certain open voids.
- Determining possible inflows that can be expected in future underground mining activities and how shallow aquifer ingress during heavy rainfall events can contribute to inflows to the deeper aquifers.

There are certain limitations and challenges to the accuracy and confidence of the modelling calibration and approach, as indicated in Chapter 6. However, the numerical model produced quantitative ingress rates during rapid recharge events through the mapped mine related voids from the shallow aquifer systems included in the East Rand basin that are comparable to similar studies conducted for this area

The study conducted has produced significant insights into the relationship among mining activities, groundwater systems, and the role of numerical modelling. By exploring previously uncharted territory in quantifying water ingress from aquifers into open voids, this research addresses critical knowledge gaps and sheds light on the potential implications for environmental sustainability and resource management. Despite challenges, the use of numerical models emerges as a promising tool to anticipate and manage risks associated with rapid recharge events, influencing groundwater quality and stability. The findings from the East Rand basin underscore the complex interactions between human activities and the natural environment, emphasising the importance of employing innovative tools like numerical modelling to guide responsible practices, safeguard resources, and promote a more balanced coexistence between mining operations and groundwater ecosystems.

6.1 Recommendations

To improve the model calibration and build confidence in the modelling output the following can be considered:

- A detailed field survey (hydrocensus) can be conducted over the sub-catchment area to collect more recent data in terms of groundwater levels, groundwater abstraction locations and identification of potential open voids not just from historic mining footprints but also naturally occurring open voids leading to the subsurface.
- Site visits to the active mines included in the sub-catchment can be conducted to gather data and information from exiting mine monitoring programs and dewatering practices to better understand the current groundwater systems in terms of drawdown created by the different mines in the East Rand basin.
- Additional hydraulic testing in the shallow alluvial aquifer systems can be conducted to gather and compare hydraulic parameters needed for calibration purposes.
- A surface water study can be conducted for the Blesbokspruit catchment, and associated tributaries included in the sub-catchment whereby flooding scenarios from the floodplains of the rivers and streams could provide estimates to calibrate the modelling approach during the saturation process and accurately apply the hydraulic head lifts to represent the surface water flooding rates and volumes.

The additional data and information will improve the numerical modelling output and provide answers to further studies that can be conducted where water ingress from shallow aquifer systems as well as deeper aquifer systems flows through open voids. The effects that the ingress potential has on gradual hydraulic head rise regionally and the contribution to decanting especially in mined out areas like the Witwatersrand Gold fields and stability to dolomitic and karst aquifers could be better understood. The effect that the water ingress has on water quality in general and how it will dilute or concentrate chemical constituents that may contaminate the natural and aquatic environmental systems could also be better understood and mitigation methods such as the identification of specific open voids and capping these voids may minimise the impacts associated with increased water ingress into the subsurface.

Chapter 7 References

Abiye, T.A., 2011. Provenance of groundwater in the crystalline aquifer of Johannesburg area, South Africa. *International Journal of the Physical Sciences*, pp. 98-111.

Baily, A., 2023. *Water Resources of South Africa 2012 Study (WR2012),* Johannesburg: Department Water and Sanitation Republic of South Africa.

Bonan, G., 2019. *Climate Change and Terrestrial Ecosystem Modelling,* Cambridge: Cambridge University Press.

Botha, A., 2018. *Generic source term determination for tailings,* Masters Dissertation *s.l.*: North-West University.

Coetzee, H., 2010. *Mine Water Management in the Witwatersrand Gold Fields with Special Emphasis on Acid Mine Drainage,* s.l.: Inter-Ministerial Committee on Acid Mine Drainage.

Coetzee, H., and Cole, P., 2022. *Estimation of Mine Water Ingress Volumes for the Witwatersrand Goldfields,* IMWA 2022.

Conrad, J., Nel, J. and Wentzel, J., 2004. *The challenges and implications of assessing groundwater recharge:* A case study – northern Sandveld, Western Cape, South Africa. Water SA, 30 (5),75-81.

Department of Water Affairs and Forestry (DWAF), 2008. Best Practice Guidelines Series A: Activity guidelines: Best Practice Guidelines Series A4. Water Management for Surface Mine

Department of Water Affairs and Forestry (DWAF), 2012. *Classification of Significant Water Resources (River, Wetlands, Groundwater and Lakes) in the Upper, Middle and Lower Vaal Water Management Areas* (WMA) 8, 9, 10: Management Classes of the Vaal River Catchment Report.

Department of Water Affairs and Forestry (DWAF), 2013. *Feasibility Study for a Long-Term Solution to address the Acid Mine Drainage associated with the East, Central and West Rand underground mining basins*. Assessment of the Water Quantity and Quality of the Witwatersrand Mine Voids. DWA Report No. PRSA 000/00/16512/2.

Department of Water Affairs and Forestry (DWAF), 2006.– *literature study.* Prepared by Witthuser, K.T. on behalf of the Directorate: National Water Resource Planning. DWAF Planning reference number 14/14/2/3/8/1. DWA, Pretoria, South Africa.

Danél, M., van Tonder, G. and Schoeman, B., 2021. *Re-watering of West Rand Dolomitic Compartments: Implications for JB Marks Local Municipality,* Paper, IMESA Conference 2021.

Dippenaar, M.A., van Rooy, J., and Rodger E., 2018. *Engineering, hydrogeological and vadose zone hydrological aspects of Proterozoic dolomites (South Africa),* Journal of African Earth Sciences. https://doi.org/10.1016/j.jafrearsci.2018.07.024

Duthe, D., 2020. *Modderfontein Groundwater Ingress Groundwater Model Specialist Investigation,* Pretoria: The Council for Geoscience.

Eckart, M., Kories H., Rengers R. and Unland W., 2004. *Application of a numerical model to facilitate mine water management in large coal fields in Germany*. / Mine Water 2004 - Process, Policy and progress, Newcastle upon Tyne, vol. 2, 209-218.

FEFLOW, 2022. FEFLOW 7.5 Documentation. Retrieved May 9, 2022, from http://www.feflow.info/html/help75/feflow/01_Introduction/intro.htm

Frimmel, H.E., 2019. *The Witwatersrand Basin and Its Gold Deposits.* [Online] Available at:https://link.springer.com/chapter/10.1007/978-3-319-78652-010 [Accessed 1992].

Hobbs, P., 2013. *Groundwater Reserve Determination for the Upper Vaal Water Management Area,* Pretoria: Water Research Commission.

Koekemoer, A., 2020. *West Wits Project Geohydrological Assessment for the Proposed Opencast and Underground Mining,* s.l.: MvB Consulting.

Lea, I., Waygood C., and Duthie D., 2001. *Water management strategies to reduce long term liabilities at Grootvlei gold mine.* Johannesburg, 8th International Congress on Mine Water & the Environment, Johannesburg, South Africa, pp. 441 - 449.

McCarthy, T.S., 2006. The Witwatersrand Supergroup. In: M. R. Johnson, C. R. Anhaeusser & R. J. Thomas, eds*. The Geology of South Africa. Pretoria: Geological Society of South Africa & Council for Geoscience*.

Marei, A., Khayat,S., Weise,S., Ghannam S., Sbaih S.M., and Geyer,S., 2010. Hydrological Sciences Journal, 55:5, 780-791, DOI: 10.1080/02626667.2010.491987

Maré, H.G., Rademeyer, J.I. and Sami, K. 2007. Application on Groundwater/Surface water Interaction Modelling in the Schoonspruit Catchment.

Midgley, D.C., Pitman, W.V. and Middleton, B.J. 1994. Volumes I to VI. Report No's 298/1.1/94 to 298/1.6/94. Water Research Commission, Pretoria, South Africa.

MIKE, 2022. MIKE SHE. Retrieved May 5, 2022, from https://www.mikepoweredbydhi.com/products/mike-she

North West University (NWU), 2016*, Council for Geoscience*, Pretoria.

Parsons, R., 2004. *Surface water-groundwater interaction in a Southern African context*. Water Research Commission, Report No TT 218/03.

Pathare, V.G. and Japtap, S.A., 2017. Surface Water - Ground Water Interactions Modelling Approaches and Their Sustainability for Indian Conditions. *International Journal of Current Research*, 9(08), 55589 - 55592.

Rodney, F., Tucker, R.P., and Viljoen, M.J., 2016. A Review of the Witwatersrand Basin. *The World's Greatest Goldfield,* 39(2), pp. 106 - 133.

Scholtz, O., 2013. *Geohydrological investigation on the farm Droogefontein portions 26, 46, 47,* Delmas, Mpumalanga: Shangoni AquiScience (Pty) Ltd.

Schrader, A., and Winde, F., 2014. *Unearthing a hidden treasure: 60 years of karst research in the Far West Rand, South Africa,* Article, Faculty of Natural Sciences, North-West University, Potchefstroom, South Africa.

Scott, R., 1995. *Flooding of Central and East Rand gold Mines: an investigation into controls over the inflow rate, water quality and the predicted impacts of flooded mines*. Water Research Commission, WRC Report no 486/1/95.

Tanner, J.L. and Hughes, D.A., 2015. *Understanding and modelling of surface and groundwater interactions*. Report for the Water Research Commission (WRC). WRC Report No. 2056/2/14.

USGS, 2021. *GSFLOW: Coupled Groundwater and Surface-Water Flow Model*. Retrieved May 5, 2022, from https://www.usgs.gov/software/gsflow-coupled-groundwater-and-surface-water-flow-model

Van Dyk, G. and Kisten, S., 2006. An explanation of the 1:500 000 general hydrogeological map. Pretoria: Department of Water Affairs.

Wall, S., 2013. *Assessment of the Water Quantity and Quality of the Witwatersrand Mine Voids,* Johannesburg: Department of Water Affairs.

Wagener, T., Boyle, D.P., Lees, M.J., Wheater, H.S., Gupta, H.V. and Sorooshian, S., 2001. *A framework for development and application of hydrological models.* Hydrology and Earth System Sciences, 5 (1), 13-26.

Wagener, T. and Gupta, H.V., 2005. *Model identification for hydrological forecasting under uncertainty. Stochastic Environmental Research and Risk Assessment*.

Water Research Commission (WRC), 2005. Water Resources of South Africa 2005. Water Research Commission Report K5/1491

Watkins, D., n.d. *30-Meter SRTM Elevation Data Downloader.* [Online] Available at: http://dwtkns.com/srtm30m [Accessed 30 April 2022].

Whitaker, S., 1986. Flow in porous media: A theoretical derivation of Darcy's law. *Transport in Porous Media,* Volume 1, pp. 1, 3-25.

Winde, F., 2015. Uranium pollution in South Africa: past research and future needs. *Hrvatski geografski glasnik*, 77(2), 33-53.

Winter, T.C., Harvey, J.W., Franke, O.L. and Alley, W.M., 1998. *Ground water and surface water: a single resource*. U.S. Geological Survey Circular 1139 (Vol. 1139).

van Wyk, E., van Tonder, G. and Vermeulen, D., 2011. *Characteristics of local groundwater recharge cycles in South African semi hard rock terrains - Rainwater input,* Bloemfontein: Institute for Groundwater Studies, University of the Free State.

Appendix A Rainfall Records

Station 476644												
Year	Jan	Feb	Mar	Apr	May	Jun	Jul	Aug	Sep	Oct	Nov	Dec
1921	81,1	113,8	9,5	17,8	20,8	0	50,8	45,7	66,3	176,4	120,2	109,9
1922	81,8	65	24,3	0	9,4	19,6	0	5,9	67,1	143,3	79,6	250,6
1923	54,6	125,3	34	19,6	0	0	4,1	37,8	19,5	80,5	43,7	80,5
1924	93,2	156,4	86,4	61,7	0	0	1,3	57	35,4	117,4	128,8	127,3
1925	70,9	108,7	95,3	32,8	0	18,3	0	21,8	28,1	96	100,6	155,9
1926	96,5	78,8	23,9	0	0	55,4	3,6	1,8	29	74,6	73,2	129,6
1927	137	98,9	25,1	14,2	0,5	0	13	11,4	116,8	27,1	80,8	136,7
1928	105,8	97	32,5	18,5	32,7	4,8	0	99,8	39,4	128	56,6	102,5
1929	161,5	63,7	7,5	25,7	0	18,6	18	1,8	160,8	111,5	128,4	135,7
1930	47,3	45,1	77,7	0	0	55,4	0	0	22,6	63,5	126,2	166,5
1931	173	142,7	16,3	13,2	0	0	0	26,4	42,5	85,5	67,8	110,1
1932	33	99,3	74,9	0	7,6	0	0	11,4	53,9	136,3	39	44,5
1933	37,7	116	76,5	49,3	6,4	44,9	40,1	41,9	15,7	233,1	189,3	141,8
1934	82,3	140,8	5,8	6,6	0	0	10,2	17,8	67,2	186,3	98,6	82,8
1935	181	130,5	26,2	145,2	0	0,5	0	30,2	18,5	33,7	106	97,6
1936	204,3	35,4	28,9	2,8	0	1,3	0	35,8	30,5	206,3	50,3	140,4
1937	31,1	41,5	104,7	6,9	5,5	7,8	8,9	17,1	69,5	40,6	144	111,3
1938	168,9	81,1	12,7	32,3	3,8	58,2	18	14,7	65,4	31,3	157	41
1939	82,9	91	33	29,9	47,7	0,3	0,6	66	60,8	269,7	141,2	76,7
1940	51,6	98,1	102,6	0	0	0	0	15,5	20,6	144,2	170	194
1941	91,9	108,2	14,8	17,3	17,6	0	30	19,8	41,2	7,4	118,2	224,5
1942	68,8	67,2	125,8	52,1	0,8	76,2	44,2	30,8	99,8	101	209,6	52,1
1943	375,5	52,6	40,9	4,1	52,1	0	0	73,2	70,7	77,8	228,6	167,7
1944	126,1	170,1	9,1	19,8	0	5,8	0	0	167,9	104,2	48,6	83,5
1945	149,3	101,2	37,3	28,9	0	0	0	0,3	32,5	83,5	40,5	232
1946	104,3	135,2	23,2	0	1,3	3,6	2,3	9,7	35,4	109,8	104,2	95,9
1947	44,6	80,7	72,9	27,4	0	1,5	0	0,8	21	92,6	102	87,3
1948	73,8	42,7	41,4	1,8	7,1	0	0	14,2	69,9	91	16,1	192,5
1949	67	98,6	26	69,6	4,1	1,6	0	0	72,4	229,9	250,4	74,9
1950	38,9	51,2	40,4	55,7	0	2,3	19,6	8,2	31,5	87,3	233,9	65,8
1951	83,9	56,9	45,9	4,3	7,9	36,1	1	1,5	89,8	19,6	100,2	139,6
1952	95,3	97,4	55,1	13,2	0	0	0	0	25,5	174,2	176,7	82,1
1953	48,7	65,6	42,3	19,8	3	0	0	25	55,2	138,8	77,5	148,5

Station 476644												
1954	210,2	43,8	70,7	28,5	6,6	0	2,3	0	23,7	148,3	41,2	241,1
1955	126	125,2	5	84,3	7,5	1,6	0	23,5	52,3	131,2	128,6	86,3
1956	126,2	123,1	24,8	55,4	31,5	67	17,7	104,3	124	130,4	131,4	93,5
1957	88,5	90,5	128,7	6,5	2,5	0	0	91,6	99,1	92,5	149,2	139,8
1958	82,6	47,6	49,7	23,1	3,8	8	0	5,1	48	175	155,2	114,7
1959	83,9	53,5	104,1	0,7	3,4	0	12,4	4,7	58,6	132,7	157,6	74,4
1960	118,9	76,7	66,9	35,2	8,6	0	0	17,6	75,1	126	145,5	160,9
1961	87,7	54,5	60,3	0	0,5	0	0,6	25,6	43,4	115	76,8	69,8
1962	24,3	52,6	59,6	29,4	58,4	18,7	0	5,2	20,3	178,1	70,1	76,9
1963	38,7	69,1	64,6	5,7	13,5	0	5,3	30,5	57,1	87,9	70,1	208,1
1964	61,9	15,3	84,9	20,9	3,1	29,5	0	0	185,6	33,9	95,8	150
1965	118,7	11,5	8,4	11,5	3,8	0	2,7	17,4	21,2	63,1	39,3	80,2
1966	113,6	132,3	81,2	19	0	0	11,9	10,9	108,4	88,5	171,5	189,9
1967	68,7	120,8	108,5	16,4	0	0	9,6	0	65,5	68,7	143	136,2
1968	23,3	191,7	64,5	72,7	1,2	0,4	4	42	64,8	104,1	71,2	94,3
1969	91,9	44,2	45,1	29,8	4,5	16,7	8,1	19,3	109,7	162,4	143,9	147,1
1970	112,9	95	112,5	26,5	12,5	0	0	57	105	133,9	102,7	188,8
1971	24,6	112,7	27,9	9,4	0	0	2,1	6,6	105,1	102,9	172,9	316,3
1972	69,3	45,9	85	0	0	0	17,5	94	89	126,3	71,6	89,2
1973	40,8	89,6	170,1	14,3	3,8	0	0,4	16	98,2	100,4	138,7	53,3
1974	175,4	117,3	121,4	17,2	6,6	1,3	0,5	1,8	48,2	171	106,9	355,5
1975	192	181,2	71,5	119	0	0	0	17,5	62,1	181,9	166,6	114,1
1976	62,6	154	17	4,3	0	0	1,5	55,8	126,8	50,4	78,5	142,7
1977	138,3	121,4	29,6	3,4	0	0	7,5	20,5	96	100	73,7	467,3
1978	44,8	76,6	42,9	15,6	4	16,8	54,6	29,3	89,8	25	119,8	37,7
1979	121,1	37,7	3,5	2,8	0	0	19	82,1	65,9	229,4	149,4	189,6
1980	141,2	79,4	41,5	0	0	0	7,5	48,6	17	160,5	120,9	151,8
1981	23,9	68,6	20,7	0,5	1,6	9,1	0	15,9	92,1	60,7	90,3	116,7
1982	44,3	30,9	20,1	15,7	35,4	4	7,5	17	62	92,3	86,6	141,7
1983	18,2	73,6	8,4	2,3	6,5	12	0	18,1	59,6	130,6	179,6	108,8
1984	90,7	40,1	95,3	6,1	2	6,2	15,2	23,1	117,4	78,6	44,1	73
1985	143,1	68,4	28,8	0	29,2	0	10,7	1,4	142,9	56	102,9	151,8
1986	155,3	187,5	9,6	1,8	1,4	0	34,7	162,6	114,8	131,7	165,3	108,4

Station 476736												
Year	Jan	Feb	Mar	Apr	May	Jun	Jul	Aug	Sep	Oct	Nov	Dec
1909	104,9	90,5	6,5	0	6,9	0	0	61,6	120,9	147,6	129,6	143,8
1910	66,9	52,4	80,1	78,2	0	0	1,6	5	102,9	35,3	160,9	110,6
1911	191,2	31,3	87,3	12,4	0	0	0	6,9	58,6	127,3	85,4	60,3
1912	49,5	77,6	73,2	4,9	0	2,5	21,3	3,8	8,2	75,6	134,1	91,8
1913	90,9	79,7	18,3	7,4	3,6	0	28,2	13,2	79,2	33,2	70,8	46,3
1914	27,7	0	25,9	0	52,7	0	36,1	0	65	171,6	173	134,1
1915	55,4	65,2	17,4	3,8	0	0	0	0	117,1	124,4	83,6	50,3
1916	124,2	61,7	46,7	20,4	15,2	5,4	52,3	21,2	32,3	71,3	89,5	138
1917	151,7	67,4	0	0,8	0	6,4	86,6	16,5	19,8	344	170,9	194,9
1918	91,6	24,1	14,3	2,9	0	0	0	4,9	188,9	98,6	145,8	75,5
1919	61,7	66,4	5,4	23,7	0	0	0,3	60,5	22,3	147,3	83,4	103,6
1920	20	15,7	3,6	0	0	29,3	0	0	105	101,4	97,7	186,7
1921	68,5	114,1	6,9	28,6	0	0	46	31,2	62,3	138,8	109,7	137,5
1922	69,3	99,2	29,7	0,8	9,4	15	0	6,4	72,3	167,5	74,4	185,3
1923	64,5	147,3	20,4	33,7	0,5	0	4,8	27,1	20,1	62,1	60,5	87,1
1924	175,3	82,9	36,9	19,1	0	1	60,6	0	30,8	157,9	153,5	106,1
1925	86,5	62,3	2,8	34	3,9	7,6	0	16,8	25,1	73,1	68,2	152,4
1926	60,3	23,4	5,1	0	54,4	2,5	1,3	0	111,3	139,3	90,7	92,4
1927	115,7	73,3	39,5	19,3	1,5	0	13,3	17,1	151,3	20,1	102,1	128,7
1928	171,5	124,6	26,6	11,9	48,7	0	0	118,3	32	135,4	48,4	106,8
1929	158,1	56,9	2,5	12,4	0	14	17,5	2,5	164,3	96,3	116,6	171,6
1930	105,7	50,3	0	0	0	51,7	0	0	16,9	47,7	122,4	182,1
1931	109,1	90,1	10,6	14	0	0	0	37,7	40	129,2	65,1	131,9
1932	35,4	47,5	57,1	1,8	5,6	0	0	12,4	52,7	62,8	90,7	57,2
1933	30,1	81,8	55,9	72,4	3	29,5	32	20,1	9,7	260,2	200,7	181,3
1934	77,5	114,2	8,1	7,3	0	0	4,6	4,1	46	162,8	84,9	83,2

Station 476736												
1935	179,1	145,1	36,4	148,8	0	0	0	22,9	16,9	40,5	162,2	89,4
1936	195	39,3	23,6	2,8	0	0	0	11,6	24,8	191,2	42,5	142,7
1937	55,1	36,5	109,2	5,9	6,9	7,9	9,6	21,8	36,6	21,6	179,1	81,4
1938	175,6	66,2	2,8	36	0	58,1	18,8	20,2	66,5	33,8	128,6	49,6
1939	103,4	87,6	23,6	29,8	45	0	0,5	74,1	60,6	258,1	77,8	105,1
1940	43	101,9	87,8	0,5	0	0,5	0	27,2	29,5	139,5	160,4	139,4
1941	112	105	26,7	16,3	17,8	0	36,3	20,6	35,3	21	131,6	215,3
1942	64,8	87,3	138,7	48,9	2	55,1	37,4	60,2	106,9	102,9	194,2	59
1943	382,5	30,5	24,3	9,6	44,8	0	0	63,3	70,1	69,8	189,8	151,7
1944	133,9	140,6	16,9	23	0	1,5	0	0	154,3	172,1	25,1	84,8
1945	107,9	42,4	39,6	0	0	0	0	0	31,3	53	89,9	110,9
1946	108,8	37,8	0	0,8	3	0,5	8,9	0	44,1	132,2	118,5	132,6
1947	71,8	104,9	66,1	26,4	0	0,5	0	1,6	38,2	141,3	114	108,6
1948	96,1	32	40,1	1,8	9,4	0	0	13,8	61,4	98,7	20,8	171,2
1949	159,6	38,6	65,5	5,9	1,8	2,8	2,6	0	90,9	158,8	150,4	59,1
1950	37	57,7	49,8	58	0,5	2,8	15,8	7,9	33,1	50,3	173,2	76,9
1951	63,4	51,1	7,2	6,8	36,6	1,3	1,3	0	96,7	113,9	126,4	74,4
1952	110	95,8	59,9	5,8	0	0	0	0,8	26,4	141,2	97,4	80
1953	65,7	47,8	20,3	2,2	0	1,5	27,5	0	64,7	90	127,9	61,9
1954	216,2	69,5	65,9	25,2	8,3	0	4,7	0	13,9	183,7	56	204
1955	134,9	7,2	82,2	6	6,5	0	22,8	0	69	166	157,3	70,7
1956	174,2	127,3	22,5	30,7	26,3	70,2	19,3	90,4	111,9	139,8	103,3	97,9
1957	92,5	64,5	131	8,5	1	0	0	88,3	83,1	52,5	114,4	155,3
1958	68,6	33,7	42	26,9	3,6	7	0	7,2	28,3	145,4	113,7	104,5
1959	60,7	47,4	79	1,5	3	0	7,5	3,1	76,8	145	130	67,3
1960	114,7	59,9	67,1	33,2	7,9	1,2	0	15	75,5	127,4	117,3	100,1
1961	89,9	55,2	57,6	0	0,3	0	0,5	18,9	57,4	91,3	66,2	74,3
1962	40,5	54	50,5	34	64,5	22,5	0	0	24,6	162,2	87,8	80,3
1963	32,4	44	53,5	9	8,6	0	0	27,3	69	119,1	56,1	228,7

Station 476736												
1964	48	35,7	74,3	8	0,4	33	0	0,2	174,2	67,3	146,3	150,5
1965	112,7	5	25,9	11,5	3	0	2,5	22,4	19,9	45,7	85,7	141,9
1966	176,3	136,9	63,7	11	0	0	16,1	6,8	103,6	99,8	153,8	195,7
1967	57,9	90,5	92,3	14	0,1	0,1	10	0,4	92,2	69,8	145,5	104,5
1968	25,3	254,2	41	71,2	0,1	0,1	3,5	38,6	47,7	85,3	90,9	85,2
1971	30,8	80	22,2	11,1	0,9	0	3,6	6,1	104,9	131,5	132,5	209,9
1972	30,1	85,8	90,7	0	0	0	18,8	81,4	105,5	83,3	68,6	85,4
1973	46,2	74,3	107,4	8,1	0	21	0,2	17,4	80,9	56,4	99,7	36,7
1974	168,7	46,6	47,6	8,7	8	0	6,5	1,9	44,3	145,6	61,3	306
1975	82	48	71	80	0	1,5	0	10,3	23,5	210	170,3	152,5
1976	56,5	78,5	18	9	0	0	2	75	97,3	71,5	82,6	117,5
1977	154	123	47,5	8	0	0	7,5	25	58	108,5	179,2	337
1978	44	96,5	16	35	0	18	67,5	29	72	30,5	61,5	52,5
1979	102,7	67	3	2	0	0	1	91,4	57	193	70,5	195,7
1980	121	83,4	47,5	0	6	0	8,4	35	31,1	153,9	190,4	167
1981	63,1	44,5	16,2	0	2	6	4	12,4	87,3	74,2	94,5	116,3
1982	61,8	28,1	46,2	8,4	34,6	4,4	7,4	15,4	74,6	24,6	102,8	79,6
1983	23,6	100,8	17,4	0	4,8	14,7	0	10,6	90,3	102	147,3	76,2
1984	82,4	55,1	0,3	9,4	0	6	12	22,1	88,7	111,3	40,4	114,1
1985	150,1	65,8	23,8	0	28,6	0	10,8	0	154,2	21,8	147	161,1
1986	148,5	186,2	3,7	0	0	0	32	167,1	106,5	132,1	182	116,7
1987	84,9	95,7	25,5	1,5	13,5	6,5	0	40,9	86,4	171,5	139,4	108,4
1988	176,1	26	45,7	6,2	65,3	0	2,2	2,5	96,3	66	101,7	112,2
1989	59,1	148,8	105	13,4	0,2	2	0	5,1	34,6	161,3	91,6	86,2
1990	94,2	159	93,7	0	7,9	0	0	8,5	32	30,6	111,7	109,7
1991	80,8	43,9	16,3	0	2,3	0	17	0,1	52	51,3	110,1	114,3
1992	128,8	61,6	31,9	2,3	0	0	0,2	36,8	30,2	71,6	103,6	134,8
1993	139,6	86,1	20,9	0	0	0	0,3	6	153,6	112,6	140,8	171,5
1994	94,3	148,3	53,9	6,1	0	0	9	12,5	73,2	71,5	137	58,2

Station 476736												
1995	225,1	89,8	82,9	4,4	2,1	0,4	3,5	0,9	184,3	130	132,6	241,9
1996	88,1	272,1	29,1	99,4	9	8,5	4	54,2	109,6	98	124,8	101,6
1997	51,3	30	11,4	0	0	0	0	61,7	49,5	171,8	76,5	112,6
1998	34,9	30,4	33	36,1	2	4,5	0	8	94,4	174,7	153,6	124,1
1999	291,9	205,3	46,5	31,5	0	0	0	37	24	66,3	249,6	140,4
2000	80	33	30,9	0	3,7	0	7,5	66	81,2	122,5	81,2	29,5
2001	82,1	35,8	24,8	31,5	13	0	0	0	160	104,5	82,2	136
2002	105	0	0	0	0	0	6,2	0	61,2	12,8	115,5	103,9
2003	138,7	188,5	25,8	12,8	2,4	24,9	3,3	13,4	59	96,2	93,7	93,7

Station 476766												
Year	Jan	Feb	Mar	Apr	May	Jun	Jul	Aug	Sep	Oct	Nov	Dec
1920	57,6	181,6	15,8	20,5	3,3	0	0	29,9	108,9	76,4	107,7	113,9
1921	58,3	136,4	6,6	26	5,8	0	44	19,6	69,4	148,3	111,7	183
1922	76,9	88,4	31,2	0	8,9	19,2	0	5,8	76,6	167,9	69,8	182,1
1923	64	171,5	16,8	28	0	0	4,5	28,4	17,8	71,7	54,1	91,6
1924	119,2	176	80,7	43,7	9,4	0	0	59,6	38,2	131,5	163,5	129,2
1925	69,7	70,6	97,6	31,6	0,8	8,4	0	0	17	78,1	104,4	118,3
1926	91,1	66,3	5	6,3	0	53,6	0	0	36,1	71,8	131,5	97,3
1927	98,7	87,6	30,5	10,7	0	0	14	12,7	144,7	15,3	66,6	126,9
1928	146,8	98,5	27,2	7,9	42,2	0	0	120,9	33,6	124,4	26,9	101
1929	168,7	52	7,3	17	0	17,2	18,3	0	138,9	95,4	145,5	125,5
1930	66,8	40,9	76,2	0	0	48	0	0	15	40,9	81,5	139,8
1931	115,3	131,6	20,3	12,2	0,8	0	0	32,8	46	120,9	73,1	83,5
1932	48	47,2	62,7	1	5,3	0,5	0	11,7	48,3	67,1	106,8	98,3
1933	38,9	61,5	80	70,9	4,5	33,3	38,4	17,8	8,4	247,4	182,8	183,7
1934	54,7	126,2	10,4	2,8	0	0	4,3	2,5	47,6	164,2	95,1	71,7
1935	161,4	140,1	46	153,5	0	0	0	22,4	13,5	41,6	133,9	89,4

Station 476766												
1936	172,5	30,7	29,2	2,1	0	0	0	11,2	27,1	191,6	36,3	146,4
1937	41,8	47,9	109,3	5,4	3,8	6,3	9,1	16,8	38,1	21,2	128,9	80,2
1938	147	69,8	21,8	33,6	0,8	65,5	16	22,1	62,1	32,7	126,2	45,5
1939	74,8	83,8	27,2	19,1	57,4	0	0	67,2	63,9	244,1	87,5	92
1940	35,8	97,4	93,5	0	0	0	0	18,3	23,7	141,9	156,5	171,6
1941	100,9	72,3	21,1	16,3	15,8	0	35,1	22,6	39,6	18,8	119,9	249,5
1942	75,2	83	127,4	53,1	1,5	52,6	37,4	44,9	109,5	109,1	192,6	68,9
1943	357,7	26,2	31,3	8,9	49,3	0	0	61,4	77,8	86,3	180,6	112,5
1944	133,6	138,6	15	23,6	0	0	0	0	145,3	179,9	29,1	70,2
1945	127,5	108,7	32,7	23,1	0	0	0	0	28,8	50,5	90,8	238
1946	133,1	106,7	21,6	0	0	0	0	8,7	37	108,9	119,1	85,3
1947	67,3	82,1	72,5	22,9	0	0,8	0	2,3	33	142,5	116,2	111,4
1948	91,9	18,3	32,6	2,5	6,8	0	0	13,2	59,9	76	17,5	182,1
1949	63,3	133,3	34,3	72,3	5,3	1	3	1,3	115,3	222	235,6	125,6
1950	33,3	42,2	50,3	62,5	0	5,1	21,1	8,1	28,8	66,6	174,3	82,1
1951	76,8	53,3	32,7	5,9	8,2	37,6	0,8	0	121,7	21,2	109,5	95,8
1952	97,6	99,7	61,5	38,1	0	0	0	0	21,5	178,5	152,1	84,1
1953	51	82,5	39,8	21	0	0	0,5	29	60,8	137,5	89,1	134,5
1954	249	70,7	85,5	24,5	3	0	2,5	0	19,9	175	45,5	239,5
1955	192,3	127,5	9,6	79,5	4,7	5	0	22,9	49,3	137,9	151,1	79,2
1956	178,7	160,5	24,7	32,2	32	76	21,5	120,9	102,5	161,5	124,6	102,3
1957	69,3	101	176,5	3,5	0	0	0	88,8	128,5	66,3	124	155,1
1958	94,5	29,7	45,9	32,5	4	10	0	6,1	48,2	170,5	163	129,5
1959	49,4	61	91	0,5	3	0	9,6	2	84,5	174,5	136,4	106,1
1960	80	70,6	61,3	32,8	6,8	0	0	22	62,5	121	116,4	86
1961	86,5	58	58	0	2	0	2	23	50	93,4	48,8	85,7
1962	40,2	60,3	48,9	41,2	64,2	21,5	0	4	17	179,1	104,9	81,8
1963	35,5	49,7	52	7,8	10,5	0	9	25	70,9	89,5	70,2	203,8
1964	56,5	14	83	11,6	1,5	27,5	0	0,4	185	62,8	134,5	142,1

Station 476766												
1965	126,5	20,7	17,7	11	0,5	0	2,2	19,7	26,2	60,6	54,6	121,1
1966	180,1	129,9	76,1	15	0	0	13,8	6,9	122,1	87,7	153,2	205,7
1967	78,1	95,9	116,6	38,8	0,1	0	9,5	0,6	104	85,5	178,2	113,3
1968	27,6	259,2	48,2	70,6	0	0	4,5	40,3	42,8	100,7	78,2	91,7
1969	95	87,9	46,7	25,1	5	13	17	25,5	123,8	132,7	171,4	139,2
1970	70,5	75,5	116,6	26,8	10	0	0,6	33	103,5	86,3	83,3	137,7
1971	28	101,2	22,2	11,7	0,4	0	3,1	9	98,8	106	138,8	165,1
1972	37	98,3	76	0	0	0	22,3	73	97,5	68,1	58,5	73
1973	51,2	107,2	120,5	10	6,1	0	0,5	15,5	83,8	67,8	156	86,8
1974	171,2	140,5	91,4	10,5	7,8	0,5	8,5	1,6	38,4	165,5	58,5	368,2
1975	112,2	98,8	62,2	72,5	0	2	0	14,2	32,5	200,9	144	188,9
1976	64	106,4	30,1	4	0	0	1	69,7	110,2	79,8	60,9	132
1977	119,2	145,6	44,1	5	0,3	0	9	15,9	97	121	123,1	333,3
1978	24,9	92,5	32,5	14,7	5,7	16,6	71,9	23,7	65,5	11,7	61,6	72,2
1979	113	73,3	13,4	2	0	0	0	80,3	56,8	175,7	174,5	212,5
1980	93,9	71,6	26,7	0,2	7,1	0	9,6	40,4	14	145,9	154,5	169,7
1981	39,4	37,5	23,6	0	0	6	0	13,5	90,5	54	88,1	93
1982	46,8	26,4	55,9	8,1	33,8	6,5	6,6	18,5	49,6	34,3	84,9	91,5
1983	31,7	87,9	7,2	0,1	4	12,5	3	7,3	64,5	138,5	197,8	76,4
1984	70,3	65,5	97,6	8,1	0	6	9,3	20	77,2	112,9	30,7	122,9
1985	138,4	69,9	30,2	0	28,2	0	8	0,1	125,3	49,8	139,3	145
1986	168,4	196,3	10,8	1	0,2	0	36,5	160,9	126,6	134,3	150,6	99,7
1987	88,9	115	31,9	1	10,1	5,4	0	44,7	68,9	167,5	108,3	91,3
1988	154,9	23,1	41,6	5	58,6	0,1	5,5	0,1	89,6	51,5	81,9	91,6
1989	56,3	136	116,8	12	0,6	1,5	0,9	4,6	31,9	177,6	96,5	81,3
1990	106,5	269,2	97,6	0	6,2	0	0	10,5	28	25	141	118,3
1991	134,2	60,7	7,1	0	0	0	34,5	1,2	52	98,9	104,8	123,1
1992	74,2	114,8	53,7	2,9	0	0	0,5	45,3	36	99,7	183,9	144,2
1993	204,5	104,4	30,3	0	0	0	0	4,5	202,6	125,7	169,2	212,5

Station 476766												
1994	87,1	172,7	60,2	3,8	0	0	14,5	14	94	99,7	181,5	77,7
1995	261	72	114	6,8	0	1,5	10,5	1,7	217,2	173,3	189,4	265,3
1996	96,3	305,3	30,8	126,6	7,8	12	5,5	59	82,8	142,8	174,2	101,3
1997	48,2	45	4,8	0	0	0	0	55,6	46	213,1	99,9	142,7
1998	43,5	31	41	39,3	7,3	0,6	0,4	8,9	79	276,4	199,2	134
1999	320,8	223,7	53,8	27	0,3	0	0	32	26	55,2	276,6	157,9
2000	129,1	35	11	43,7	4,2	0	6,5	80,5	95,9	166,5	114,7	62,5
2001	84,6	67	24,3	34,7	16	0	23,3	12	26	97,5	84,7	145,5
2002	110,5	57,5	0	0	20,5	0	6	0	89,9	9,5	122,3	109,2
2003	204,8	21,1	13	2	25,7	3	0	0	58,5	100,6	148,2	148,5
2004	11,5	54	20	0	0	8,2	19	0	38,8	115,7	171,1	22,6
2005	55,5	109	18	0,6	0	0	110,2	0	15,4	97,2	1,5	223
2006	16,3	16,5	83,2	0	36	0	0	0	8	119	71	59

Station 476835												
Year	Jan	Feb	Mar	Apr	May	Jun	Jul	Aug	Sep	Oct	Nov	Dec
1905	54,2	63,2	16,8	6,9	0	0	0	34,3	9,2	135,8	90,8	78,4
1906	68,4	78,8	3,3	0	0	0	77,5	0	79,5	98,8	87,9	147,4
1907	77,9	99,5	7,6	0	0,8	16,1	5,5	16,1	75,9	139,6	87,5	74,8
1908	206,6	80,8	2	11,2	0	18,8	43,7	16,3	71,5	93	88,7	314,9
1909	142,7	12,4	0	3,3	0,5	0	41,4	0	29	140,9	132,4	106,3
1910	58,2	60,7	57,2	85,3	0	0	1	6,4	102,3	20,3	138,6	120,3
1911	17,6	91,8	11	0	0	0	5,1	0	47	80,8	164,2	209,2
1912	83,1	52,3	1,5	0	7,6	35,3	3,3	0	28,9	39	103,6	39,2
1913	45,5	49,1	22,9	6,6	5,1	0	25,5	16,3	100,6	25,6	48,3	115,3
1914	45,4	35	2,5	25,9	0	39,1	7,2	11,2	42,7	169	183,1	4,9
1915	58,2	75,9	26,9	3,3	0	0	0	0	122,2	167,6	112,8	45,2
1916	114,9	64,8	45,8	15,5	12,2	16	43	21,7	45,4	65,1	126	93,7

Station 476835												
1917	197,1	76,3	0	2,9	0	12,7	71,2	21,1	32,1	436,2	116,8	177,7
1918	151,1	17,7	18,6	4,1	1,3	6,1	0	10,4	169,2	138,7	140,9	72,2
1919	36,5	98,4	0	18,3	0	0	0	35,3	41,4	109,8	78,4	141,2
1920	71,2	306,2	13,5	25,7	0,8	0	0	20,3	114	116,5	25,7	153,3
1921	48,1	110,9	9,9	3,5	28,1	0	40,7	23,4	69,3	107,9	109,2	83,7
1922	84,6	18,8	1,8	9,4	19,8	1,2	8,3	0	139,6	136,2	134,3	67,1
1923	82,9	117,9	7,2	28,2	0	0	4,6	37,5	17,3	72,7	60	144,7
1924	86,4	154,5	159,3	25,7	4	0	0,8	38,9	50,3	95,5	125,9	113,6
1925	131,1	64,7	24,7	31,5	3,8	6,4	0	15,2	30	80,2	108,2	205,8
1926	79,7	70,7	17,1	0	0	36,7	0,8	0,8	33,2	93,9	90,1	101,9
1927	133,5	56,6	16,7	21,1	3	0	6,3	21,1	127,3	31,8	114,7	135,4
1928	117,1	97	20,8	10,9	41,1	0	1,8	111,3	45	116,9	48,9	234,7
1929	160,2	85,7	5,6	6,4	0,8	14,7	14,2	0,8	155,4	184,3	106,7	174,9
1930	72,4	38,1	70,7	0	0	48,3	0	0	18,5	62,4	110,2	159,1
1931	119,5	97,9	10,4	19,4	1,3	0	1,2	51,1	47,4	111,8	83,1	120,7
1932	43,8	89,1	36,2	0	0	0	0	14,2	44,7	161,3	76,9	65,9
1933	75,7	51,6	35,7	41,4	6,6	15,8	26,2	12,7	9,7	315,2	226,2	143,9
1934	51,9	83,3	11,8	3,1	0	0	13,2	2,1	62,5	141,3	85,8	60,4
1935	91,3	141,5	41,2	132,1	0	0	0	22,9	62	14,5	75,3	84,6
1936	130,8	32,3	20,6	3	0	1,8	0	2	25,6	149,9	45,7	124,7
1937	54,8	52,9	81,2	7,4	9,2	9,1	9,6	31,5	37,6	21,5	170,2	79
1938	152,6	57,6	3,9	58,2	0	51,9	22,9	16,8	63,7	42,6	141,7	130,7
1939	68,5	31	39,2	25,7	25,9	0	0	54,3	75,9	260,5	107,3	89,9
1940	84,9	69,3	87,8	0	0	0,5	0	11,7	8,7	161,7	171,5	121,4
1941	87,8	62,7	55,7	8,4	22,1	0	29,8	30,5	29,9	26,1	56,9	138,2
1942	90,1	94,3	133,4	52,8	2	66,5	28,3	62,2	116,9	98,3	192,5	49,3
1943	224,7	67,9	20,8	9,4	46,3	0	0	55,4	73,4	73,8	154,4	132,5
1944	109,2	120	20,8	21,1	0	5,8	0	0	145,3	60,5	39,1	86,1
1945	89,1	75,3	32,6	18,3	0	0	0	0	27,3	74,9	76,1	222,1

Station 476835												
1946	176,5	104,6	40,1	0,3	0	2,5	0	7,9	71,1	93,1	125,5	133,5
1947	55,3	109,7	75,9	28,2	0	1,3	0	17,5	18,8	71,5	160	114,1
1948	107,8	62,8	28,3	1,8	10	0	0	16	71,1	72,8	55,2	212
1949	11	64,6	28,2	59,7	11,5	0	3,5	3	140	257,1	244,4	109,7

Appendix B Groundwater Chloride Concentrations

Sample ID	Latitude	Longitude	Groundwater Cl (mg/l)
102	-26,057780	28,400000	48,2
433	-26,285400	28,529590	74,0
2628AD00118	-26,308330	28,288890	40,5
2628AD00192	-26,306940	28,333330	156,0
2628AD00350	-26,328260	28,341110	40,6
431D	-26,284753	28,528619	79,3
431S	-26,285420	28,529620	141,3
6L13-12	-26,212907	28,463114	718,2
B21	-26,356166	28,309000	2528,3
B41	-26,354672	28,300719	460,7
B9D	-26,202250	28,448669	261,6
BH7	-26,397403	28,445706	4,4
BHC46	-26,224125	28,431031	11,0
CEN74	-26,300041	28,360796	7,9
DA68	-26,182477	28,494377	24,7
G10D	-26,217977	28,445000	2431,9
G23D	-26,217986	28,444989	7437,1
G3D	-26,216850	28,443597	78,6
G8D	-26,217819	28,441025	75,6
GA16S	-26,227880	28,317670	1012,7
GAA12D	-26,199411	28,446918	569,1
GAA13D	-26,197923	28,442553	33,4
GAA13S	-26,197923	28,442553	26,2
GC1	-26,274985	28,278551	19,1
GP141	-26,338000	28,524110	31,4
GP142	-26,346726	28,514374	280,0
GP143	-26,331709	28,482316	230,8
HR1	-26,258330	28,350000	17,2
HR3	-26,308334	28,288888	44,1
ME1	-26,179520	28,428130	7,9
PD3	-26,209526	28,430171	107,6
ZBH26D	-26,327216	28,509185	167,2
DN08	-26,232040	28,559630	35,2
DN09	-26,232820	28,563920	20,5
DN13	-26,228740	28,565180	46,1
DN20	-26,217350	28,554570	23,2
DN21	-26,222480	28,553310	19,3
DN22	-26,216090	28,542110	21,8
DN23	-26,207590	28,541430	11,5
DN24	-26,212140	28,540750	16,0
DN25	-26,215160	28,557830	9,4
DN26	-26,235360	28,574910	7,5
DN28	-26,251500	28,562460	5,0

Sample ID	Latitude	Longitude	Groundwater Cl (mg/l)
DN29	-26,243580	28,577850	20,4
DN30	-26,186610	28,558960	88,8
DN32	-26,196970	28,563000	90,2
DN33	-26,205650	28,553960	13,9
DN34	-26,188270	28,560610	17,8
DN35	-26,187630	28,560130	3,8
DN36	-26,182030	28,562460	34,9
DN39	-26,183470	28,557220	3,5
DN40	-26,183170	28,556730	31,6
DN42	-26,182050	28,556940	22,8
BH1	-26,175920	27,840310	82,0
BH2	-26,179250	27,843360	42,0
BH3	-26,178420	27,828780	15,0
BH4	-26,200940	27,900970	62,0
Witbh1	-26,183140	27,856780	42,0
Witbh3	-26,170916	27,821916	12,0
Witbh5	-26,171110	27,886250	8,0
Witbh7	-26,178530	27,861250	20,0
DD	-26,176305	27,862833	71,0
BH1	-26,229720	28,042780	50,0
BH2	-25,992500	28,117500	9,7
SP1	-25,985000	28,331670	1,5
SP2	-26,021670	27,564720	5,2
SP3	-25,874440	27,782220	4,4
BH3	-26,246670	27,716940	1,5
BH4	-26,233890	27,803060	1,5
BH5	-26,234720	27,725280	1,5
BH6	-26,233060	27,783330	1,5
BH7	-26,235280	27,749440	3,5
BH8	-26,236670	27,796670	1,5
BH9	-26,247220	27,749720	1,5
BH10	-26,243330	27,796390	3,8
BH11	-26,245830	27,683610	1,5
BH12	-26,228330	27,734440	1,5
BH13	-26,245560	27,683610	1,5
BH14	-26,245560	27,721110	21,2
BH15	-26,221110	27,775280	105,5
BH15	-26,240280	27,804170	1,5
BH16	-25,810280	28,148610	18,8
BH17	-25,883330	28,316670	29,2
BH18	-25,900000	28,316670	19,0
BH19	-25,893610	28,306940	36,2
BH20	-25,816670	28,100000	5,7
BH21	-25,825000	28,122220	58,9
BH22	-25,820830	28,122220	49,0

Sample ID	Latitude	Longitude	Groundwater Cl (mg/l)
BH23	-25,783330	28,187500	21,0
BH24	-25,812500	28,152780	18,7
BH25	-25,829170	28,175000	56,6
BH26	-25,827780	28,169440	60,2
BH27	-25,791670	28,208330	1,5
BH28	-25,827780	28,116670	56,8
BH29	-25,784720	28,205560	1,5
BH30	-26,033330	28,466670	1,5
BH31	-26,116670	28,433330	9,0
BH32	-26,083330	28,500000	3,0
BH33	-26,016670	28,450000	1,5
BH34	-25,896390	28,312500	20,0
BH35	-25,902500	28,317220	7,2
BH36	-26,016110	27,708060	61,8
BH37	-26,104440	27,600280	11,0
BH38	-26,093610	27,622220	1,5
BH39	-26,047060	27,709420	138,0
BH40	-26,053610	27,627500	132,5
BH41	-26,051940	27,654440	8,3
BH42	-26,091390	27,592500	6,8
BH43	-26,045560	27,649440	37,7
BH44	-26,050000	27,694440	19,6
BH45	-26,033890	27,681670	3,1
BH46	-26,050830	27,672500	39,0
BH47	-26,079170	27,666390	1,5
BH48	-26,094170	27,665560	1,5
BH49	-26,088890	27,696110	1,5
BH50	-26,095000	27,598610	1,5
BH51	-26,077220	27,601670	1,5
BH52	-26,005830	28,423330	2,0
BH53	-26,108060	27,722780	25,6
BH54	-26,113610	27,722780	21,1
BH55	-26,113330	27,722780	17,5
BH56	-25,895280	28,307220	8,4
BH57	-25,889170	28,314720	1,5
BH58	-25,897220	28,304170	43,5
BH59	-26,248610	27,743890	83,6
BH60	-25,833330	28,166670	7,2
BH61	-25,971670	27,793060	16,9
BH62	-26,058330	27,586110	1,5
BH63	-26,140280	27,630560	1,5
BH64	-26,143060	27,615280	1,5
BH65	-26,133330	27,663890	108,3
BH66	-26,127780	27,594440	4,4
BH67	-26,072220	27,626390	1,5

Sample ID	Latitude	Longitude	Groundwater Cl (mg/l)
BH68	-25,888890	27,513890	85,5
BH69	-25,808330	28,154170	9,0
BH70	-26,224170	28,334720	3,7
BH71	-26,053610	27,705830	106,0
BH72	-26,077250	27,699120	2,5
BH73	-26,010390	28,413580	6,8
KNOPPIESFONTEIN (DUP NAME 3214)	-26,100000	28,450000	16,5
KNOPPIESFONTEIN (DUP NAME 3215)	-26,116667	28,433333	9,0
KNOPPIESFONTEIN (DUP NAME 3632)	-26,119444	28,445556	12,3
KNOPPIESFONTEIN (DUP NAME 3770)	-26,100000	28,416667	8,5
KNOPPIESFONTEIN (DUP NAME 3783)	-26,101389	28,420833	11,1
KNOPPIESFONTEIN (DUP NAME 4001)	-26,086111	28,441667	12,7
KLIPFONTEIN (DUP NAME 21104)	-26,168333	28,450000	1,5
WELGEDACHT (DUP NAME 21106)	-26,185556	28,491667	4,7
VARKFONTEIN (DUP NAME 21110)	-26,042778	28,397778	1,5
VARKFONTEIN (DUP NAME 21111)	-26,052222	28,395833	1,5
VARKFONTEIN (DUP NAME 21112)	-26,078333	28,387500	3,4
HOLFONTEIN (DUP NAME 21113)	-26,155556	28,493333	40,5
KNOPPIESFONTEIN (DUP NAME 21114)	-26,090833	28,417500	8,9
KNOPPIESFONTEIN (DUP NAME 21115)	-26,104444	28,443611	1,5
GROOTVALY (DUP NAME 21153)	-26,228611	28,505556	71,8
VARKFONTEIN (DUP NAME 21161)	-26,071667	28,395833	7,1
VLAKPLAAS (DUP NAME 23484)	-26,224167	28,334722	3,7
GROOTVALY (DUP NAME 21154)	-26,243889	28,505000	23,1
GROOTVALY (DUP NAME 21155)	-26,260556	28,485556	888,8
GROOTVALY (DUP NAME 21155)	-26,260556	28,485556	270,5
STRYDPAN (DUP NAME 21160)	-26,240278	28,616667	121,9
VISCHKUIL	-26,301944	28,588333	9,8
BLOEMENDAL (DUP NAME 21268)	-26,319167	28,583333	9,6
GROOTVALLEY (DUP NAME 22680)	-26,250000	28,488889	942,4
BRAKPAN (DUP NAME 25281)	-26,264722	28,381389	45,9
BRAKPAN (DUP NAME 25282)	-26,259167	28,380833	29,5
BRAKPAN (DUP NAME 25283)	-26,260000	28,381667	9,8
NIGEL	-26,468611	28,471389	1,5
Minimum			**1,5**
Maximum			**7437,1**
Average			**163,5**

Appendix C Recharge Estimations and Assumptions

Sample ID	Latitude	Longitude	Cl (mg/l)	Average Annual Recharge (mm)	Recharge %	Assumption
G23D	-26,217986	28,444989	7437,1	0,1	0,0	Mining activity
B21	-26,356166	28,309000	2528,3	0,4	0,1	Mining activity
G10D	-26,217977	28,445000	2431,9	0,4	0,1	Mining activity
GA16S	-26,227880	28,317670	1012,7	1,0	0,1	Mining activity
GROOTVALLEY (DUP NAME 22680)	-26,250000	28,488889	942,4	1,1	0,1	Mining activity
GROOTVALY (DUP NAME 21155)	-26,260556	28,485556	888,8	1,1	0,2	Mining activity
6L13-12	-26,212907	28,463114	718,2	1,4	0,2	Mining activity
GAA12D	-26,199411	28,446918	569,1	1,8	0,2	Accepted
B41	-26,354672	28,300719	460,7	2,2	0,3	Accepted
GP142	-26,346726	28,514374	280,0	3,6	0,5	Accepted
GROOTVALY (DUP NAME 21155)	-26,260556	28,485556	270,5	3,8	0,5	Accepted
B9D	-26,202250	28,448669	261,6	3,9	0,5	Accepted
GP143	-26,331709	28,482316	230,8	4,4	0,6	Accepted
ZBH26D	-26,327216	28,509185	167,2	6,1	0,8	Accepted
2628AD00192	-26,306940	28,333330	156,0	6,5	0,9	Accepted
431S	-26,285420	28,529620	141,3	7,2	1,0	Accepted
BH39	-26,047060	27,709420	138,0	7,4	1,0	Accepted
BH40	-26,053610	27,627500	132,5	7,7	1,0	Accepted
STRYDPAN (DUP NAME 21160)	-26,240278	28,616667	121,9	8,4	1,1	Accepted
BH65	-26,133330	27,663890	108,3	9,4	1,3	Accepted
PD3	-26,209526	28,430171	107,6	9,5	1,3	Accepted
BH71	-26,053610	27,705830	106,0	9,6	1,3	Accepted
BH15	-26,221110	27,775280	105,5	9,7	1,3	Accepted
DN32	-26,196970	28,563000	90,2	11,3	1,5	Accepted
DN30	-26,186610	28,558960	88,8	11,5	1,6	Accepted
BH68	-25,888890	27,513890	85,5	11,9	1,6	Accepted
BH59	-26,248610	27,743890	83,6	12,2	1,7	Accepted
BH1	-26,175920	27,840310	82,0	12,4	1,7	Accepted
431D	-26,284753	28,528619	79,3	12,9	1,7	Accepted
G3D	-26,216850	28,443597	78,6	13,0	1,8	Accepted
G8D	-26,217819	28,441025	75,6	13,5	1,8	Accepted
433	-26,285400	28,529590	74,0	13,8	1,9	Accepted
GROOTVALY (DUP NAME 21153)	-26,228611	28,505556	71,8	14,2	1,9	Accepted
DD	-26,176305	27,862833	71,0	14,4	2,0	Accepted
BH4	-26,200940	27,900970	62,0	16,4	2,2	Accepted
BH36	-26,016110	27,708060	61,8	16,5	2,2	Accepted
BH26	-25,827780	28,169440	60,2	16,9	2,3	Accepted
BH21	-25,825000	28,122220	58,9	17,3	2,4	Accepted
BH28	-25,827780	28,116670	56,8	17,9	2,4	Accepted
BH25	-25,829170	28,175000	56,6	18,0	2,5	Accepted
BH1	-26,229720	28,042780	50,0	20,4	2,8	Accepted

Sample ID	Latitude	Longitude	Cl (mg/l)	Average Annual Recharge (mm)	Recharge %	Assumption
BH22	-25,820830	28,122220	49,0	20,8	2,8	Accepted
102	-26,057780	28,400000	48,2	21,2	2,9	Accepted
DN13	-26,228740	28,565180	46,1	22,1	3,0	Accepted
BRAKPAN (DUP NAME 25281)	-26,264722	28,381389	45,9	22,2	3,0	Accepted
HR3	-26,308334	28,288888	44,1	23,1	3,1	Accepted
BH58	-25,897220	28,304170	43,5	23,4	3,2	Accepted
BH2	-26,179250	27,843360	42,0	24,3	3,3	Accepted
Witbh1	-26,183140	27,856780	42,0	24,3	3,3	Accepted
2628AD00350	-26,328260	28,341110	40,6	25,1	3,4	Accepted
HOLFONTEIN (DUP NAME 21113)	-26,155556	28,493333	40,5	25,2	3,4	Accepted
2628AD00118	-26,308330	28,288890	40,5	25,2	3,4	Accepted
BH46	-26,050830	27,672500	39,0	26,1	3,6	Accepted
BH43	-26,045560	27,649440	37,7	27,0	3,7	Accepted
BH19	-25,893610	28,306940	36,2	28,2	3,8	Accepted
DN08	-26,232040	28,559630	35,2	29,0	3,9	Accepted
DN36	-26,182030	28,562460	34,9	29,2	4,0	Accepted
GAA13D	-26,197923	28,442553	33,4	30,6	4,2	Accepted
DN40	-26,183170	28,556730	31,6	32,3	4,4	Accepted
GP141	-26,338000	28,524110	31,4	32,4	4,4	Accepted
BRAKPAN (DUP NAME 25282)	-26,259167	28,380833	29,5	34,6	4,7	Accepted
BH17	-25,883330	28,316670	29,2	34,9	4,7	Accepted
GAA13S	-26,197923	28,442553	26,2	38,8	5,3	Accepted
BH53	-26,108060	27,722780	25,6	39,9	5,4	Accepted
DA68	-26,182477	28,494377	24,7	41,2	5,6	Accepted
DN20	-26,217350	28,554570	23,2	43,9	6,0	Accepted
GROOTVALY (DUP NAME 21154)	-26,243889	28,505000	23,1	44,1	6,0	Accepted
DN42	-26,182050	28,556940	22,8	44,7	6,1	Accepted
DN22	-26,216090	28,542110	21,8	46,8	6,4	Accepted
BH14	-26,245560	27,721110	21,2	48,1	6,5	Accepted
BH54	-26,113610	27,722780	21,1	48,4	6,6	Accepted
BH23	-25,783330	28,187500	21,0	48,5	6,6	Accepted
DN09	-26,232820	28,563920	20,5	49,7	6,8	Accepted
DN29	-26,243580	28,577850	20,4	50,0	6,8	Accepted
Witbh7	-26,178530	27,861250	20,0	51,0	6,9	Accepted
BH34	-25,896390	28,312500	20,0	51,0	6,9	Accepted
BH44	-26,050000	27,694440	19,6	52,0	7,1	Accepted
DN21	-26,222480	28,553310	19,3	52,8	7,2	Accepted
GC1	-26,274985	28,278551	19,1	53,3	7,3	Accepted
BH18	-25,900000	28,316670	19,0	53,7	7,3	Accepted
BH16	-25,810280	28,148610	18,8	54,2	7,4	Accepted
BH24	-25,812500	28,152780	18,7	54,5	7,4	Accepted
DN34	-26,188270	28,560610	17,8	57,3	7,8	Accepted
BH55	-26,113330	27,722780	17,5	58,2	7,9	Accepted

Sample ID	Latitude	Longitude	Cl (mg/l)	Average Annual Recharge (mm)	Recharge %	Assumption
HR1	-26,258330	28,350000	17,2	59,4	8,1	Accepted
BH61	-25,971670	27,793060	16,9	60,3	8,2	Accepted
KNOPPIESFONTEIN (DUP NAME 3214)	-26,100000	28,450000	16,5	61,8	8,4	Accepted
DN24	-26,212140	28,540750	16,0	63,7	8,7	Accepted
BH3	-26,178420	27,828780	15,0	68,0	9,2	Accepted
DN33	-26,205650	28,553960	13,9	73,3	10,0	Accepted
KNOPPIESFONTEIN (DUP NAME 4001)	-26,086111	28,441667	12,7	80,3	10,9	Accepted
KNOPPIESFONTEIN (DUP NAME 3632)	-26,119444	28,445556	12,3	82,9	11,3	Accepted
Witbh3	-26,170916	27,821916	12,0	85,0	11,6	Accepted
DN23	-26,207590	28,541430	11,5	88,6	12,1	Accepted
KNOPPIESFONTEIN (DUP NAME 3783)	-26,101389	28,420833	11,1	91,8	12,5	Accepted
BHC46	-26,224125	28,431031	11,0	92,5	12,6	Accepted
BH37	-26,104440	27,600280	11,0	92,7	12,6	Accepted
VISCHKUIL	-26,301944	28,588333	9,8	104,0	14,2	Accepted
BRAKPAN (DUP NAME 25283)	-26,260000	28,381667	9,8	104,0	14,2	Accepted
BH2	-25,992500	28,117500	9,7	105,1	14,3	Accepted
BLOEMENDAL (DUP NAME 21268)	-26,319167	28,583333	9,6	106,2	14,4	Accepted
DN25	-26,215160	28,557830	9,4	108,4	14,8	Accepted
BH31	-26,116670	28,433330	9,0	113,3	15,4	Accepted
BH69	-25,808330	28,154170	9,0	113,3	15,4	Accepted
KNOPPIESFONTEIN (DUP NAME 3215)	-26,116667	28,433333	9,0	113,3	15,4	Accepted
KNOPPIESFONTEIN (DUP NAME 21114)	-26,090833	28,417500	8,9	114,5	15,6	Accepted
KNOPPIESFONTEIN (DUP NAME 3770)	-26,100000	28,416667	8,5	119,9	16,3	Accepted
BH56	-25,895280	28,307220	8,4	121,4	16,5	Accepted
BH41	-26,051940	27,654440	8,3	122,8	16,7	Accepted
Witbh5	-26,171110	27,886250	8,0	127,4	17,3	Accepted
ME1	-26,179520	28,428130	7,9	129,0	17,6	Accepted
CEN74	-26,300041	28,360796	7,9	129,4	17,6	Accepted
DN26	-26,235360	28,574910	7,5	135,4	18,4	Accepted
BH35	-25,902500	28,317220	7,2	141,6	19,3	Accepted
BH60	-25,833330	28,166670	7,2	141,6	19,3	Accepted
VARKFONTEIN (DUP NAME 21161)	-26,071667	28,395833	7,1	143,6	19,5	Accepted
BH73	-26,010390	28,413580	6,8	149,0	20,3	Accepted
BH42	-26,091390	27,592500	6,8	149,9	20,4	Accepted
BH20	-25,816670	28,100000	5,7	178,8	24,3	Accepted
SP2	-26,021670	27,564720	5,2	196,0	26,7	Accepted
DN28	-26,251500	28,562460	5,0	205,5	28,0	Accepted
WELGEDACHT (DUP NAME 21106)	-26,185556	28,491667	4,7	216,9	29,5	Accepted
SP3	-25,874440	27,782220	4,4	231,7	31,5	Accepted
BH66	-26,127780	27,594440	4,4	231,7	31,5	Accepted
BH7	-26,397403	28,445706	4,4	232,2	31,6	Accepted
DN35	-26,187630	28,560130	3,8	268,3	36,5	Accepted
BH10	-26,243330	27,796390	3,8	268,3	36,5	Accepted

Sample ID	Latitude	Longitude	Cl (mg/l)	Average Annual Recharge (mm)	Recharge %	Assumption
BH70	-26,224170	28,334720	3,7	275,5	37,5	Accepted
VLAKPLAAS (DUP NAME 23484)	-26,224167	28,334722	3,7	275,5	37,5	Accepted
DN39	-26,183470	28,557220	3,5	291,3	39,6	Accepted
BH7	-26,235280	27,749440	3,5	291,3	39,6	Accepted
VARKFONTEIN (DUP NAME 21112)	-26,078333	28,387500	3,4	299,8	40,8	Accepted
BH45	-26,033890	27,681670	3,1	328,8	44,7	Accepted
BH32	-26,083330	28,500000	3,0	339,8	46,2	Accepted
BH72	-26,077250	27,699120	2,5	407,8	55,5	Accepted
BH52	-26,005830	28,423330	2,0	509,7	69,3	Accepted
SP1	-25,985000	28,331670	1,5	679,6	92,5	Detection limit
BH3	-26,246670	27,716940	1,5	679,6	92,5	Detection limit
BH4	-26,233890	27,803060	1,5	679,6	92,5	Detection limit
BH5	-26,234720	27,725280	1,5	679,6	92,5	Detection limit
BH6	-26,233060	27,783330	1,5	679,6	92,5	Detection limit
BH8	-26,236670	27,796670	1,5	679,6	92,5	Detection limit
BH9	-26,247220	27,749720	1,5	679,6	92,5	Detection limit
BH11	-26,245830	27,683610	1,5	679,6	92,5	Detection limit
BH12	-26,228330	27,734440	1,5	679,6	92,5	Detection limit
BH13	-26,245560	27,683610	1,5	679,6	92,5	Detection limit
BH15	-26,240280	27,804170	1,5	679,6	92,5	Detection limit
BH27	-25,791670	28,208330	1,5	679,6	92,5	Detection limit
BH29	-25,784720	28,205560	1,5	679,6	92,5	Detection limit
BH30	-26,033330	28,466670	1,5	679,6	92,5	Detection limit
BH33	-26,016670	28,450000	1,5	679,6	92,5	Detection limit
BH38	-26,093610	27,622220	1,5	679,6	92,5	Detection limit
BH47	-26,079170	27,666390	1,5	679,6	92,5	Detection limit
BH48	-26,094170	27,665560	1,5	679,6	92,5	Detection limit
BH49	-26,088890	27,696110	1,5	679,6	92,5	Detection limit
BH50	-26,095000	27,598610	1,5	679,6	92,5	Detection limit
BH51	-26,077220	27,601670	1,5	679,6	92,5	Detection limit
BH57	-25,889170	28,314720	1,5	679,6	92,5	Detection limit
BH62	-26,058330	27,586110	1,5	679,6	92,5	Detection limit
BH63	-26,140280	27,630560	1,5	679,6	92,5	Detection limit
BH64	-26,143060	27,615280	1,5	679,6	92,5	Detection limit
BH67	-26,072220	27,626390	1,5	679,6	92,5	Detection limit
KLIPFONTEIN (DUP NAME 21104)	-26,168333	28,450000	1,5	679,6	92,5	Detection limit
VARKFONTEIN (DUP NAME 21110)	-26,042778	28,397778	1,5	679,6	92,5	Detection limit
VARKFONTEIN (DUP NAME 21111)	-26,052222	28,395833	1,5	679,6	92,5	Detection limit
KNOPPIESFONTEIN (DUP NAME 21115)	-26,104444	28,443611	1,5	679,6	92,5	Detection limit
NIGEL	-26,468611	28,471389	1,5	679,6	92,5	Detection limit
Minimum (Accepted)			**2,0**	**1,8**	**0,2**	
Maximum (Accepted)			**569,1**	**509,7**	**69,3**	
Average (Accepted)			**49,2**	**82,6**	**11,2**	

Appendix D Recharge Potential and related Geology

Sample ID	Cl (mg/l)	Average Annual Recharge (mm/a)	Recharge (%)	Geology
DN08	35,2	29,0	3,9	Alluvium
BLOEMENDAL (DUP NAME 21268)	9,6	106,2	14,4	Alluvium
GAA12D	569,1	1,8	0,2	Diamictite
B9D	261,6	3,9	0,5	Diamictite
102	48,2	21,2	2,9	Diamictite
GAA13D	33,4	30,6	4,2	Diamictite
GAA13S	26,2	38,8	5,3	Diamictite
DA68	24,7	41,2	5,6	Diamictite
KNOPPIESFONTEIN (DUP NAME 3214)	16,5	61,8	8,4	Diamictite
KNOPPIESFONTEIN (DUP NAME 4001)	12,7	80,3	10,9	Diamictite
BH31	9,0	113,3	15,4	Diamictite
KNOPPIESFONTEIN (DUP NAME 3215)	9,0	113,3	15,4	Diamictite
ME1	7,9	129,0	17,6	Diamictite
GP143	230,8	4,4	0,6	Dolomite and Limestone
ZBH26D	167,2	6,1	0,8	Dolomite and Limestone
G3D	78,6	13,0	1,8	Dolomite and Limestone
G8D	75,6	13,5	1,8	Dolomite and Limestone
GROOTVALY (DUP NAME 21153)	71,8	14,2	1,9	Dolomite and Limestone
KNOPPIESFONTEIN (DUP NAME 3632)	12,3	82,9	11,3	Dolomite and Limestone
BHC46	11,0	92,5	12,6	Dolomite and Limestone
VARKFONTEIN (DUP NAME 21161)	7,1	143,6	19,5	Dolomite and Limestone
WELGEDACHT (DUP NAME 21106)	4,7	216,9	29,5	Dolomite and Limestone
GP142	280,0	3,6	0,5	Sandstone and Shale
GROOTVALY (DUP NAME 21155)	270,5	3,8	0,5	Sandstone and Shale
431S	141,3	7,2	1,0	Sandstone and Shale
STRYDPAN (DUP NAME 21160)	121,9	8,4	1,1	Sandstone and Shale
PD3	107,6	9,5	1,3	Sandstone and Shale
DN32	90,2	11,3	1,5	Sandstone and Shale
DN30	88,8	11,5	1,6	Sandstone and Shale
431D	79,3	12,9	1,7	Sandstone and Shale
433	74,0	13,8	1,9	Sandstone and Shale
DN13	46,1	22,1	3,0	Sandstone and Shale
BRAKPAN (DUP NAME 25281)	45,9	22,2	3,0	Sandstone and Shale
HOLFONTEIN (DUP NAME 21113)	40,5	25,2	3,4	Sandstone and Shale
DN36	34,9	29,2	4,0	Sandstone and Shale
GP141	31,4	32,4	4,4	Sandstone and Shale
BRAKPAN (DUP NAME 25282)	29,5	34,6	4,7	Sandstone and Shale

DN20	23,2	43,9	6,0	Sandstone and Shale
GROOTVALY (DUP NAME 21154)	23,1	44,1	6,0	Sandstone and Shale
DN22	21,8	46,8	6,4	Sandstone and Shale
DN09	20,5	49,7	6,8	Sandstone and Shale
DN29	20,4	50,0	6,8	Sandstone and Shale
DN21	19,3	52,8	7,2	Sandstone and Shale
DN34	17,8	57,3	7,8	Sandstone and Shale
DN24	16,0	63,7	8,7	Sandstone and Shale
DN33	13,9	73,3	10,0	Sandstone and Shale
DN23	11,5	88,6	12,1	Sandstone and Shale
KNOPPIESFONTEIN (DUP NAME 3783)	11,1	91,8	12,5	Sandstone and Shale
VISCHKUIL	9,8	104,0	14,2	Sandstone and Shale
BRAKPAN (DUP NAME 25283)	9,8	104,0	14,2	Sandstone and Shale
DN25	9,4	108,4	14,8	Sandstone and Shale
KNOPPIESFONTEIN (DUP NAME 21114)	8,9	114,5	15,6	Sandstone and Shale
KNOPPIESFONTEIN (DUP NAME 3770)	8,5	119,9	16,3	Sandstone and Shale
DN26	7,5	135,4	18,4	Sandstone and Shale
DN28	5,0	205,5	28,0	Sandstone and Shale
BH7	4,4	232,2	31,6	Sandstone and Shale
DN35	3,8	268,3	36,5	Sandstone and Shale
BH70	3,7	275,5	37,5	Sandstone and Shale
VLAKPLAAS (DUP NAME 23484)	3,7	275,5	37,5	Sandstone and Shale
VARKFONTEIN (DUP NAME 21112)	3,4	299,8	40,8	Sandstone and Shale

Appendix E Groundwater Levels

Site ID	Latitude	Longitude	Groundwater level (mbgl)
Well_1	-26,036120	27,700000	7,9
Well_2	-25,856390	28,166950	15,0
Well_3	-25,896390	28,312500	22,0
Well_4	-25,927500	28,219450	30,0
Well_5	-26,017400	27,711360	30,0
Well_6	-26,080560	27,576390	53,0
Well_7	-25,898620	28,302780	67,0
Well_8	-25,969450	28,280560	76,0
Well_9	-25,916890	28,338560	10,0
Well_10	-25,889160	28,208880	40,0
Well_11	-25,892220	28,321950	63,0
Well_12	-26,068250	27,647360	92,0
Well_13	-26,050800	27,672480	74,0
Well_13	-25,882220	28,256660	107,0
Well_14	-26,016670	28,285550	116,0
Well_15	-25,908610	28,316950	134,0
Well_16	-26,046250	27,678720	132,0
Well_17	-25,856940	28,233330	148,0
Well_18	-25,949610	28,341940	19,0
Well_19	-25,950000	28,268060	169,0
A2N0783	-26,046990	28,380850	14,6
B2N0024	-26,055380	28,433090	29,0
C2N0113	-26,143223	28,519330	138,4
C2N0887	-26,088780	28,448400	8,1
C2N0888	-26,110556	28,441667	2,7
C2N0889	-26,119167	28,445278	6,3
C2N0890	-26,082530	28,433020	2,5
C2N0891	-26,085910	28,444120	9,0
C2N0892	-26,088056	28,448889	13,9
C2N0893	-26,101500	28,449290	3,5
C2N0894	-26,173710	28,521030	57,3
C2N1113	-26,139167	28,518056	49,6
C2N1114	-26,144320	28,521260	49,0
431D	-26,284753	28,528619	10,1
431S	-26,285420	28,529620	9,8
6L13-12	-26,212907	28,463114	3,1
B21	-26,356166	28,309000	2,4
B9D	-26,202250	28,448669	21,2
BH7	-26,397403	28,445706	31,1
CEN74	-26,300041	28,360796	11,5
G14D	-26,217986	28,444989	8,6
G23D	-26,217986	28,444989	13,0
G8D	-26,217819	28,441025	12,5

Site ID	Latitude	Longitude	Groundwater level (mbgl)
GAA12D	-26,199411	28,446918	23,9
GAA13D	-26,197923	28,442553	22,6
GAA13S	-26,197923	28,442553	21,9
GP141	-26,338000	28,524110	8,1
GP142	-26,346726	28,514374	6,8
GP143	-26,331709	28,482316	2,1
PD3	-26,209526	28,430171	22,2
G3D	-26,216850	28,443597	9,3
431S	-26,285420	28,529620	9,8
G10D	-26,217977	28,445000	13,0
B41	-26,354672	28,300719	2,5
GA16S	-26,225055	28,315486	26,4
3	-26,215841	28,441486	9,8
6	-26,209570	28,430143	22,2
ZBH26D	-26,327216	28,509185	1,2
ZBH26S	-26,327216	28,509185	1,0
DN08	-26,232040	28,559630	3,5
DN09	-26,232820	28,563920	5,4
DN13	-26,228740	28,565180	4,9
DN21	-26,222480	28,553310	12,8
DN23	-26,207590	28,541430	10,2
DN24	-26,212140	28,540750	20,5
DN25	-26,215160	28,557830	5,8
DN26	-26,235360	28,574910	8,3
DN27	-26,250510	28,562480	12,1
DN28	-26,251500	28,562460	11,9
DN29	-26,243580	28,577850	8,6
DN43	-26,207960	28,573490	31,0
DN45	-26,204140	28,560240	25,6
DN46	-26,221520	28,541400	100,0
DN47	-26,223030	28,538820	34,5
DN48	-26,222670	28,538170	34,3
DN49	-26,220910	28,539250	16,6
DN50	-26,224160	28,540960	33,8
DN51	-26,225180	28,540180	17,3
DN53	-26,225290	28,531050	16,6
DN54	-26,225920	28,537190	20,4
DN55	-26,225390	28,536760	29,0
DN56	-26,225350	28,537320	10,2
DN57	-26,225480	28,537290	100,5
DN59	-26,218020	28,539130	32,1
DN61	-26,221280	28,535520	49,7
DN62	-26,220130	28,534720	22,3
DN63	-26,220000	28,536530	57,0
DN64	-26,225150	28,532940	18,5

Site ID	Latitude	Longitude	Groundwater level (mbgl)
DN65	-26,224270	28,532660	19,8
DN66	-26,225440	28,534560	48,2
DN67	-26,222850	28,532640	25,6
DN68	-26,221160	28,532930	16,4
DN70	-26,219330	28,531550	66,4
DN71	-26,217610	28,533990	11,6
DN72	-26,226150	28,539080	28,0
DN30	-26,186610	28,558960	89,0
DN31	-26,190520	28,553710	91,0
DN32	-26,196970	28,563000	94,6
DN34	-26,188270	28,560610	40,2
DN35	-26,187630	28,560130	20,1
DN36	-26,182030	28,562460	77,1
DN38	-26,184440	28,559550	1,2
DN39	-26,183470	28,557220	21,4
DN40	-26,183170	28,556730	20,2
DN42	-26,182050	28,556940	60,1
BH1	-26,175920	27,840310	2,5
BH2	-26,179250	27,843360	0,3
BH3	-26,178420	27,828780	13,0
BH4	-26,200940	27,900970	20,9
WITBH1	-26,183140	27,856780	36,6
WITBH5	-26,171110	27,886250	10,1
WITBH7	-26,178530	27,861250	7,9
Minimum			**0,3**
Maximum			**169,0**
Average			**32,9**

Appendix F Time Dependant Recharge Model Input

Date	Rainfall (mm/month)	Rainfall (m/d)	Alluvium	Sandstone and Shale	Basaltic lava	Diamictite	Dolomite and Limestone	Quartzite and Conglomerate	Quartzite and Shale	Granite and Gneiss	Diabase	Dolerite Dykes	Faults
Jan-94	87,1	2,9E-03	2,3E-04	8,7E-05	2,9E-05	7,3E-05	2,9E-04	5,8E-05	2,9E-05	2,9E-05	1,5E-05	1,5E-05	2,3E-04
Feb-94	172,7	5,8E-03	4,6E-04	1,7E-04	5,8E-05	1,4E-04	5,8E-04	1,2E-04	5,8E-05	5,8E-05	2,9E-05	2,9E-05	4,6E-04
Mar-94	60,2	2,0E-03	1,6E-04	6,0E-05	2,0E-05	5,0E-05	2,0E-04	4,0E-05	2,0E-05	2,0E-05	1,0E-05	1,0E-05	1,6E-04
Apr-94	3,8	1,3E-04	1,0E-05	3,8E-06	1,3E-06	3,2E-06	1,3E-05	2,5E-06	1,3E-06	1,3E-06	6,3E-07	6,3E-07	1,0E-05
May-94	0	0,0E+00	0,0E+00	0,0E+00	0,0E+00	0,0E+00	0,0E+00	0,0E+00	0,0E+00	0,0E+00	0,0E+00	0,0E+00	0,0E+00
Jun-94	0	0,0E+00	0,0E+00	0,0E+00	0,0E+00	0,0E+00	0,0E+00	0,0E+00	0,0E+00	0,0E+00	0,0E+00	0,0E+00	0,0E+00
Jul-94	14,5	4,8E-04	3,9E-05	1,5E-05	4,8E-06	1,2E-05	4,8E-05	9,7E-06	4,8E-06	4,8E-06	2,4E-06	2,4E-06	3,9E-05
Aug-94	14	4,7E-04	3,7E-05	1,4E-05	4,7E-06	1,2E-05	4,7E-05	9,3E-06	4,7E-06	4,7E-06	2,3E-06	2,3E-06	3,7E-05
Sep-94	94	3,1E-03	2,5E-04	9,4E-05	3,1E-05	7,8E-05	3,1E-04	6,3E-05	3,1E-05	3,1E-05	1,6E-05	1,6E-05	2,5E-04
Oct-94	99,7	3,3E-03	2,7E-04	1,0E-04	3,3E-05	8,3E-05	3,3E-04	6,6E-05	3,3E-05	3,3E-05	1,7E-05	1,7E-05	2,7E-04
Nov-94	181,5	6,1E-03	4,8E-04	1,8E-04	6,1E-05	1,5E-04	6,1E-04	1,2E-04	6,1E-05	6,1E-05	3,0E-05	3,0E-05	4,8E-04
Dec-94	77,7	2,6E-03	2,1E-04	7,8E-05	2,6E-05	6,5E-05	2,6E-04	5,2E-05	2,6E-05	2,6E-05	1,3E-05	1,3E-05	2,1E-04
Jan-95	261	8,7E-03	7,0E-04	2,6E-04	8,7E-05	2,2E-04	8,7E-04	1,7E-04	8,7E-05	8,7E-05	4,4E-05	4,4E-05	7,0E-04
Feb-95	72	2,4E-03	1,9E-04	7,2E-05	2,4E-05	6,0E-05	2,4E-04	4,8E-05	2,4E-05	2,4E-05	1,2E-05	1,2E-05	1,9E-04
Mar-95	114	3,8E-03	3,0E-04	1,1E-04	3,8E-05	9,5E-05	3,8E-04	7,6E-05	3,8E-05	3,8E-05	1,9E-05	1,9E-05	3,0E-04
Apr-95	6,8	2,3E-04	1,8E-05	6,8E-06	2,3E-06	5,7E-06	2,3E-05	4,5E-06	2,3E-06	2,3E-06	1,1E-06	1,1E-06	1,8E-05
May-95	0	0,0E+00	0,0E+00	0,0E+00	0,0E+00	0,0E+00	0,0E+00	0,0E+00	0,0E+00	0,0E+00	0,0E+00	0,0E+00	0,0E+00
Jun-95	1,5	5,0E-05	4,0E-06	1,5E-06	5,0E-07	1,3E-06	5,0E-06	1,0E-06	5,0E-07	5,0E-07	2,5E-07	2,5E-07	4,0E-06
Jul-95	10,5	3,5E-04	2,8E-05	1,1E-05	3,5E-06	8,8E-06	3,5E-05	7,0E-06	3,5E-06	3,5E-06	1,8E-06	1,8E-06	2,8E-05
Aug-95	1,7	5,7E-05	4,5E-06	1,7E-06	5,7E-07	1,4E-06	5,7E-06	1,1E-06	5,7E-07	5,7E-07	2,8E-07	2,8E-07	4,5E-06
Sep-95	217,2	7,2E-03	5,8E-04	2,2E-04	7,2E-05	1,8E-04	7,2E-04	1,4E-04	7,2E-05	7,2E-05	3,6E-05	3,6E-05	5,8E-04
Oct-95	173,3	5,8E-03	4,6E-04	1,7E-04	5,8E-05	1,4E-04	5,8E-04	1,2E-04	5,8E-05	5,8E-05	2,9E-05	2,9E-05	4,6E-04
Nov-95	189,4	6,3E-03	5,1E-04	1,9E-04	6,3E-05	1,6E-04	6,3E-04	1,3E-04	6,3E-05	6,3E-05	3,2E-05	3,2E-05	5,1E-04
Dec-95	265,3	8,8E-03	7,1E-04	2,7E-04	8,8E-05	2,2E-04	8,8E-04	1,8E-04	8,8E-05	8,8E-05	4,4E-05	4,4E-05	7,1E-04
Jan-96	96,3	3,2E-03	2,6E-04	9,6E-05	3,2E-05	8,0E-05	3,2E-04	6,4E-05	3,2E-05	3,2E-05	1,6E-05	1,6E-05	2,6E-04
Feb-96	305,3	1,0E-02	8,1E-04	3,1E-04	1,0E-04	2,5E-04	1,0E-03	2,0E-04	1,0E-04	1,0E-04	5,1E-05	5,1E-05	8,1E-04
Mar-96	30,8	1,0E-03	8,2E-05	3,1E-05	1,0E-05	2,6E-05	1,0E-04	2,1E-05	1,0E-05	1,0E-05	5,1E-06	5,1E-06	8,2E-05
Apr-96	126,6	4,2E-03	3,4E-04	1,3E-04	4,2E-05	1,1E-04	4,2E-04	8,4E-05	4,2E-05	4,2E-05	2,1E-05	2,1E-05	3,4E-04
May-96	7,8	2,6E-04	2,1E-05	7,8E-06	2,6E-06	6,5E-06	2,6E-05	5,2E-06	2,6E-06	2,6E-06	1,3E-06	1,3E-06	2,1E-05
Jun-96	12	4,0E-04	3,2E-05	1,2E-05	4,0E-06	1,0E-05	4,0E-05	8,0E-06	4,0E-06	4,0E-06	2,0E-06	2,0E-06	3,2E-05
Jul-96	5,5	1,8E-04	1,5E-05	5,5E-06	1,8E-06	4,6E-06	1,8E-05	3,7E-06	1,8E-06	1,8E-06	9,2E-07	9,2E-07	1,5E-05
Aug-96	59	2,0E-03	1,6E-04	5,9E-05	2,0E-05	4,9E-05	2,0E-04	3,9E-05	2,0E-05	2,0E-05	9,8E-06	9,8E-06	1,6E-04
Sep-96	82,8	2,8E-03	2,2E-04	8,3E-05	2,8E-05	6,9E-05	2,8E-04	5,5E-05	2,8E-05	2,8E-05	1,4E-05	1,4E-05	2,2E-04
Oct-96	142,8	4,8E-03	3,8E-04	1,4E-04	4,8E-05	1,2E-04	4,8E-04	9,5E-05	4,8E-05	4,8E-05	2,4E-05	2,4E-05	3,8E-04
Nov-96	174,2	5,8E-03	4,6E-04	1,7E-04	5,8E-05	1,5E-04	5,8E-04	1,2E-04	5,8E-05	5,8E-05	2,9E-05	2,9E-05	4,6E-04
Dec-96	101,3	3,4E-03	2,7E-04	1,0E-04	3,4E-05	8,4E-05	3,4E-04	6,8E-05	3,4E-05	3,4E-05	1,7E-05	1,7E-05	2,7E-04